CHAPTER 5

RESULTS AND DISCUSSION

5.1 Meteorological parameters of the study Area

CMPDIL (Singrauli) and NCL headquarter office is the only source which provides meteorological data such as climate, annual rainfall and relative humidity of the study area.

5.1.1 Climate

The climate of the area is dry moist, tropical with well-defined summer from April to mid-June, rainy season from mid-June to September and winter from November to February. The temperature varies from a maximum of 44°C to a minimum of 8°C. Singrauli receives maximum rainfall during the south-west monsoon.

5.1.2 Annual rainfall patterns

Rainfall is the main source for groundwater recharging, apart from seepage from the surface water bodies. Rainfall data during 2009–2018 period obtained from the India CMPDIL Singrauli, It shows that monthly and annual average rainfall (Table 5.1).

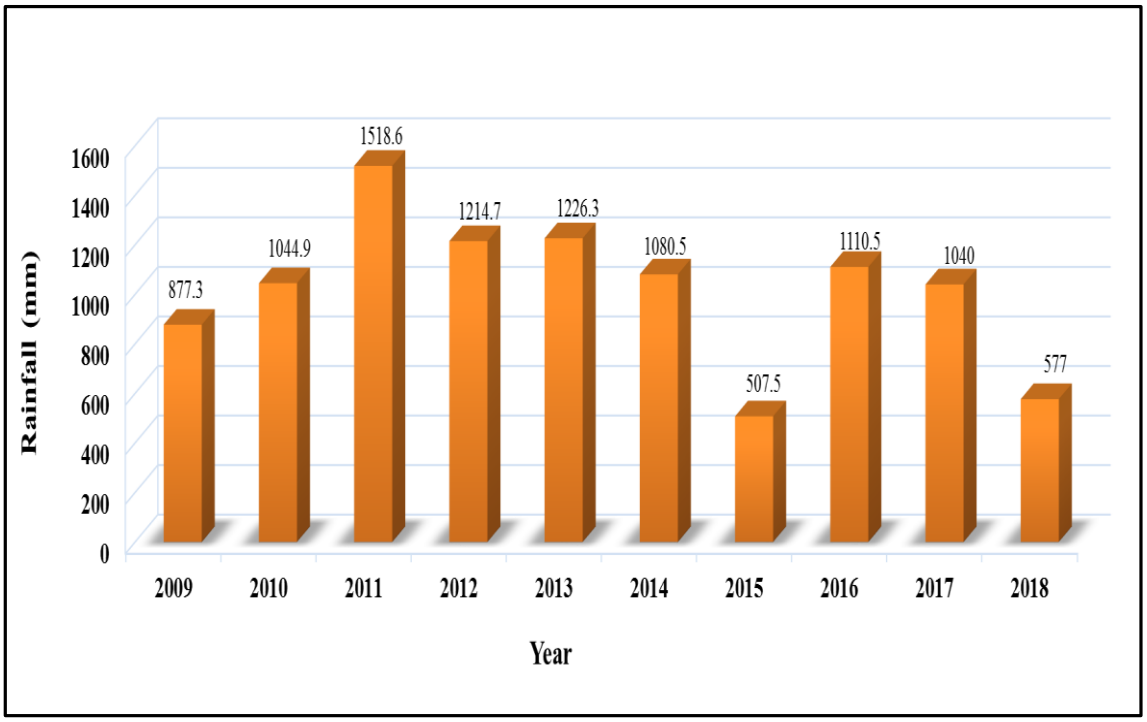

Figure. 5.1 Graph representing annual average rainfall

The average annual rainfall received of the study area is 1206 mm. The trend of the rainfall pattern of the study area was found decreasing. The maximum rainfall recorded as 1518 mm in the year 2011 and the minimum was 507 mm in the year 2015 during the last 10 years. The maximum rainfall takes place during the southwest monsoon period. In Fig 5.1 the bar graph is showing annual average rainfall (mm).

Table: 5.1 Annual rainfall data of the study area during 2009-2018 period

Year **Month**	**2009 (mm)**	**2010**	**2011**	**2012**	**2013**	**2014**	**2015**	**2016**	**2017**	**2018**
JAN	4.8	5.6	4.0	35.0	0.0	56.2	45.0	6.8	0.0	0.0
FEB	0.0	7.2	2.8	1.6	91.5	60.1	12.0	0.0	0.0	9.0
MAR	1.6	0.0	0.0	2.4	14.4	36.6	47.0	17.1	2.0	13.0
APR	2.0	0.0	34.2	0.0	17.1	11.9	11.9	0.0	0.0	3.0
MAY	24.6	55.7	14.3	0.0	8.0	23.9	12.0	8.8	8.0	20.0
JUNE	43.8	51.8	414.2	24.0	138.0	100.2	31.1	26.7	104.	59.0
JULY	318.1	347.7	273.8	500.2	295.2	279.7	153.1	166	490	165
AUG	241.3	308.8	373.6	388.5	370.7	197.3	148.1	424	257	235
SEPT	132.9	254.6	400.1	220.7	107.1	259.3	29.0	435.0	120	65
OCT	42.2	10.	0.0	10.4	184.3	46.1	14.3	19.1	59	2.0
NOV	64.4	0.0	0.0	18.3	0.0	0.0	0.0	0.0	0.0	6.0
DEC	1.6	3.2	1.6	13.6	0.0	11.2	4.0	0.0	0.0	0.0
Annual	**877.3**	**1044.9**	**1518.6**	**1214.7**	**1226.3**	**1082.5**	**507.50**	**1110.5**	**1040**	**577**

(Data Source: NCL Singrauli)

5.1.3 Relative humidity

The area experiences high relative humidity during the south west monsoon period. The maximum relative humidity varies from 55% to 88% during July to September and 33% to 55% in winter season (October to February). In summer (March to June) relative humidity is only 14% (CMPDI, 2005).

5.2 Assessment of groundwater level fluctuation of the study area

Open-cast coal mining activities and underground mining, usually impact on both hydro-geological parameters and water quality (Bai et al. 2011; Pan et al. 2012; Tiwari et al., 2015; Zeng et al., 2018; Verma et al., 2020). The various hydro-geological parameters such as slope, elevation, geology, soil and drainage pattern may cause disturbed by open cast coal mining activities. Due to the disturbing of hydro-geological parameters of the coal mining area, which have a significant impact on aquifer potential, groundwater flow direction and groundwater level.

The groundwater levels in and around mining areas vary to a great extent from place to place. The groundwater level values (mbgl) during pre-monsoon and post-monsoon periods give the fluctuation values at any place. These values are obtained by regular (monthly) monitoring of water level into selected dug-wells and other water source structure.

The objective of this research was to assess the impact of hydrogeological parameters on groundwater level fluctuation in the study area. The various hydrogeological parameters that have been considered here which can affect the aquifer recharge are soil, geology, drainage pattern, elevation, and slope. The objective was achieved by the preparation of thematic maps of various hydrogeological parameters and the comparative GIS-based maps analysis has been performed between individual hydrogeological parameters and water level fluctuation maps,

5.2.1 Groundwater level monitoring stations

A total of eighty-six dug-wells were selected for the monitoring of groundwater level around different coal mining blocks of Singrauli coalfields for pre and post-monsoon for the season 2016 as given in Appendix A.1 and selected dug-wells coded from DW-1 to

DW-86. The detailed methodology adopted for carrying out the research is discussed in the previous Chapter IV. The well location map of the study area is shown in Fig. 5.2.

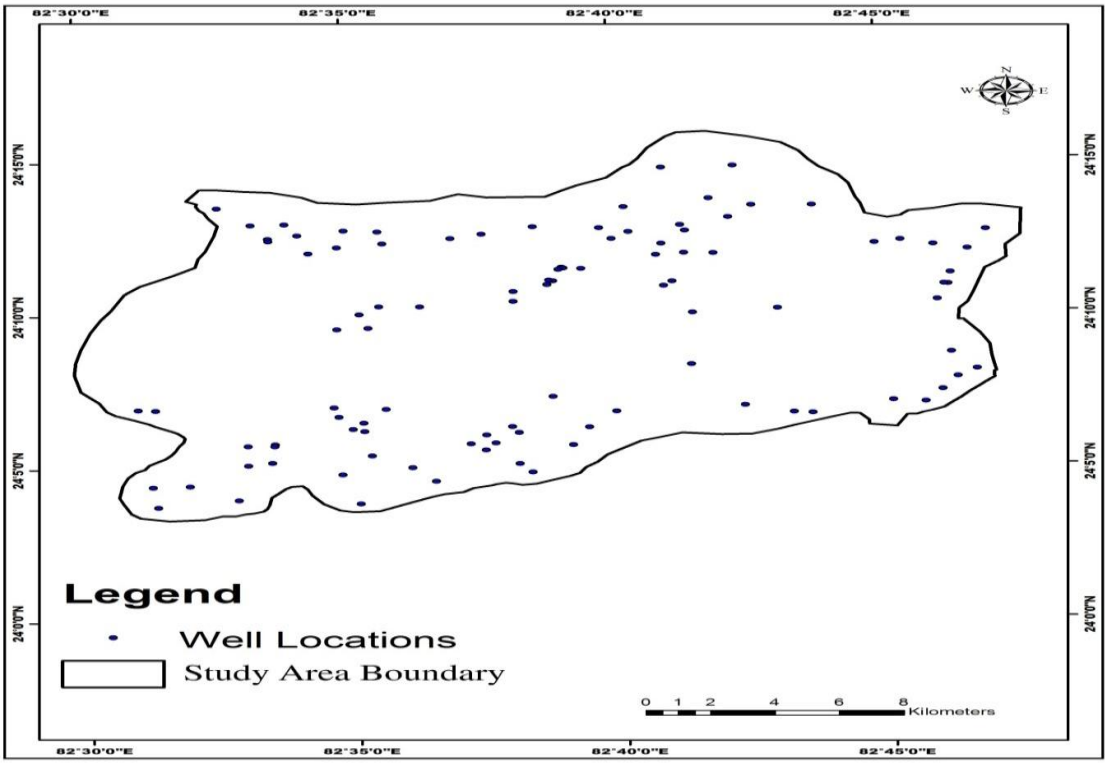

Figure 5.2 Location map of the monitoring dug-wells of the study area

5.2.2 Comparative analysis of WLF with various hydrogeological parameters using GIS

By using ArcGIS, Comparative analysis of water level fluctuation (WLF) has been done to estimate the aggregate effect of the various hydrogeological factors on groundwater recharge. It has been discussed in the below section separately with various hydrogeological factors viz. soil, geology, drainage, elevation and slope of the study area. In a comparative analysis, the thematic maps of various hydrogeological factors has been compared with field-collected groundwater level data map (pre and post-monsoon) and groundwater level fluctuations map to determine the overall water level situation of the study area.

5.2.2.1 GIS analysis of WLF under different slope classes

The occurrence and movement of groundwater are governed strongly by slope; therefore slope can be considered as an important factor in runoff flows and infiltration (Tiwari et al., 2015).A higher degree of slope results in the rapid runoff of rainfall water and increased erosion rate with feeble recharge potential (Magesh et al. 2011a, b).Gentle slope regions are having the capability to hold the surface water in the same position for a longer duration. Therefore, a region with gentle slope is having more prospects of groundwater as the infiltration process predominates.

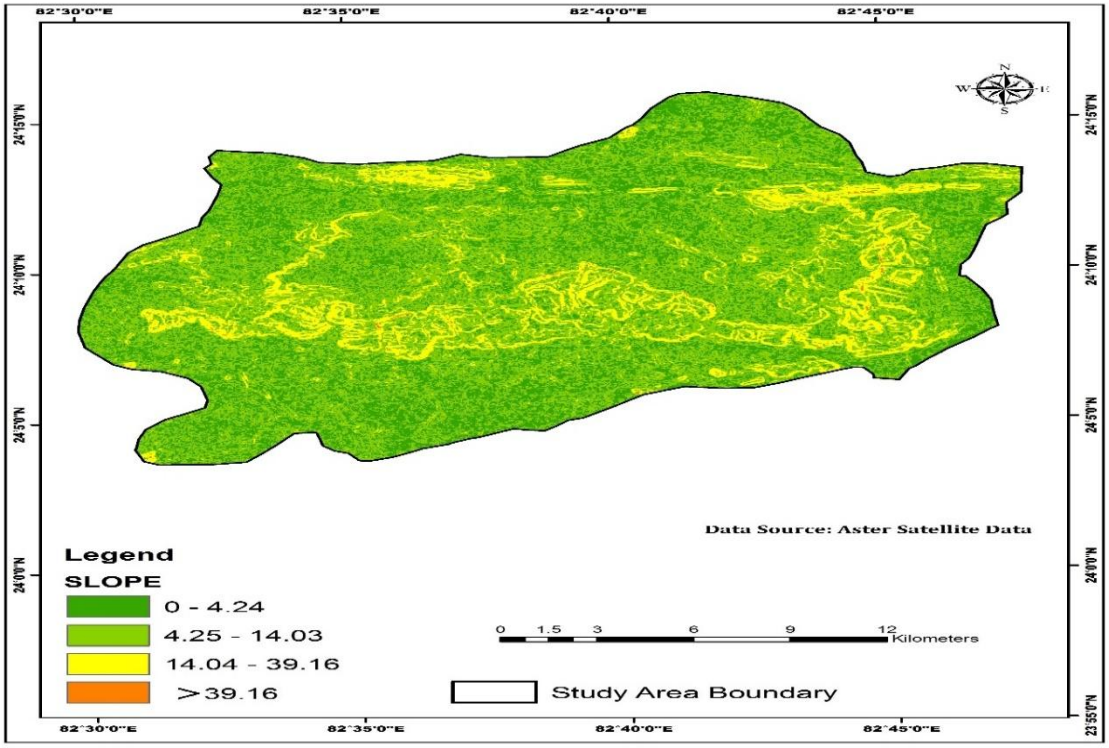

Figure 5.3 Slope map of the study area

The slope has been categorized into four classes i.e. gentle (0°- 4.24°), moderate (4.25°-14.03°), steep (14.04°- 39.16°) and very steep (> 39.16°) are shown in Fig. 5.3. From the slope map of the study area, it can be seen that the steep slope has occurred at the central portion of the study area in W-shape due to the overburden dump. Except for the middle areas, the slope of the rest area is the distribution from 0-14.03°.

Concerning the WLF map and slope map, it can be understood that slope has a direct relationship with WLF within an area. It very well may be seen from the water level fluctuation map (Fig.5.10) that WLF in south-western and some portion of the north-eastern portion show moderate to higher WLF from 1.6 to 3.3 mbgl. This may be attributed to the fact that most of the non-hilly areas are present in these areas which come under gentle to moderate slope category which forms the perfect hydrogeological condition for recharging of groundwater.

With respect to water level fluctuation map and slope map, it can be seen from water level fluctuation map that WLF in central regions shows lower water level fluctuation from 0.59 to 1.5 mbgl which may be attributed to the presence of overburden dump as well steep slope which forms runoff zone over them and thereby less chance of rainwater infiltration. Thus, the combined effect of slope and mining activities on the water level fluctuation in the central portion of the study area.

5.2.2.2 GIS analysis of WLF under different elevation classes

Plainer areas, having lower elevation tend to retain water longer inducing greater infiltration of recharge of water. A large amount of runoff and a smaller amount of infiltration are associated with areas with steep elevation angle (Thapa et al., 2017). Different studies have shown that there is a direct influence of slope, elevation, and surface topography on groundwater recharge and water table fluctuation (Moore et al. 1988). The elevation of the study area lies within 232–495 m above the mean sea level as shown in Fig.5.4.

It can be observed from WLF map (Fig.5.10) and elevation map (Fig.5.4) that wells lie in higher elevation range (350-495m) show lower WLF values whereas the wells lie in lower elevation range (233-350m) show higher WLF values, as lower plains are

considered as good recharge zone and areas having higher elevation have less potential for rainwater infiltration (Murthy 2000).

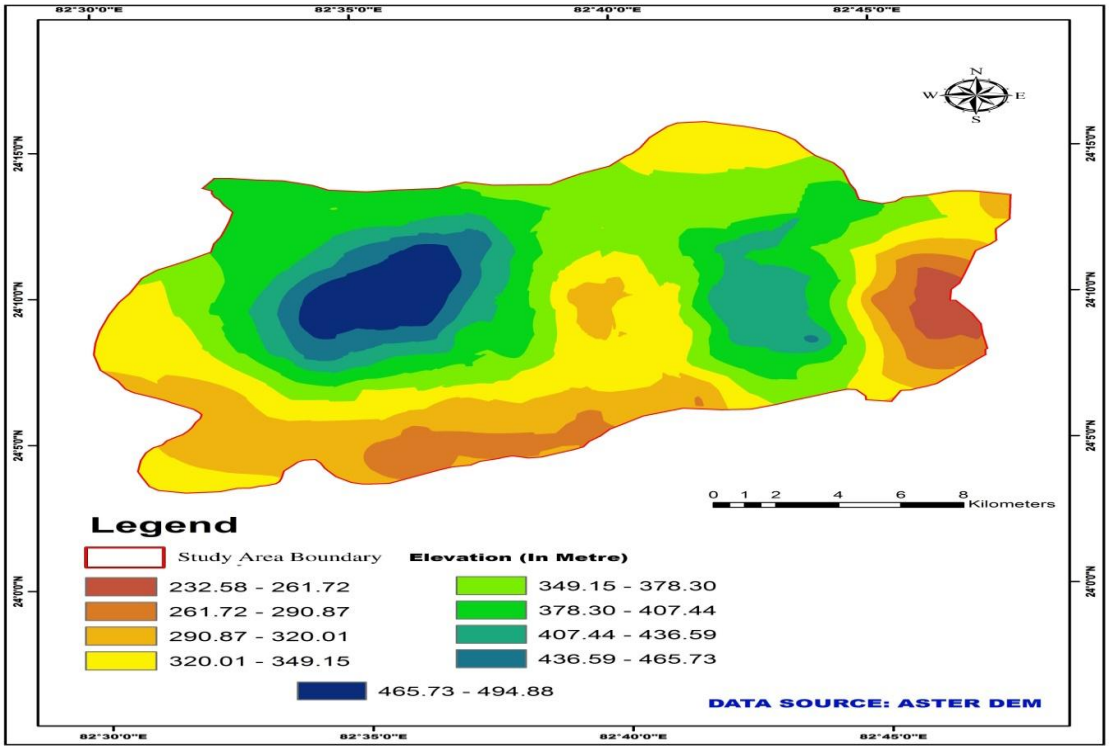

Figure 5.4 Elevation map of the study area

The recharge zone is the western higher plain (>350m) covered with forests and the discharge area is Govind Ballabh Pant Sagar located in the south-east (< 290m). The depth to water levels (>18 mbgl) during pre-monsoon are very high at few locations (DW-27,63 and 64), this may be due to the elevation at that point is very high so the internal flow of groundwater from higher to lower elevation areas.

5.2.2.3 GIS analysis of WLF under different geological formation

The geological formation is the most important factor for delineating the groundwater level fluctuation. In the study area, the geology consists of Barakar Formation, Mahadeva, Barren Measures, Metamorphics, Raniganj, Talchir formations and Igneous intrusive as shown in Fig 5.5.

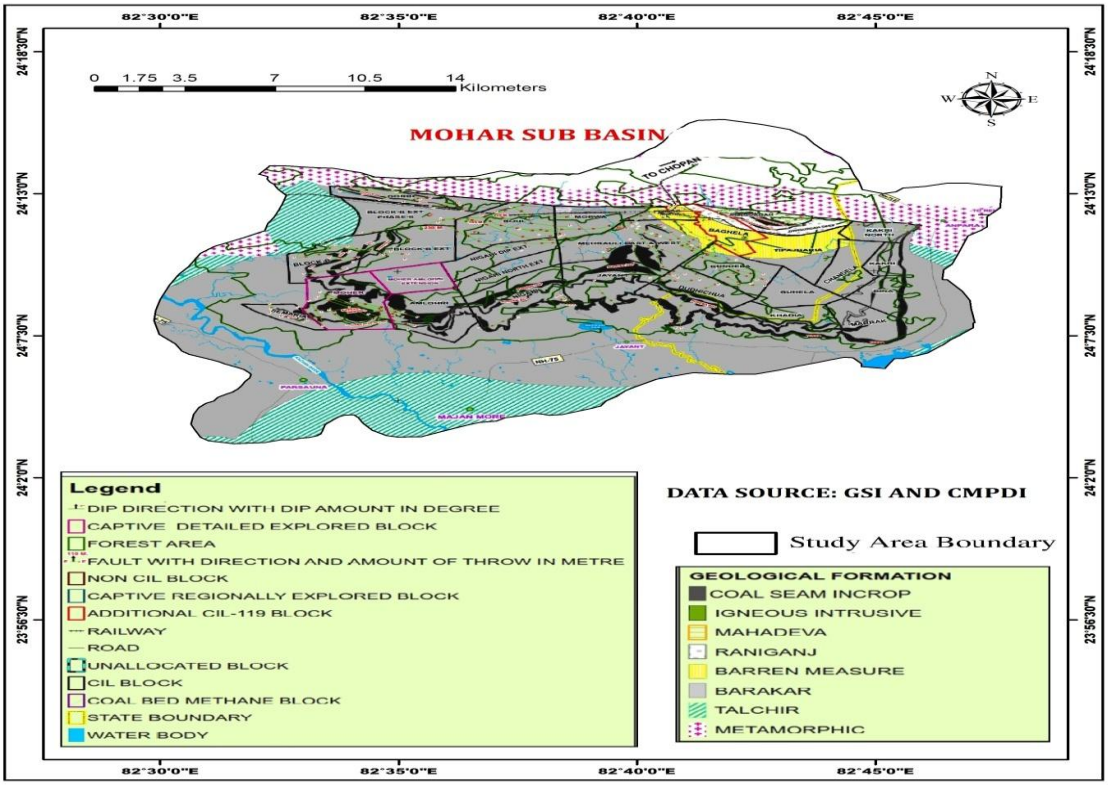

Figure 5.5 Geological map of the study area

Concerning WLF, it can be observed from WLF maps (Fig. 5.10) and geological maps (Fig. 5.5) that wells lie in Barakar Formation, Talchir Formation, Barren Measures and Raniganj formation show the higher value of WLF, while wells in the central, eastern side of Barakar formation and north-eastern side of metamorphic rock show lower WLF. This may be due to the lithological behaviour of the different geological formation. Such behaviour of WLF with respect to different geological formation can be explained on the basis of the stratigraphic sequence of Singrauli coalfield that has been tabulated in Table 3.1.

Geology of the coal seams present in Barakar formation is disturbed due to mining activities which affect the infiltration rate of rainwater to aquifers. The lithology of Barakar Formation consists of sandstone, siltstone, shale, carbonaceous shale and coal seams. Sandstone and siltstone have good water holding capacity of surface water. The

presence of coal seams in Barakar Formation at the central region of the study area, which affects the infiltration rate of rainwater to aquifers, therefore, minimum groundwater level fluctuation have shown at the central and eastern side of Barakar formation

The Talchir formation of comprised of sandstone, siltstone pebbly sandstone and boulder bed have also good water holding capability of surface water, therefore it shows maximum groundwater level fluctuation in these formations.

The Barren Mesures and Raniganj formation cover an area in the north-eastern part of the study area and both are disposed in a semi-circular pattern are shown in Fig. 5.5.The northern part of the study area is covered with metamorphic rock. In metamorphic, a very little amount of surface water infiltrates into the aquifer through secondary porosity like lineaments, cracks in rocks.

5.2.2.4 GIS analysis of WLF under drainage pattern

Drainage is one of the most important parameters for recharging of the aquifer in an area. This causes variation in the recharging of aquifer. In the drainage map of the study area, it can be seen that the dendritic drainage pattern of the study area. Which developed into the branches and trunk of the trees and indicates the homogeneity and uniformity in hydrogeological properties as shown in Fig. 5.6.

Five main perennial streams traverse through Singrauli are Kachan, Mayar, Motwani, Baliya Nala and Bijul. The perennial streams are Motwani and Balia Nala in the south and terminate into Govind Ballabh Pant Reservoir. The north-flowing streams join the Bijul River which is a tributary of Son. The south-flowing streams join the Kachan and Mayar, these two major rivers confluence near Tusa and terminate into Govind Ballabh Pant Reservoir. The streams which maintain the perennial flow in the study area are Mehrauli Nala in the north and Baliya Nala and Matwani Nala in the south.

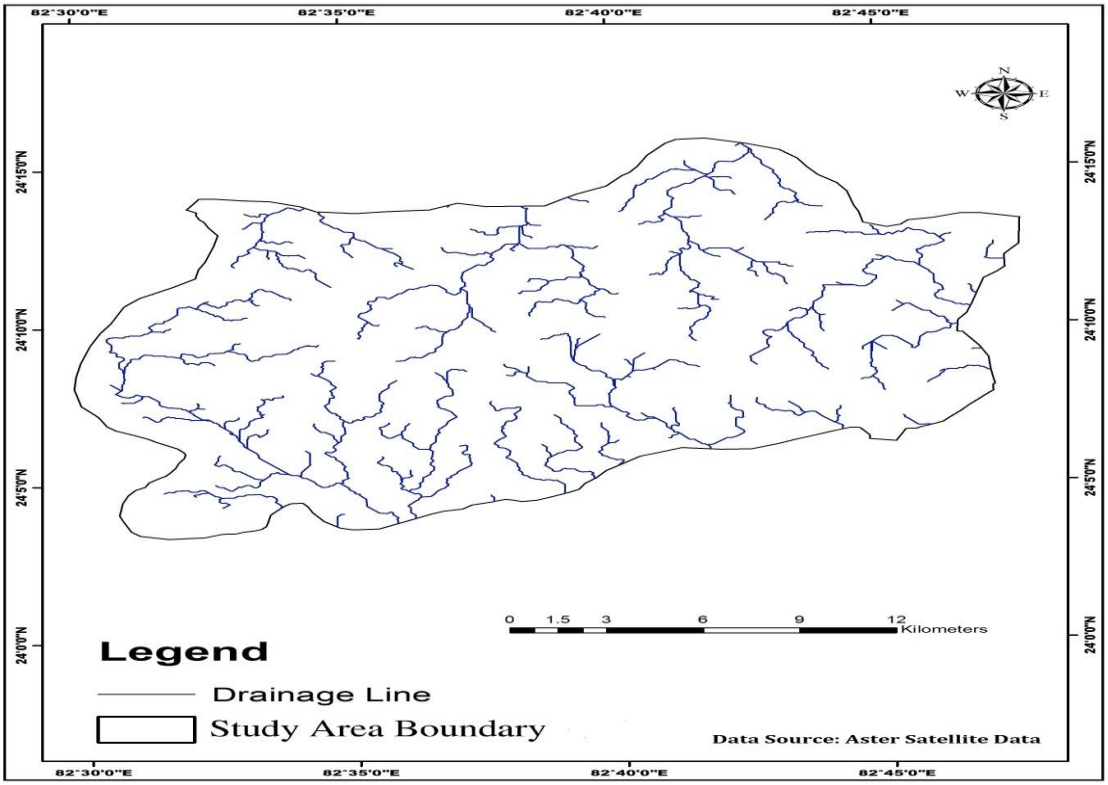

Figure 5.6 Drainage map of the study area

Streams with very high branching patterns usually spread runoff more evenly across the landscape, resulting in lower and usually slower discharges per stream segment whereas streams with low branching usually funnel water to few streams segments result in higher discharge (Tiwari et al., 2017). It can be observed from WLF map (Fig.5.10) and drainage map (Fig.5.6) that wells lie in high branching areas (south-west and north-east) show higher WLF values whereas the wells lie in low branching areas show lower WLF values, As it is known that as lower discharge rate in streams are considered as good recharge zone and areas having higher discharge rate in streams have lowers the recharge rate of aquifers.

5.2.2.5 GIS analysis of WLF under different soil classes

Soil is the most important factor for the depletion of groundwater level. The rates of water percolating through the soil are depending upon the soil texture and structure. In the study

area, there are eight types of soil present in the study area such as clay, silty-loamy, fine-loamy, loamy, coarse-loamy, sandy-clay, clay-loamy and sandy-loamy. The major part of the study area about 118.41 km^2 is covered by sandy clay soil, about 93.25 km^2 covered by sandy-loamy soil, about 57.25 km^2 covered by coarse-loamy and about 75.28 km^2 covered by loamy soil and the rest of the area is covered by clay, silty-loamy, fine-loamy, and clay-loamy soils as shown in Fig. 5.7. The soil layer were totally disturbed at the mining block regions (W-shaped) of the study area due to the expansion of coal mining activities so mining areas were not considered for these comparing analysis between water level fluctuation and soil.

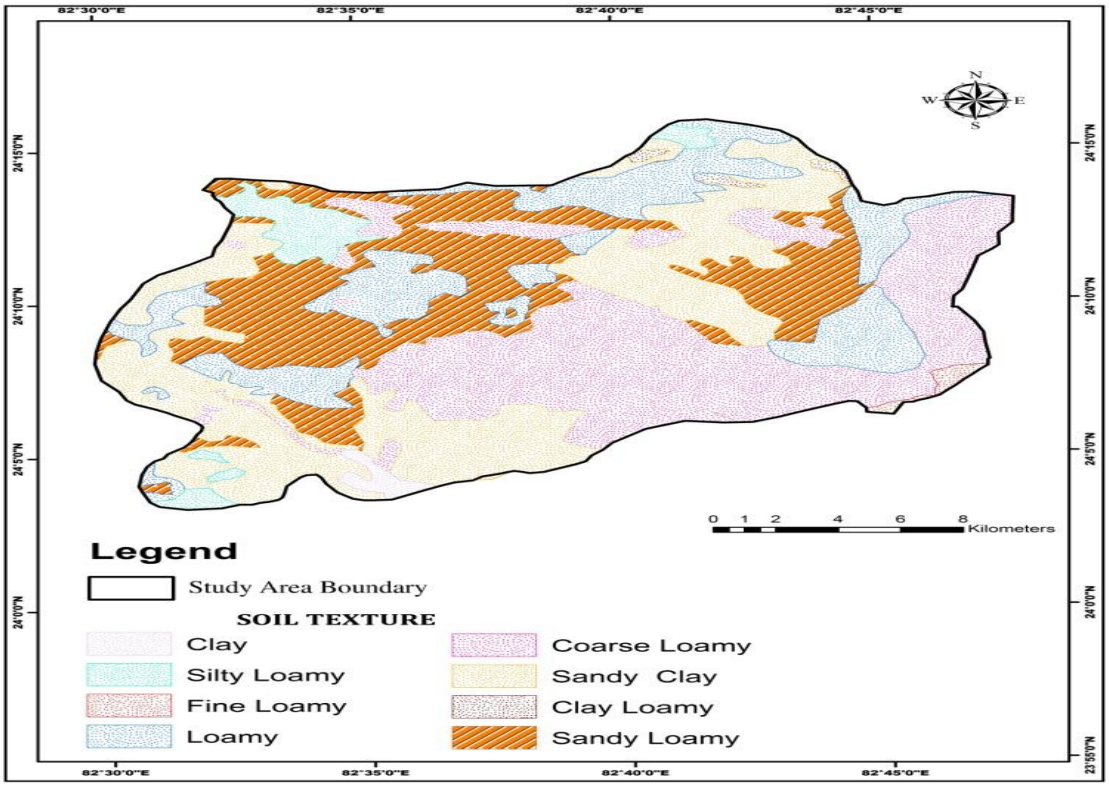

Figure 5.7 Soil map of the study area

Concerning water level fluctuation (WLF), it can be observed from the WLF map (Fig.5.10) and soil map (Fig.5.7) that wells lie in the sandy clay and some portion of silty loamy and sandy loamy soil show higher WLF whereas wells in coarse loamy soil show

lower WLF. Such Behaviour of water level fluctuation in the study area is associated with hydraulic properties such as hydraulic conductivity, Infiltration, porosity and physical properties of different soils.

Loamy, sandy-loamy, coarse loamy and silty loamy soils have higher porosity in the study areas whereas sandy clay, fine-loamy, clay, and clay loamy soils possess lower porosity. The coarse loamy soil possesses higher magnitude of hydraulic conductivity and porosity, it can be observed that wells lie in coarse loamy soil show lower value of water level fluctuation this may be due to the presence of high built-up areas occurred in these regions.

5.2.3 Depth to groundwater level during pre-monsoon

The groundwater levels around mining areas vary to a great extent from place to place. The spatial distribution of depth to the groundwater level during pre-monsoon in the study area is presented in Fig. 5.8.

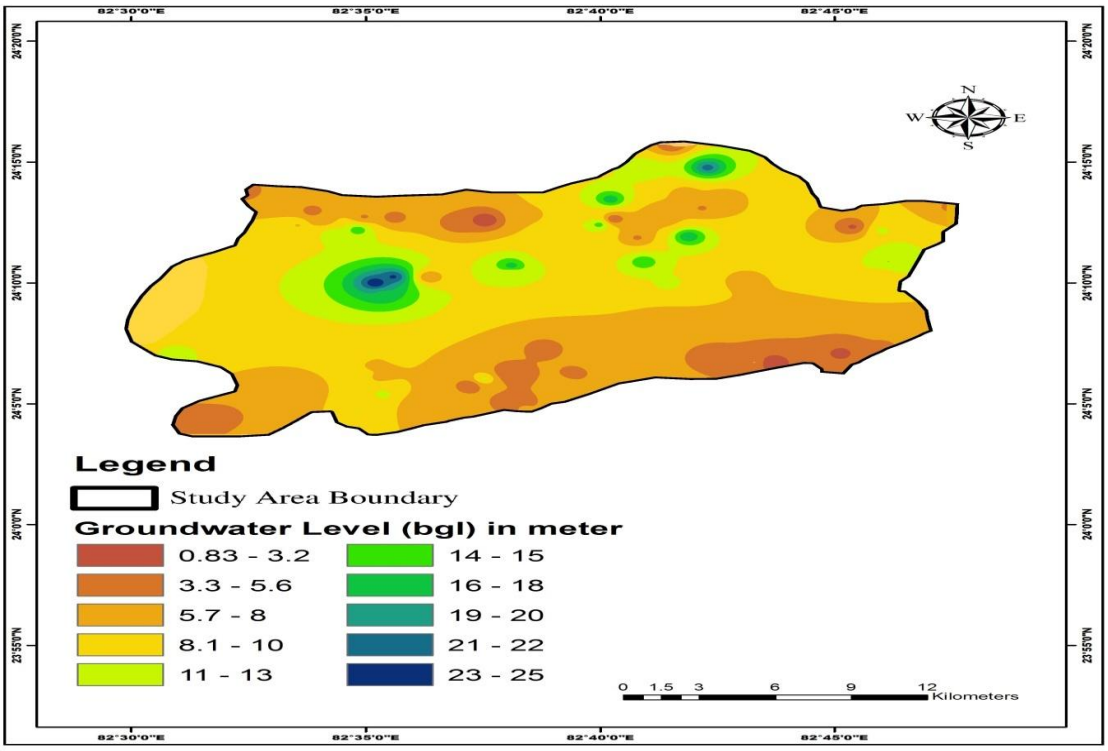

Figure 5.8 Groundwater level map during the pre-monsoon season

The depth to the water level in the study area varied between 0.83 and 25 meters below ground level (mbgl). The lower 0.83 to 5.6 (mbgl) depth to water level values were observed in the southern and upper portion of north-west regions of the study area. Medium 5.7 to 10 (mbgl) depth to water level values were observed in the central region and higher (>10 mbgl) depth to water level values were observed in the few places of the central and north-east portion of the study area. The depth to water level are observed is very high (>20 mbgl) at few locations such as Khadia Tola (490 m) and Mukhiya Tola (482 m), this may be due to the elevation at that point is very high.

5.2.4 Depth to groundwater level during post-monsoon

In the post-monsoon season, depth to water level had been recorded in November and data varied from 1 to 25 meters below ground level (mbgl). The variations of depth to water table were classified into ten classes are shown in Fig. 5.9.

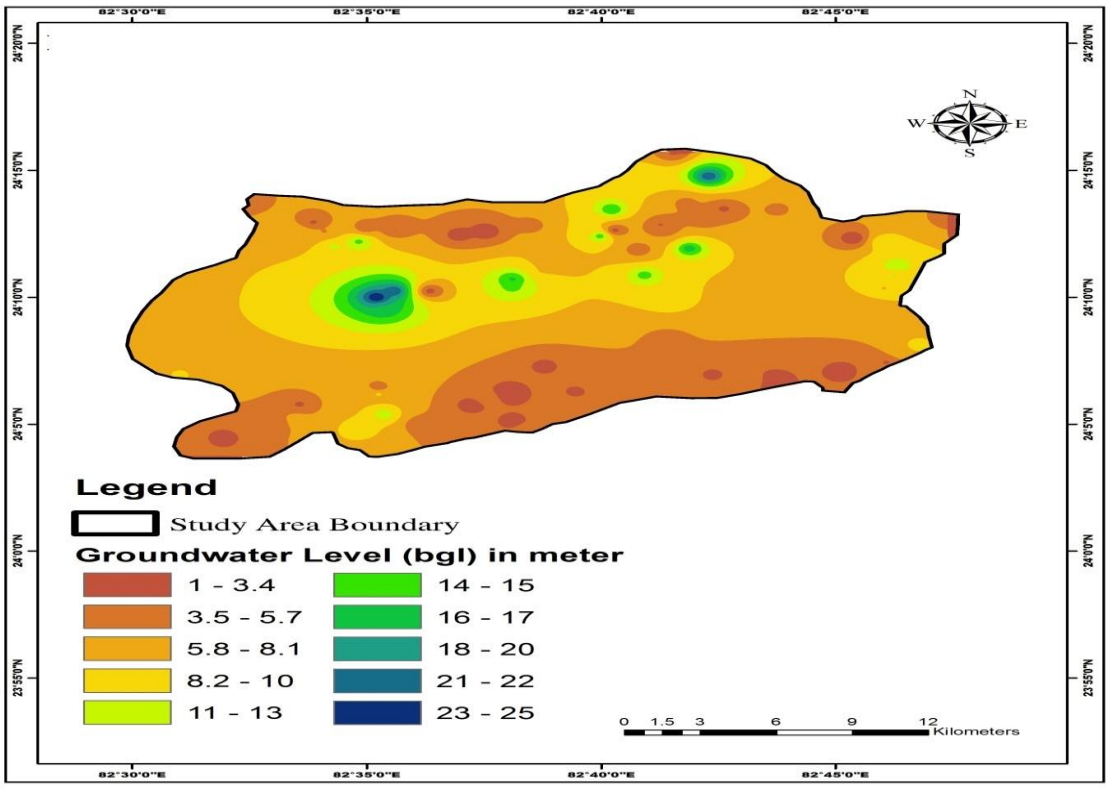

Figure 5.9 Groundwater level map during the post-monsoon season

The minimum depth to water level values ranges from1 to 5.7 (mbgl) were observed in the southern and few portions of northern regions. Medium 5.8 to 10 (mbgl) depth to water level values were observed in the eastern and central regions of the study area and higher (>10 mbgl) depth to water level values were observed in the few places of the central portion of the study area.

5.2.5 Water level fluctuation (WLF) of the study area

Comparative analysis has been done to assess the combined effect of the various hydrogeological factors on recharge of groundwater that has been discussed in the above section. The spatial distribution map and bar graph of water level fluctuations of groundwater in the study region is presented in Fig. 5.10 and Fig. 5.12.

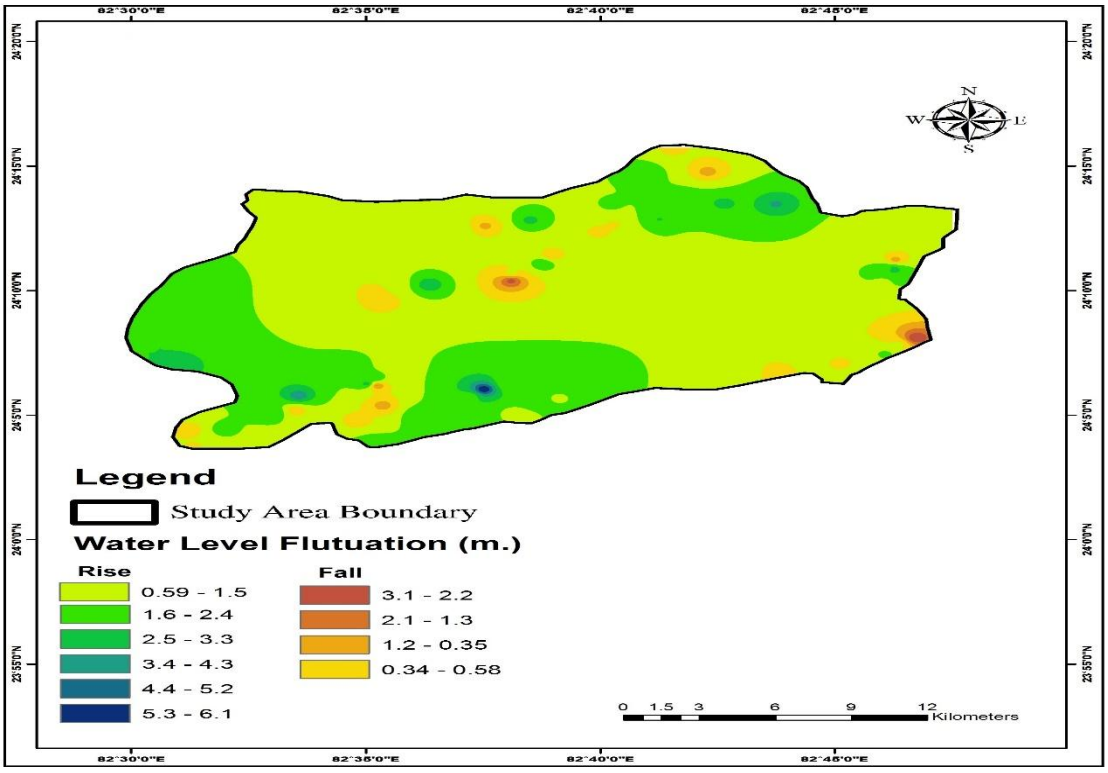

Figure 5.10 Groundwater level fluctuation map of the study area

Based on the measurements of eighty-six dug-wells, the variations of water level fluctuations was classified into two categories: (1) Rise (0.59m to 6.1m) (2) Fall (-0.58m

to -3.1m). From the fluctuation map, It has been found that the south-west and few portions of the north-east region of the study area have shown a higher level of WLF (>1.5m) whereas north-west, south-east and central areas have shown lower WLF (0.59m-1.5m).It can be observed from the WLF map, WLF showed negative values at the few locations (near Jayant mine block and NTPC plant) of the study area this may be due to the following reasons: (1) Presence of steep slope, higher elevation and man-made activities such as mining of coal. (2) Excessive draft of groundwater than the actual aquifer yield in the wells.

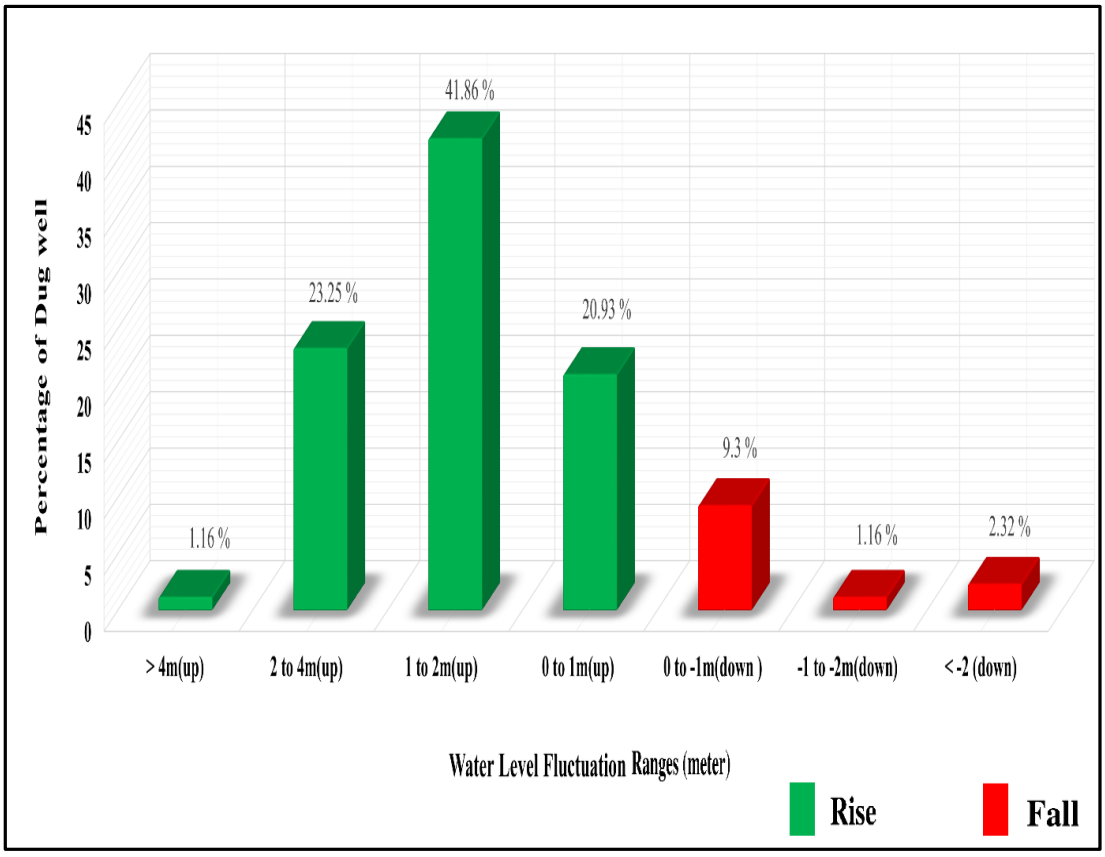

Figure 5.11 Graph showing WLF v/s Percentage of dug-wells of the study area

The WLF range of 1.6 m to 4.3 m was observed in large area. The maximum positive fluctuation indicates that the area is acting as recharge area whereas negative fluctuation indicates that the area is acting as discharge area.

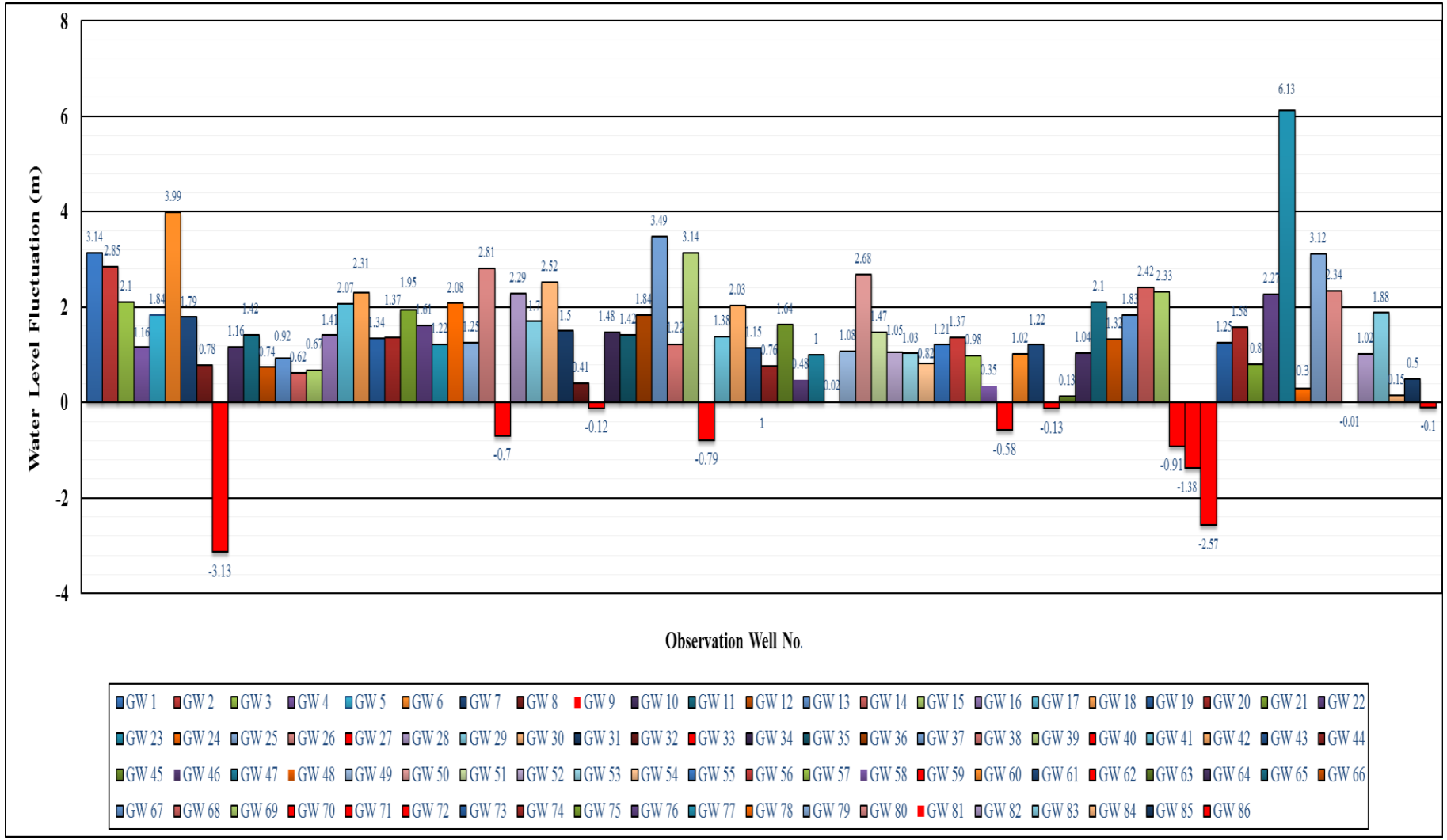

Figure 5.12 Bar graph showing WLF of dug wells

The WLF values play an important role in deciding the artificial recharge structure sites. The recharge areas are more suitable for the construction of rainwater harvesting structures as compared to discharge areas.

The graph plotted between WLF (in meter) and percentage of dug-wells of the study area are shown in Fig. 5.11. We can see that from this graph, the WLF had been categorized into two categories rise and fall based on their fluctuation values. On the basis of the graph, it has been found that the majority of dug-wells (41.86%) occur in the range of 1m to 2m (WLF).

5.3 Delineation of groundwater potential zones using remote sensing, GIS and MIF techniques

The Singrauli coalfield region in the state Madhya Pradesh and the adjoining southern part of the state of Uttar Pradesh (Sonebhadra District) and popularly known as ‘‘Energy Capital of India’’ It encompasses 11 opencast coal mines blocks and five coal based Thermal power Plants. The rapid population increase, excessive groundwater withdrawal for industrial purposes and expansion of coal mining activities are causing stress on the natural resources mainly the groundwater in this region. This activity resulted in significant changes in the land use pattern of the region, and the high-groundwater abstraction for getting fresh water has led to water crisis especially during the summer season when the groundwater levels become low.

The objective of this study is to delineation of groundwater potential zones using MIF, GIS and RS techniques. The results of this study should be helpful to the decision-makers in groundwater management and identifying suitable sites for artificial recharge in the study area.

5.3.1 Multi Influencing factors (MIF) of groundwater potential zones

Six influencing factors such as lineament, land-use, geology, drainage, slope, and soil have been used to delineation of groundwater potential zones. The interrelationship between these factors and their effect is shown in Fig.5.13. Each relationship is weighted according to its strength. The representative weight of a factor of the potential zone is the sum of all weights from each factor. A factor with a higher weight value shows a larger impact and a factor with a lower weight value shows a smaller impact on groundwater potential zones. The integration of these factors with their potential weights is computed through weighted overlay analysis in ArcGIS software.

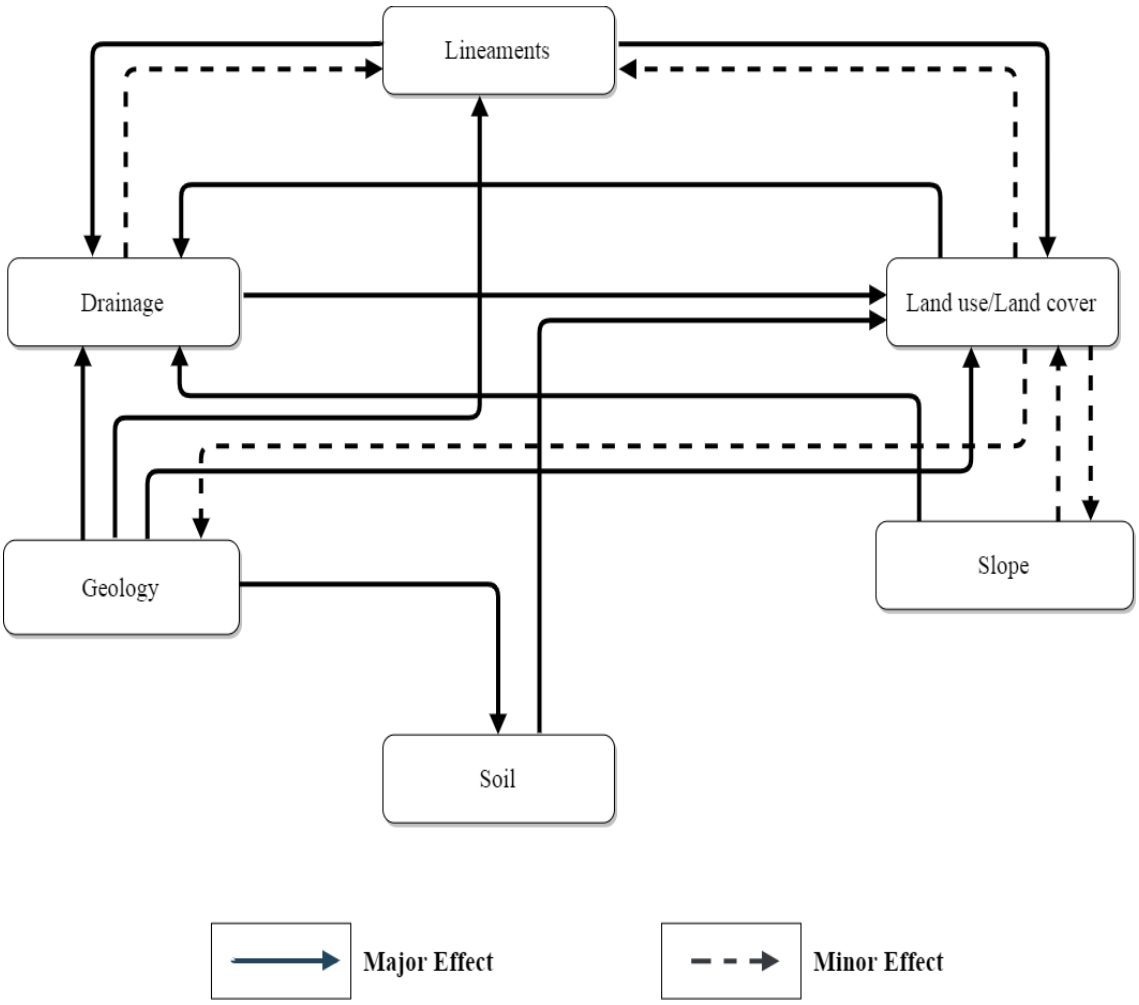

Figure 5.13 Interrelationship between the multi influencing factors concerning the groundwater potential zone

5.3.2 Assigning of weights

The multi influencing factors (MIF) for groundwater potential zones namely Geology, lineaments, land-use, drainage, slope, and soil were examined and assigned an appropriate weight are shown in Table 5.2. The effect of each influencing factor may contribute to delineate the groundwater potential zones. Moreover, these factors are interdependent. The weights of each factor were computed statistically using the multi-influencing factor (MIF) technique followed by heuristic approaches/knowledge-driven method for assigning ranks to each sub-classes of factor map. The interrelationship

among factors classes and assigning of ranks to factor's sub-classes was established based on author's expertise as well as literature review (Kaliraj et al. 2014; Senthil-Kumar and Shankar 2014; Dinesan et al. 2015; Razandi et al. 2015; Taheri et al. 2015; Taheri et al. 2016; Jothibasu and Anbazhagan 2016; Senanayake et al. 2016; Thapa et al. 2016; Zabihi et al.2016; Patra et al. 2018; Gnanachandrasamy et al. 2018).

Factors having major influence were marked as major effects and were assigned a weight of 1.0 whereas, the minor influence was marked as a minor effect with a weight of 0.5 (Magesh et al. 2012). Table 5.2 represents relative rates of each factor calculated by the cumulative sum of both major and minor effect followed by the proposed score calculation of each influencing factor using the formula as follows:

$$\text{Proposed Score} = \left[\frac{(X+Y)}{\sum(X+Y)}\right] \times 100 \qquad (5.1)$$

Where X represents the major effect of factors and Y represents the minor effect of factors. Table 5.3 shows the assigned weightage and domain effect of the thematic layers.

Table 5.2 Effect of influencing factor, relative rates and score for each potential factor.

Factor	**Major effect (X)**	**Minor effect (Y)**	**Proposed relative Rates (X+Y)**	**Proposed score of each influencing factor**
LULC	1	0.5+0.5+0.5	2.5	20
Lineament	1+1	0	2	16
Drainage	1	0.5	1.5	12
Slope	1	0.5	1.5	12
Soil	1	0	1	8
Geology	1+1+1+1	0	4	32
			∑12.5	∑100

Table 5.3 Weightage assigned to each factor based on their effect on the GWPZ

Factor	Domain of effect	Weightage
LULC	Water body	20
	Crop Land	16
	Forest Area	14
	Fallow Land	9
	Mining Area	4
	Built-up Area	3
Lineament Density	0-0.23	1
	0.24-0.65	6
	0.66-1.16	11
	1.17-2.43	16
Drainage Density	0-0.34	12
	0.35.0.85	9
	0.86-1.41	6
	1.42-2.92	3
Slope	0-4.24	12
	4.25-14.03	9
	14.04-39.16	6
	> 39.16	3
Soil	Coarse Loamy	8
	Sandy Loamy	7
	Loamy	6
	Silt Loamy	5
	Fine Loamy	4
	Sandy Clay	3
	Clay Loamy	2
	Clay	1
Geology	Barakar	32
	Talchir	26
	Barren Measure	22
	Raniganj	16
	Mahadeva	10
	Metamorphic	7
	Igneous Intrusive	5
	Coal Seam Incrop	3

5.3.3 Weighted Overlay Method

Weighted overlay analysis was used to explore the groundwater potential zones in the study region. After assigning weights and ranks to factors and their subclasses, all the inputs were integrated through a weighted overlay method by using the following equation.

$$GWPZ= \sum_{i}^{n} LULC_x\, LULC_y + S_xS_y + DD_xDD_y + Sl_xSl_y + LD_xLD_y + G_xG_y \qquad (5.2)$$

Where 'y' represents the feature rank within a layer, and 'x' represents the layer weight calculated using MIF method. S is soil, G represents Geology, LULC is land use land cover, LD is lineament density, DD is drainage density and Sl is the slope.

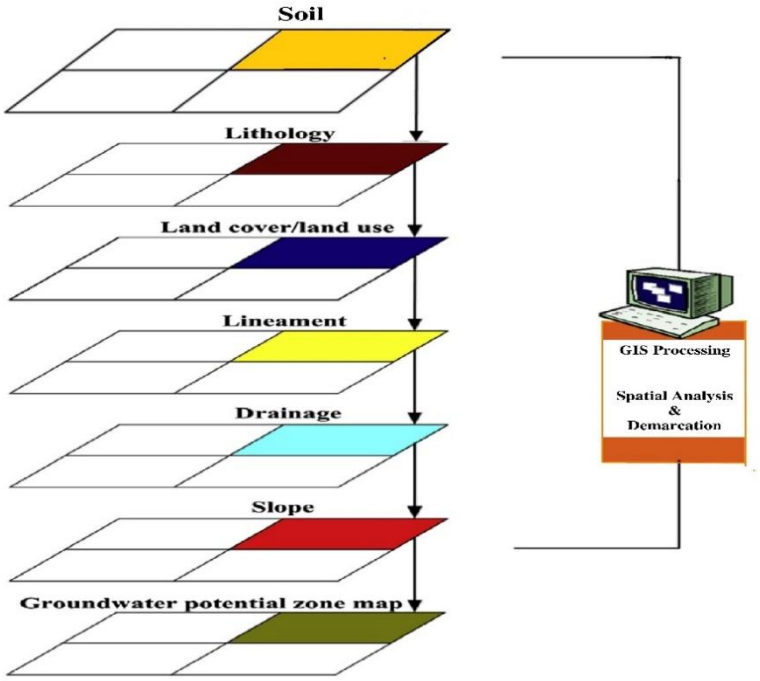

Figure 5.14 GIS techniques used for groundwater potential zone

After computed the final weights of all the thematic layers and their individual features, all the thematic layers were converted into raster format and added with one another using a Raster calculator in ArcGIS software to delineate groundwater potential zone.

5.3.4 Hydrologic Thematic Layers

In this study, six influencing factors, such as land use/land cover, lineament density, drainage density, slope, geological and soil, which influence the potentiality of groundwater availability has been studied individually as well as combined using GIS software to prepare the map of groundwater potential zones. All the parameters considered in this study are discussed below.

5.3.4.1 Land use /land cover (LULC)

Land use/land cover is an important factor of groundwater recharge (Shaban et al., 2006; Kaliraj et al., 2014; Ghosh et al., 2016).Accurate and reliable information about the present and future LULC will help in management of resources (Singh et al., 2014; Singh et al., 2015; Singh et al., 2018b).

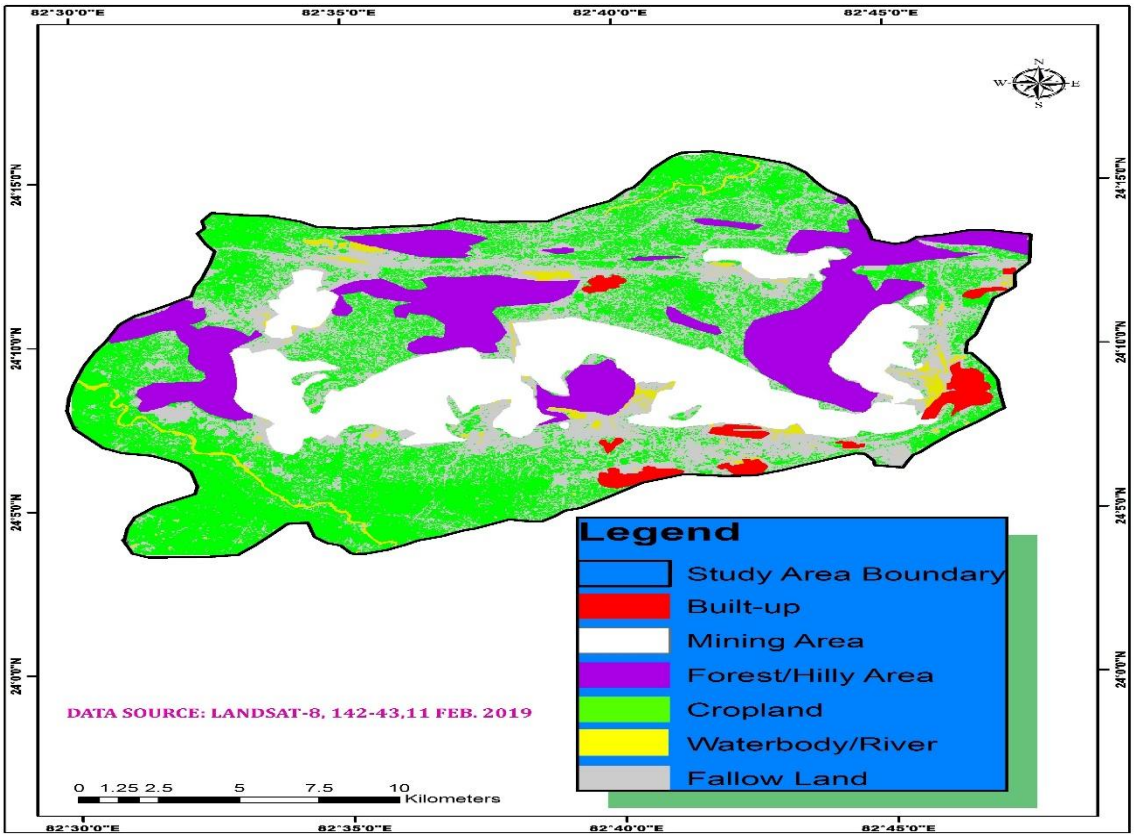

Figure 5.15 Land use/land cover (LULC) map of the study area

The major land-use (2019) type of study area are cropland, fallow land, open cast mining areas, forest land, build-up area and water bodies occupying area of 149.88 km^2 (33.51%), 117.70 km^2 (26.43%), 88.53 km^2 (19.88%), 71.82 km^2 (16.13%), 9.24 km^2 (2.07%) and 8.01 km^2 (1.79%), respectively (Fig. 5.15). Water bodies and agricultural land were given the highest ranking over other LULC features because of their continuous recharge to ground (Srivastava and Bhattacharya, 2006), whereas highly built-up areas experience less infiltration rate due to the concretization of the surface. The mining activities have disturbed aquifer geometry which results decrease in groundwater potential of the study area.

5.3.4.2 Lineament density

Lineaments represent the zones of faulting, fracturing, joints, and dykes resulting in increased secondary porosity and permeability. These factors are hydro-geologically very important as they provide the pathways for groundwater movement. Lineament density of an area can indirectly reveal the groundwater potential since the presence of lineaments usually denotes a permeable zone. Areas with higher lineament density are good for groundwater potential zones (Haridas et al., 1998).Lineament density of the study area was calculated by using the following expression:

$$L_d = \sum_{i=0}^{n} Li / A \quad (5.3)$$

Where, L_d is lineament density, L_i is the total length of all lineaments (km) and A is the area of the grid (km^2).

The lineament density map of the study area is shown in Fig. 5.16, and it reveals that high lineament density is observed in the center and Northern region of the study area with a value ranging from 0 to 2.43 km/km^2.The highest ranking was assigned to the highest lineament density interval.

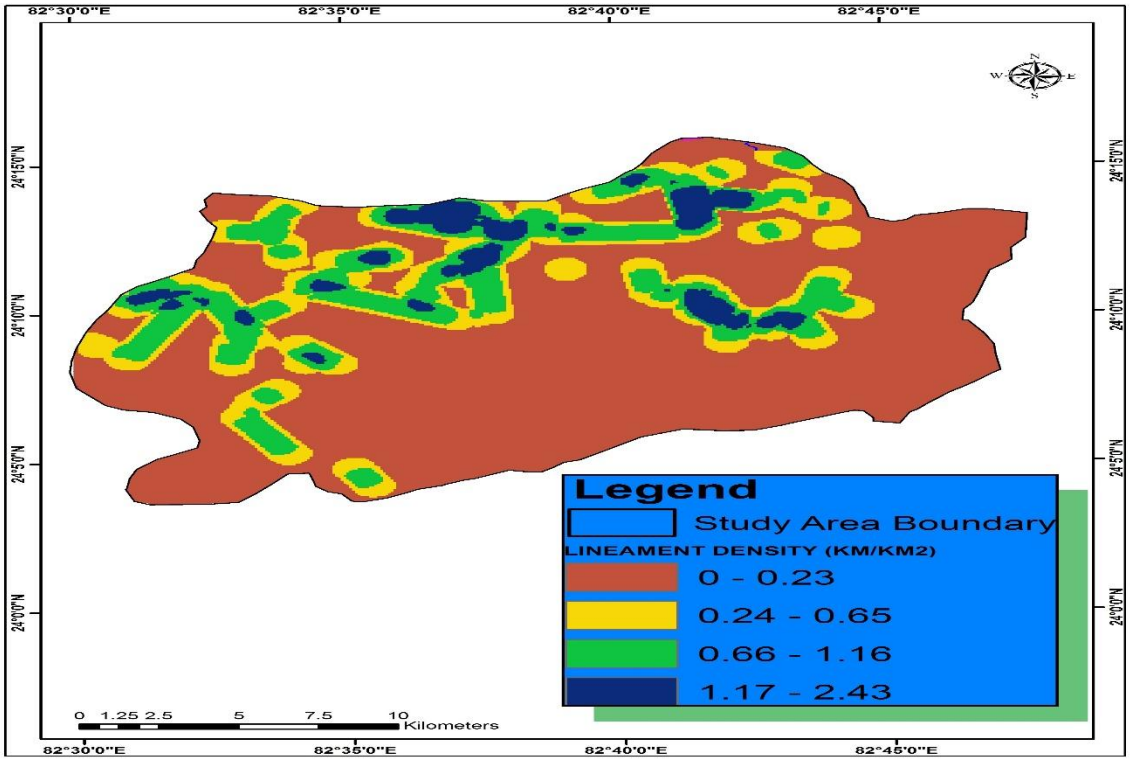

Figure 5.16 Lineament density map of the study area

5.3.4.3 Drainage density

Drainage density is defined as the closeness of the spacing of stream channels. It is a measure of the total length of the stream segment of all orders per unit area. The suitability of groundwater potential zones are indirectly related to drainage density because of its relation with surface runoff and permeability. The less permeable rock is, the less the infiltration of rainfall, which conversely tends to be concentrated in surface runoff (N.S. Magesh et al. 2012).The drainage density of the study area is calculated using the line density analysis tool in ArcGIS software. The drainage density was calculated by using the following equation:

$$D_d = \frac{\sum_{i=0}^{n}(Di)}{A} \tag{5.4}$$

Where D_d is drainage density (km/km^2), Di is the total length of streams and A is an area of a grid (km^2).

The study area has been grouped into four classes are shown in Fig. 5.17. These classes have been assigned to 'very good' (1.42-2.92 km/km^2), 'good' (0.86-1.42 km/km^2), 'poor' (0.35-0.85 km/km^2) and 'very poor' (0-0.34 km/km^2) respectively. Drainage density is inversely related to the soil infiltration capacity; high weight is given to low density, and high density is assigned less weight.

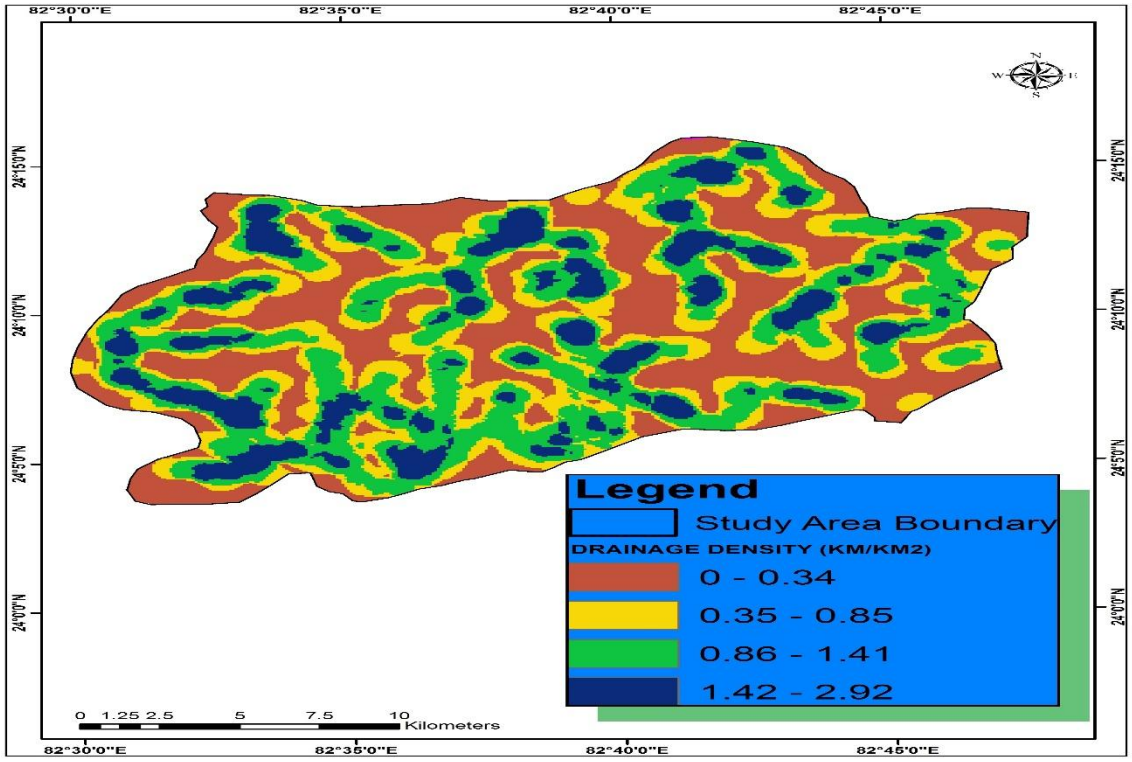

Figure 5.17 Drainage density map of the study area

5.3.4.4 Slope

The slope is the most significant factor for the identification of groundwater potential zones. Discussion of the slope with respect to water level fluctuation clearly shows that there is a direct positive relation of the slope with the water table in the terrain of singrauli coalfield. The higher degree of slope results in rapid runoff and increased erosion rate with feeble recharge potential (Magesh et al., 2011a, b). The infiltration of surface water is directly influenced by the slope gradient. Steep slopes result in rapid downward water

flow resulting from insufficient time to infiltrate. Flat areas provide higher retention time for the infiltration of rainwater (Thapa, Raju, et al 2017).

On the basis of slope angle, the entire study area is divided into four sub-classes. The areas having 0-4.24° slope fall into the 'very good' category because of the nearly flat terrain and relatively high infiltration rate. The areas with 4.25°-14.03° slope are considered as 'good' for groundwater storage due to slightly undulating topography with some runoff. The areas having a slope of 14.04°-39.16° cause relatively high runoff and low infiltration, and hence are categorized as 'poor' and the areas having a slope >39.16° are considered as 'very poor' due to higher slope and runoff. Fig. 5.3 illustrates the slope map of the study area. The ranks were assigned based on the degree of slope. Higher ranks was assigned to lower degree slope classes that would allow more groundwater retention and lesser runoff due to the flat terrain. While lesser ranks was assigned to steeper slopes because of more run-off and less infiltration (Nag & Ghosh 2013).

5.3.4.5 Geology

The geology is one of the significant factor for the detection of groundwater prospective zones. The study area mainly covered by seven types of geological formation namely, Barakar Formation, Mahadeva, Barren Measures, Metamorphics, Raniganj, Talchir formations and Igneous intrusive as shown in Fig. 5.5. On the basis of WLF study, the maximum water level fluctuation are shown by the wells associated with Barakar & Talchir formation areas, this may due to lithological behaviour as well as anthropogenic activities. The general stratigraphy of the singrauli coalfield is given in Table 3.1 (Chapter 3).

Rank has been assigned to different features based on the available porosity. Sandstone have much higher porosity; hence have higher groundwater prospect. Shale has compact

structure, hence given the lowest rank. Shale is formed due to rock compaction and is typically deposited in very slow-moving water. Rocks have classified based on available porosity as sandstone, boulder beds, laterite, basalt, schist, gneiss, granite, and granulite where sandstone represents high porosity. Whereas metamorphic rocks and coal seams represent very less to nil porosity.

5.3.4.6 Soil

Soil is an important factor for delineating the groundwater potential zones of the study area. The permeability of the soil is directly related to the effective porosity of the soil and is greatly influenced by grains shape, size grains, adsorbed water, voids ratio, the degree of saturation and impurities present (Punmia et al.2005). The analysis of the soil type reveals that the study area is covered with eight different soil types (Fig. 5.7) namely, Coarse loamy, sandy loamy, loamy, silty-loamy, fine-loamy, sandy-clay, clay-loamy and clay soils. Ranks have been subjective to each soil unit after taking into account the types of soil and their infiltration rate. The coarse loamy and sandy loamy soil has a higher infiltration rate hence it has given the highest rank while clay loamy and clay soil has a least infiltration rate assigned to low priority.

5.3.5 Ground water potential zone map of the study area

The groundwater potential zones for the study area were generated through the integration of various thematic maps such as lineament, land-use, Geology, drainage, slope, and soil using remote sensing and GIS techniques. The delineation of groundwater potential zones for the study area was made by grouping of the interpreted layers through weighted multi influencing factor and finally assigned different potential zones. The groundwater potential zone of this study area can be divided into four grades, namely very good, good, poor, and very poor are shown in Figure 5.18.

It has been found that very good to good groundwater potential occurs in the plains as it includes cropland, gentle to moderate slope, Talchir and Barakar formation and pediplains. Land use, geology and slope have played a significant role in the very good groundwater potential zone. Poor to very poor groundwater potential was found out in the mining area and forest/hilly area with steep slope, metamorphic, coal seam and built-up area. Infiltration of this area is very low due to rapid runoff with steep slopes and built-up area that were reducing recharge of the water into the subsurface.

A comparative analysis was done by comparing the groundwater level fluctuation map (Fig.5.10) with the groundwater potential zone map (Fig.5.18). After comparing it was found that the maximum water level fluctuation area (south-west, north-west and north-east) shows very good groundwater potential zone whereas the lowest water level fluctuation area shows poor groundwater potential zone.

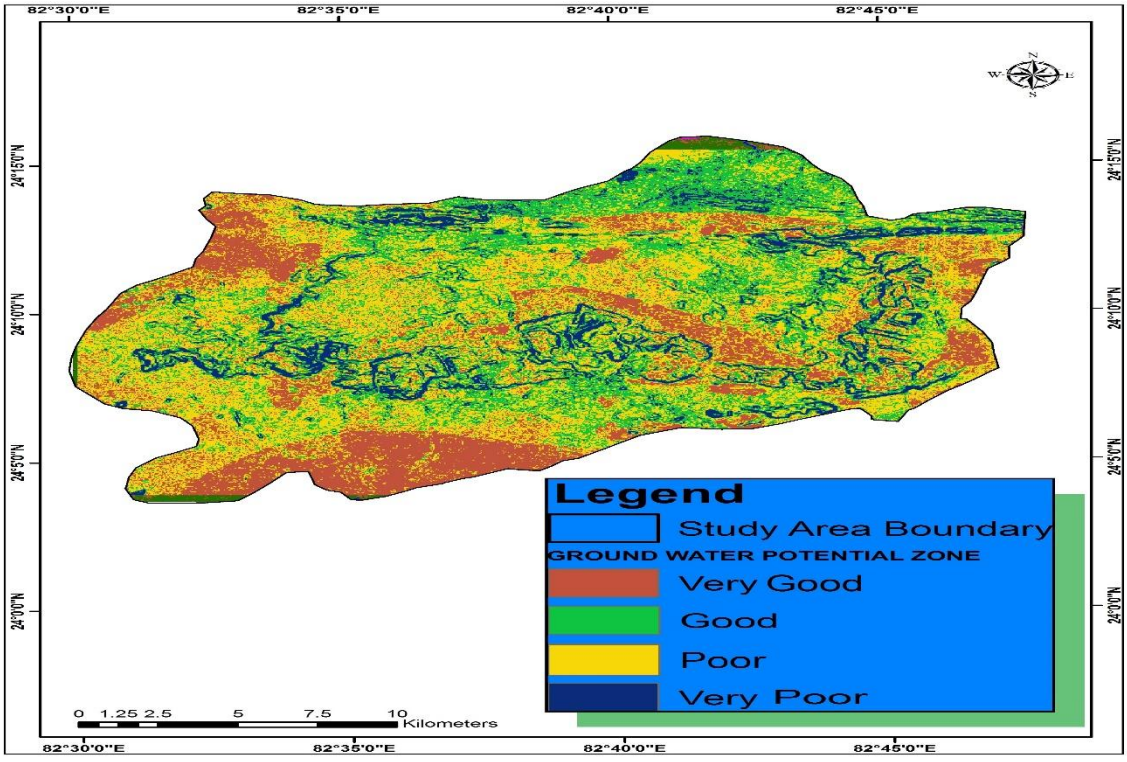

Figure 5.18 Groundwater potential zone map of the study area

5.4 Qualitative Assessment of Groundwater

Groundwater plays major life support to mankind. It is the major source to meet the domestic, irrigation and industrial water demands (Magesh et al. 2011).Groundwater chemistry of the study region having complex contamination. A total of forty-six (46) groundwater samples around different mining projects (NCL) were collected from hand pumps during the summer month of May, 2018 (Fig. 5.19 & Table 5.4) and analyzed for thirteen major physicochemical parameters (pH, EC, TDS, Total Hardness, Bicarbonate, Cl^-, F^-, NO_3^-, SO_4^{2-}, Ca^{2+}, Na^+, Mg^{2+}, K^+) and seven heavy metals (Fe, Cu, Pb, Cd, Cr, Ni, Zn). The collected water samples were analyzed to assess suitability for domestic and irrigation purposes.

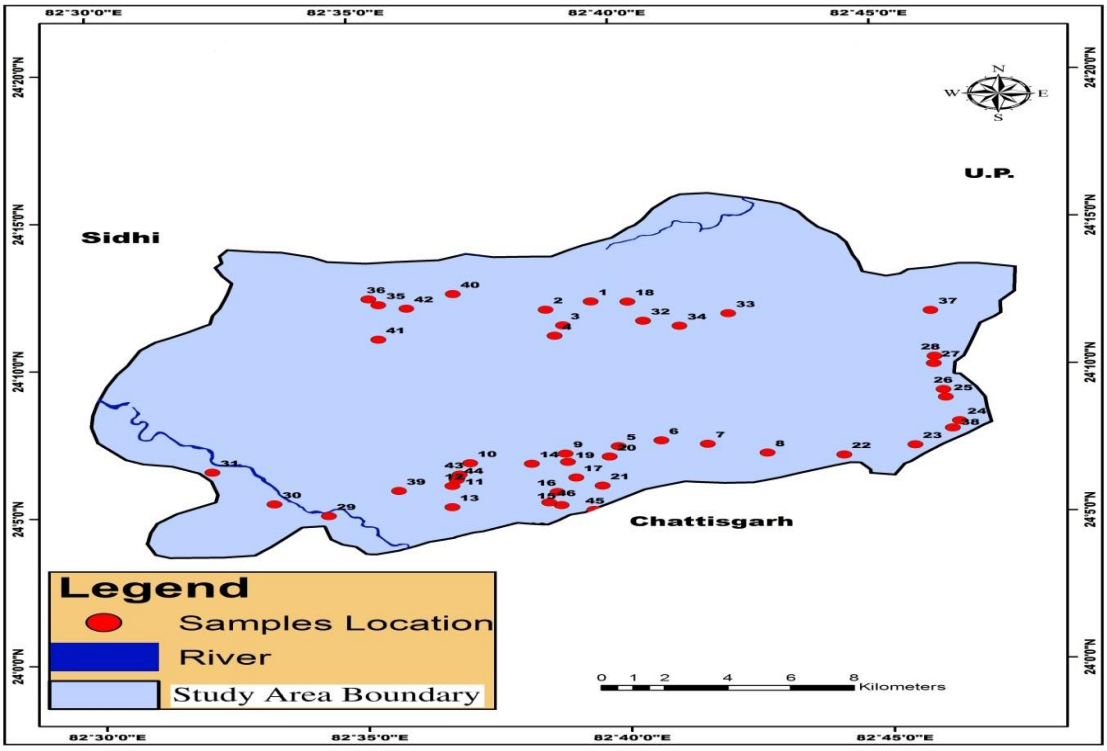

Figure 5.19 Location map of groundwater sampling stations

The groundwater samples were collected in one liter narrow-mouth pre-washed polyethylene bottles. Suspended sediments were eliminated from the groundwater samples in the laboratory by using 0.22 µm Nylon syringe filters.

Table 5.4 Details of sampling stations of the groundwater samples

Sample Code	Sampling Location	Latitude (N)	Longitude (E)
GW 1	Near Black Diamond Filling Station	24º12'13"	82º39'30"
GW 2	Shukla Mod	24º11'57"	82º38'38"
GW 3	Old Ganesh Temple	24º11'25"	82º38'57"
GW 4	Near Rewa Tower	24º11'04"	82º38'47"
GW 5	Near UP/MP Border	24º07'18"	82º39'56"
GW 6	Ambedkar Nagar	24º07'29"	82º40'45"
GW 7	Shakti Nagar Sabji Mandi	24º07'21"	82º41'38"
GW 8	Sarvottam Automobiles & Works	24º07'02"	82º42'46"
GW 9	Bharat Gas Godown	24º07'04"	82º38'55"
GW 10	Near Sangam Auto Mobile	24º06'46"	82º37'05"
GW 11	NawaNagar	24º06'16"	82º36'50"
GW 12	Near Gupta Misthan Bhandaar	24º06'00"	82º36'44"
GW 13	Arvind Kumar shah Gandhi chauraha	24º05'17"	82º36'43"
GW 14	CMPDI	24º06'44"	82º38'16"
GW 15	Near Saraswati Shishu Mandir School	24º05'19"	82º38'48"
GW 16	Vindhyanagar	24º05'46"	82º38'44"
GW 17	Near Dudhichua Ground	24º06'15"	82º39'06"
GW 18	Divisional Forest Office Gorbi	24º12'00"	82º40'12"
GW 19	Indira Guest House	24º06'47"	82º38'57"
GW 20	Gol Market	24º06'57"	82º39'45"
GW 21	Near Coal Mines Association NCL	24º07'02"	82º39'36"
GW 22	Agrawal Market	24º06'56"	82º44'13"
GW 23	Near Yogichaura post office	24º07'15"	82º45'35"
GW 24	Near Pradip Restaurant Koharaul	24º08'03"	82º46'27"
GW 25	Near Police Chowki Beena	24º08'52"	82º46'12"
GW 26	Near Arya Samaj Mandir	24º09'08"	82º46'10"
GW 27	Bansi	24º10'0.8"	82º46'0.4"
GW 28	Bansi	24º10'15"	82º46'1.3"
GW 29	Naugarh	24º05'01"	82º34'21"
GW 30	Parsauna	24º05'26"	82º33'19"
GW 31	Naugai	24º06'31"	82º32'10"
GW 32	Near Domestic GAS Station	24º11'32"	82º40'29"
GW 33	Jhingurda Post Office	24º11'46"	82º42'6.9"
GW 34	Ambedkar Nagar	24º11'21"	82º41'10"
GW 35	NCL Gorbi Stadium	24º12'09"	82º35'26"
GW 36	Rajarshi Secondary School, Gorbi	24º12'21"	82º35'15"
GW 37	Anpara	24º11'48"	82º45'58"
GW 38	Kahroul	24º07'49"	82º46'19"
GW 39	Amlori	24º05'51"	82º35'42"
GW 40	Near IOCL Pump	24º12'30"	82º36'52"
GW 41	-------	24º10'59"	82º35'25"
GW 42	-------	24º12'02"	82º35'58"
GW 43	NawaNagar	24º06'23"	82º36'53"
GW 44	NawaNagar	24º06'12"	82º36'49"
GW45	Vindhyanagar	24º05'02"	82º39'28"
GW46	Near Shahpur Post office	24º05'25"	82º38'34"

The concentration of major ions and heavy metals of groundwater samples were estimated at the Department of Mining Engineering, Central Instrumental Facility (CIF) Centre of IIT (BHU) and Interdisciplinary School of Life Sciences (ISLS) BHU. The summarised result is given in Appendix A.2.

5.4.1 Characteristics of physicochemical parameters and heavy metals along with spatial distribution maps

The physicochemical and heavy metals of the analytical results of groundwater were compared with the standard guidelines values recommended by the WHO (2011) are tabulated in Table 5.5 and ArcGIS mapping technique was adopted to prepare the spatial distribution map of major ions and heavy metals.

Table 5.5 Statistical summary of physicochemical parameters and heavy metals and its comparison with WHO (2011) Standards.

Parameters	Minimum	Maximum	AM	Median	SD	WHO (2011)
pH	6.69	7.92	7.47	7.58	0.31	6.5-8.5
EC	50	1331	584.8	547	261.38	1400
TDS	25	667	293.33	276	130.62	500
Total Hardness	16.308	540.29	199.69	192.59	99.57	500
Bicarbonate(HCO_3)	16.57	241.20	92.4	84.94	46.09	200
Fluoride (F)	0.27	1.79	0.64	0.54	0.38	1.5
Chloride (Cl)	2.181	444.92	58.55	33.48	76.93	250
Nitrate (NO_3)	0.48	144.84	14.66	6.29	24.7	45
Sulphate (SO_4)	0.6	212.80	47.1	33.5	46.91	150
Sodium (Na)	4	192.09	43.21	32.28	38.27	50
Potassium (K)	0.256	20.756	4.63	2.72	5.64	15
Magnesium (Mg)	1.168	61.504	20.33	18.44	14.68	50
Calcium (Ca)	4.608	118.085	46.54	45.12	27.04	75
Iron (Fe)	0.71	1.48	1.02	0.93	0.21	1
Copper (Cu)	1.107	1.674	1.30	1.29	0.13	1.5
Lead (Pb)	0.105	0.325	0.16	0.14	0.05	0.15
Cadmium (Cd)	0.012	0.198	0.084	0.073	0.055	0.1
Chromium (Cr)	0.001	0.061	0.0108	0.008	0.01	0.0122
Nickel (Ni)	0.092	0.294	0.182	0.1725	0.0592	0.2
Zinc (Zn)	1.397	5.318	3.204	3.24	1.1099	5

5.4.1.1 pH and Electrical Conductivity (EC)

pH is a measure of the Hydrogen ion (H^+) concentration, which determines the acidic or basic quality of water solution. At 25ºC, when pH<7, a water solution is acidic, when pH =7, a water solution is neutral, when pH>7, a water solution is basic.

$$pH = - \log [H^+] \quad (5.5)$$

According to WHO guidelines, drinking water should have a pH range of 6.5–8.5 and values out of this range would impair the Potability of water. The observed pH values of the groundwater varied from 6.69 to 7.92 with a mean value of 7.46 which indicates that groundwater is slightly acidic to alkaline in nature.

The Electrical Conductivity (EC) content represents the concentrations of ionized elements contained in water. The concentration of EC values range between 50 to 1331 μs/cm and mean 584.80 μs/cm in groundwater of the study area.

5.4.1.2 Total Dissolved Solid (TDS)

The TDS in water includes all dissolved material in solution, whether ionized or not, it does not include suspended sediments, colloids, and dissolved gases. TDS is the numerical sum of all mineral constituents dissolved in water and is expressed in mg/l. The values of TDS (mg/l) ranges from 25–667 and mean 293.32. Since the groundwater of the study area lies under freshwater class and the TDS values for all water samples are below 1000 mg/l, it may be used for drinking and irrigation purposes (Davis and De Weist 1966).

5.4.1.3 Bicarbonate (HCO_3^-)

Bicarbonate determines the alkalinity of freshwater. Natural processes, such as the dissolution of carbonate minerals and dissolution of the atmospheric and soil CO_2 could

be the source of Bicarbonate in the groundwater (Jeong 2001). The bicarbonate hazard is generally described in terms of RSC. The residual sodium carbonate (RSC) is a valuable parameter that has a significant effect on the suitability of water for irrigation uses (Adhikary et al. 2011). Excessive amounts of bicarbonate in irrigation water affect plants and agricultural soil physically and chemically, thus reducing productivity. Bicarbonate concentration in the groundwater samples of the study area ranges from 16.57 to 241.20 mg/l.

5.4.1.4 Chloride (Cl^-)

The concentration of Chloride in surface and groundwater from both natural and anthropogenic sources, such as run-off containing road de-icing salts, the use of inorganic fertilizers, landfill leachates, septic tank effluents, animal feeds, industrial effluents, irrigation drainage, and seawater intrusion in coastal areas. Chlorides are leached from various rocks into soil and water by weathering. (CDWQ, Canada 1978).

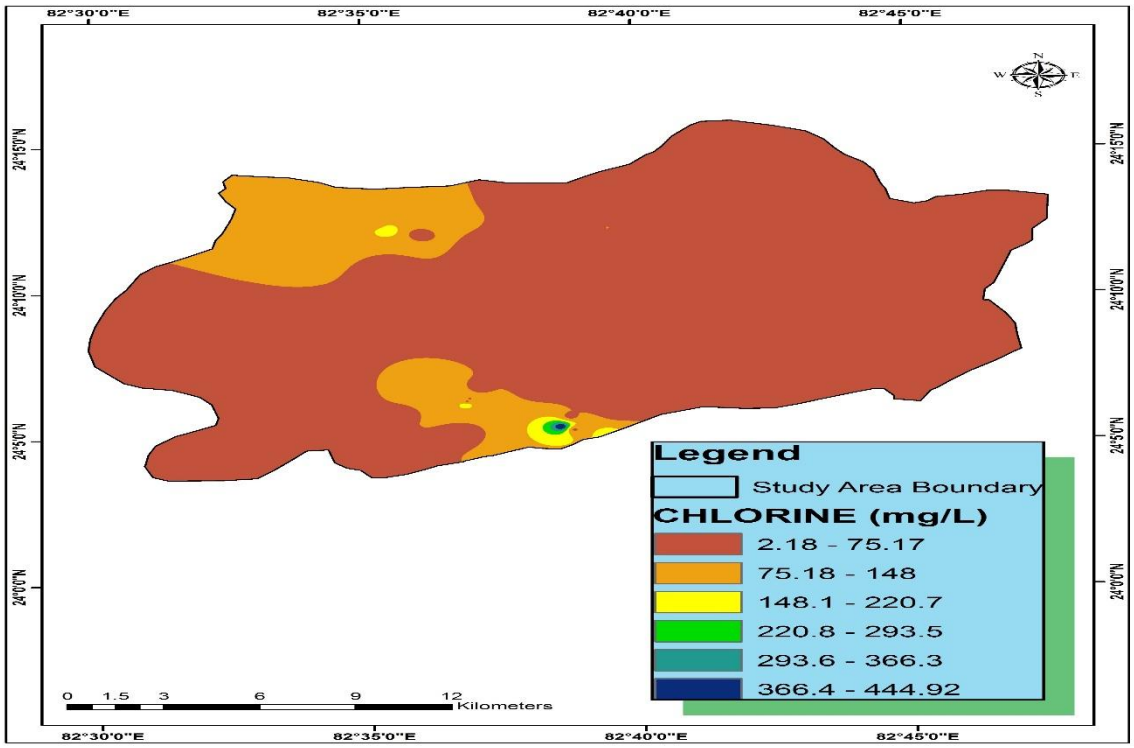

Figure 5.20 Spatial distribution of Chloride in the study area

High concentrations of chloride give a salty taste to water (WHO 2004). However, chloride concentrations above about 250 mg/l can give rise to a detectable taste in water (WHO 2004; Sawyer and McCarty 1978). The high concentration of chloride may be injurious to some people suffering from diseases of the heart and kidneys. Taste, indigestion, corrosion, and palatability are affected (CPCB 2008). The concentrations of chloride were observed in groundwater samples ranges from 2.18 to 444.91 mg/l and the mean value is 58.54 mg/l. The highest concentrations (444.91 mg/l) of chloride were found in the samples (GW-46) from the Vindhya Nagar (near Thermal power station) and exceeded the limit (>250 mg/l) prescribed by WHO (2011). The spatial distribution of chloride concentration in the groundwater of the study area is illustrated in Fig. 5.20.

5.4.1.5 Sulphate (SO_4^{2-})

Sulphate in water resources is commonly derived from the oxidative weathering of sulphide minerals, such as pyrite (FeS_2); however, gypsum (CaSO4·2H2O) and anhydrite (CaSO4) can also be a sulphate source (Han et al. 2013; Singh et al. 2011). The higher concentration of sulphate in groundwater samples might be due to the oxidation of sulphide in the aquifer materials or due to the leaching of terrestrial sulphate salts. The sulphate concentration in the groundwater ranges from 0.6 to 212.80 mg/l and mean value is 49.23 mg/l. The maximum concentrations of sulphate was observed in the groundwater samples (GW-44 and 46) and exceeded the permissible limit (>150 mg/l) recommended by WHO (2011).It can be seen from the spatial distribution map that the few portions of north-west and southern regions have shown higher concentration of sulphate ion .The spatial distribution of Sulphate concentration in the groundwater of the study area is illustrated in Fig. 5.21.

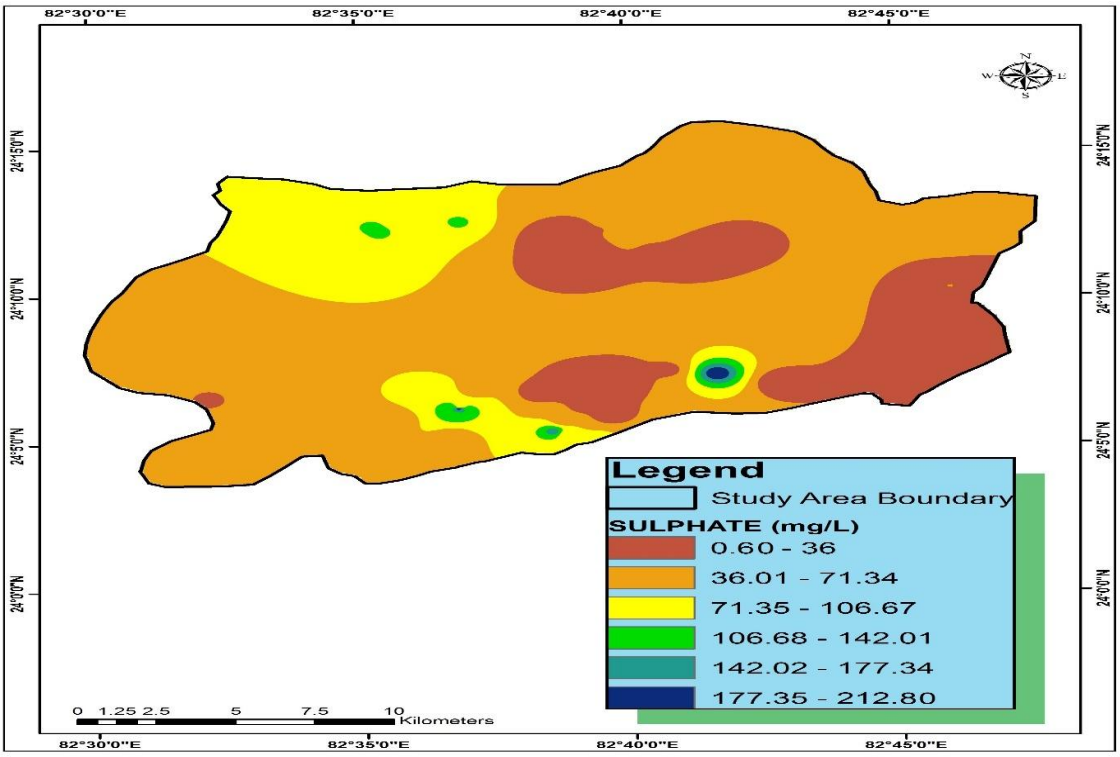

Figure 5.21 Spatial distribution of Sulphate in the study area

5.4.1.6 Nitrate (NO_3^-)

The chief sources of Nitrate are atmospheric precipitation, fertilizers, and discharges of municipal or domestic sewage (Appelo and Postma 1996). Unwarranted nitrate intake in drinking water has been linked with the risk of methemoglobinemia or 'blue baby syndrome' in humans, stomach cancer, nitrate poisoning in animals and adversely affects CNS and cardiovascular system (Mason 2002; Raju et al. 2009; Stadler et al. 2012; CPCB 2008). Additionally, biological nitrogen fixation and the use of explosives in mining areas are possible nitrate sources in mine water (Singh et al. 2012). The nitrate concentration ranges from 0.48 to 144.84 mg/l and the average value is 17.75 mg/l. Among the 46 groundwater samples, 3 water samples (GW-43, 44 & GW-46) show nitrate concentration above the limit (>45 mg/l) prescribed by WHO (2011). The spatial distribution of nitrate concentration in the groundwater of the study area is illustrated in Fig. 5.22.

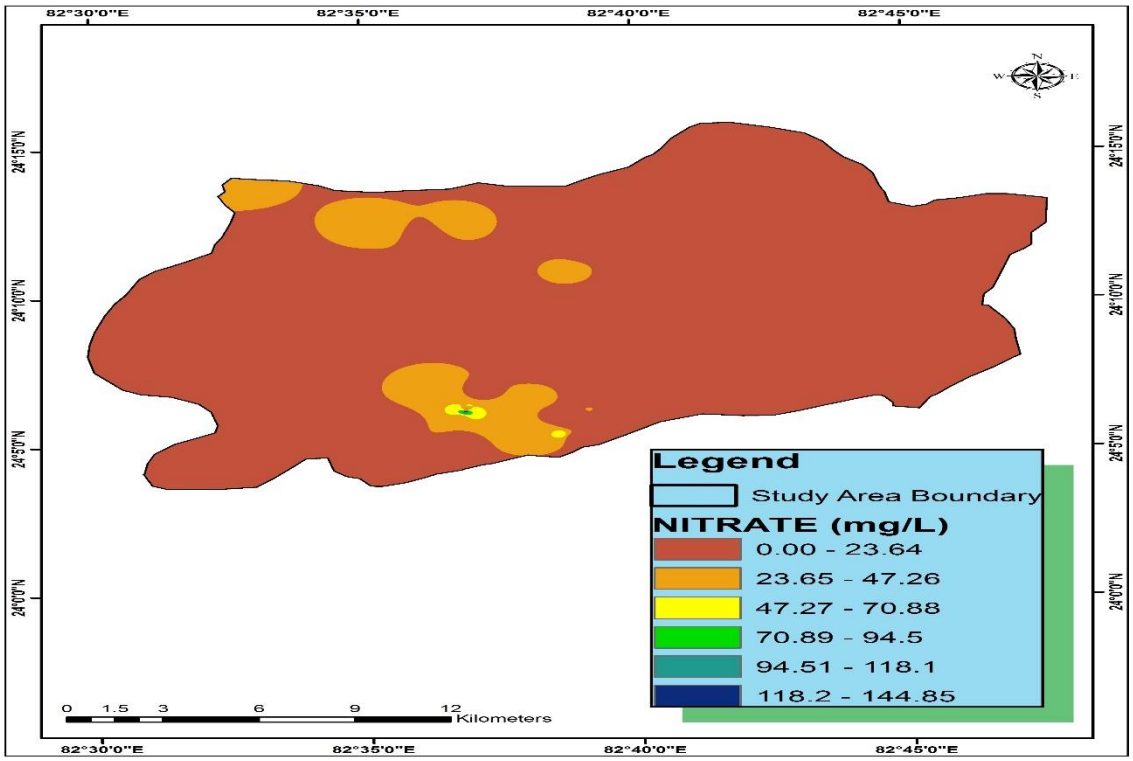

Figure 5.22 Spatial distribution of Nitrate in the study area

5.4.1.7 Fluoride (F^-)

In the last few decades, the majority of the aquifers are contaminated due to the high concentration of fluoride (F^-), which is one of the most omnipresent chemical contaminants of the world aquifers (U.K. Singh et al. 2018). About fluoride, 11% (approx.) of the groundwater samples (n = 5) of the study area show fluoride concentration higher than the WHO (2011) prescribed permissible limit of 1.5 mg/l in drinking water. Which makes the water unsuitable for drinking purposes. The high fluoride content in groundwater leads to dental and skeletal fluorosis such as mottling of teeth and deformation of ligaments (CPCB 2008).The concentration of fluoride contamination ranges from 0.27 to 1.79 mg/l and mean 0.637 mg/l. The fluoride contamination in the groundwater indicates the presence of fluoride bearing minerals (Krishna Kumar et al. 2011; Ramachandramoorthy et al. 2010). Spatial distribution of fluoride was classified on the basis of its concentration as (0.27-0.52, 0.53-0.78, 0.79-

1.03, 1.04-1.28, 1.29-1.54 and 1.55-1.79 mg/l).The spatial distribution of fluoride concentration in the groundwater of the study area is illustrated in Fig.5.23.

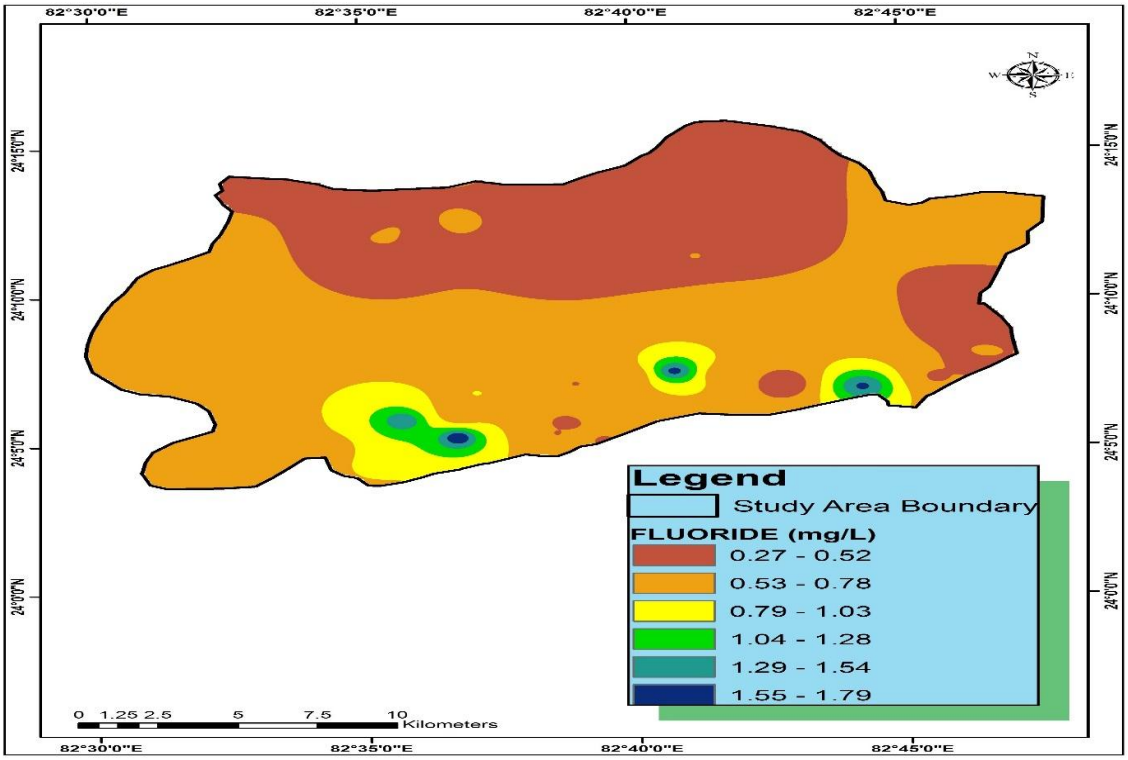

Figure 5.23 Spatial distribution of Fluoride in the study area

5.4.1.8 Calcium (Ca^{2+})

The calcium and magnesium in waters are generally used to classify the suitability of water. Calcium is the most abundant alkaline earth in the groundwater of the aquifer of the study region. The chemical breakdown of calcic-plagioclase feldspars and pyroxenes may be responsible for calcium in the groundwater (Ganyaglo et al. 2010). Calcium can also originate as lime in agricultural fertilizers. Water hardness is caused by the presence of dissolved calcium, magnesium and sometimes iron. Calcium ion concentration varies between 4.61 and 118.08 mg/l with an average of 46.54 mg/l. The maximum allowable limit of magnesium ion concentration in groundwater is 75 mg/l as per WHO (2011). The spatial distribution of calcium concentration in the study area is shown in Fig. 5.24.

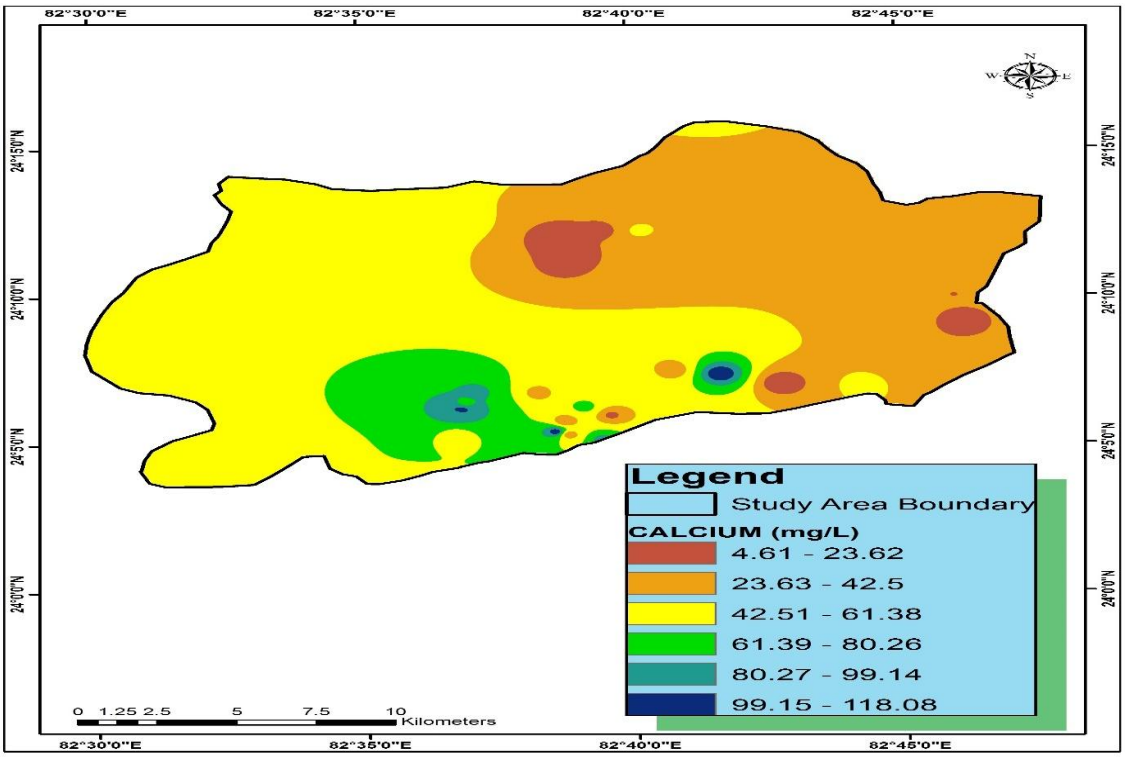

Figure 5.24 Spatial distribution of Calcium in the study area

5.4.1.9 Magnesium (Mg^{2+})

Magnesium ions present in the groundwater is particularly derived from leaching of limestone, dolomites, gypsum, and anhydrite. The major source of magnesium in the groundwater is the ion exchange of minerals in rocks and soils by water (Aghazadeh and Asghari 2010). The presence of calcium and magnesium make hard water. The magnesium concentration in the groundwater ranges from 1.17mg/l to 61.50 mg/l. The principal source of magnesium in natural water is the ferromagnesium mineral in igneous rock and magnesium carbonate in sedimentary rock. The maximum allowable limit of magnesium ion concentration in groundwater is 50 mg/l as per WHO (2011). The maximum concentrations of magnesium was observed in the groundwater samples at few locations (GW-1, 13, 20, 23, and 44) and exceeded the permissible limit recommended by WHO (2011).The spatial distribution of magnesium concentration in the groundwater of the study area is shown in Fig. 5.25.

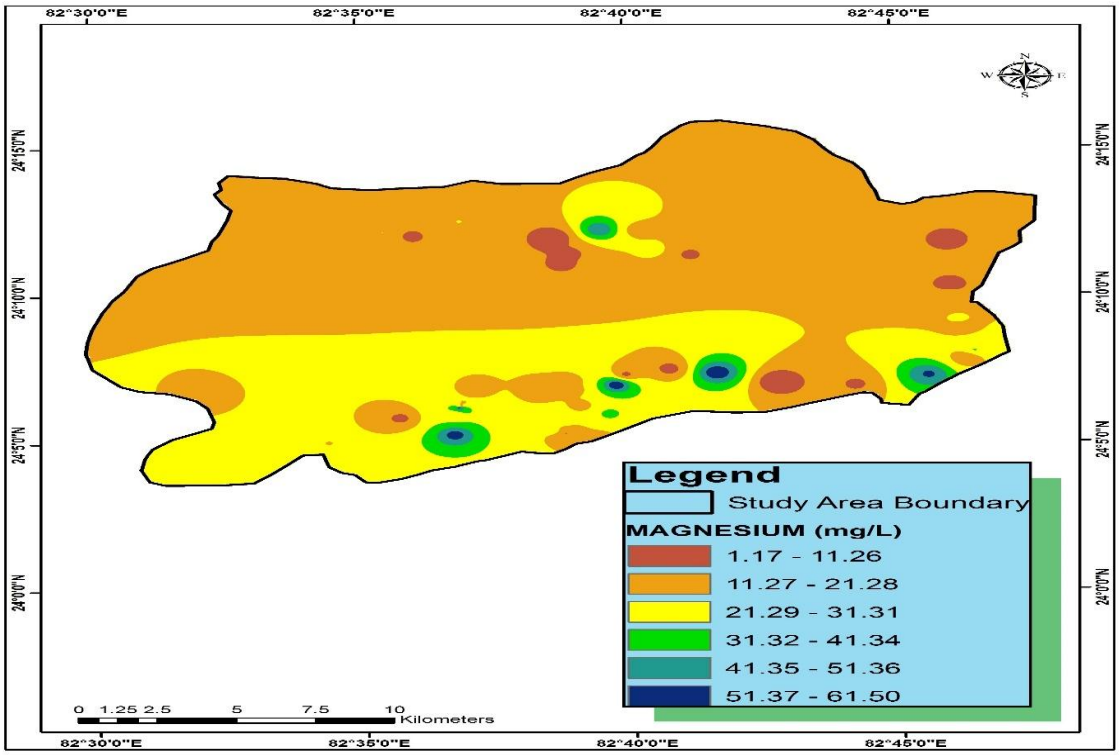

Figure 5.25 Spatial distribution of Magnesium in the study area

5.4.1.10 Sodium (Na^+)

Sodium concentration plays an important role in evaluating the groundwater quality for irrigation because sodium causes an increase in the hardness of soil as well as a reduction in its permeability (Tijani 1994). The concentration of the sodium in irrigation water is also known as the sodium percentage. The sodium percentage has been used to classify the chemical composition of the groundwater. Sodium in high concentrations tends to be absorbed by clay grains, displacing Mg^{2+} and Ca^{2+}, which reduces the permeability of soils (Ravi Kumar et al. 2011). The concentration of sodium varies from 4 to 192.09 mg/l. The highest concentrations (175.14 & 192.09 mg/l) of sodium was found in the water samples (GW-15 & GW-16) and exceeded the limit (>50 mg/l) prescribed by WHO (2011). The spatial distribution of sodium concentration in the groundwater of the study area is illustrated in Fig. 5.26.

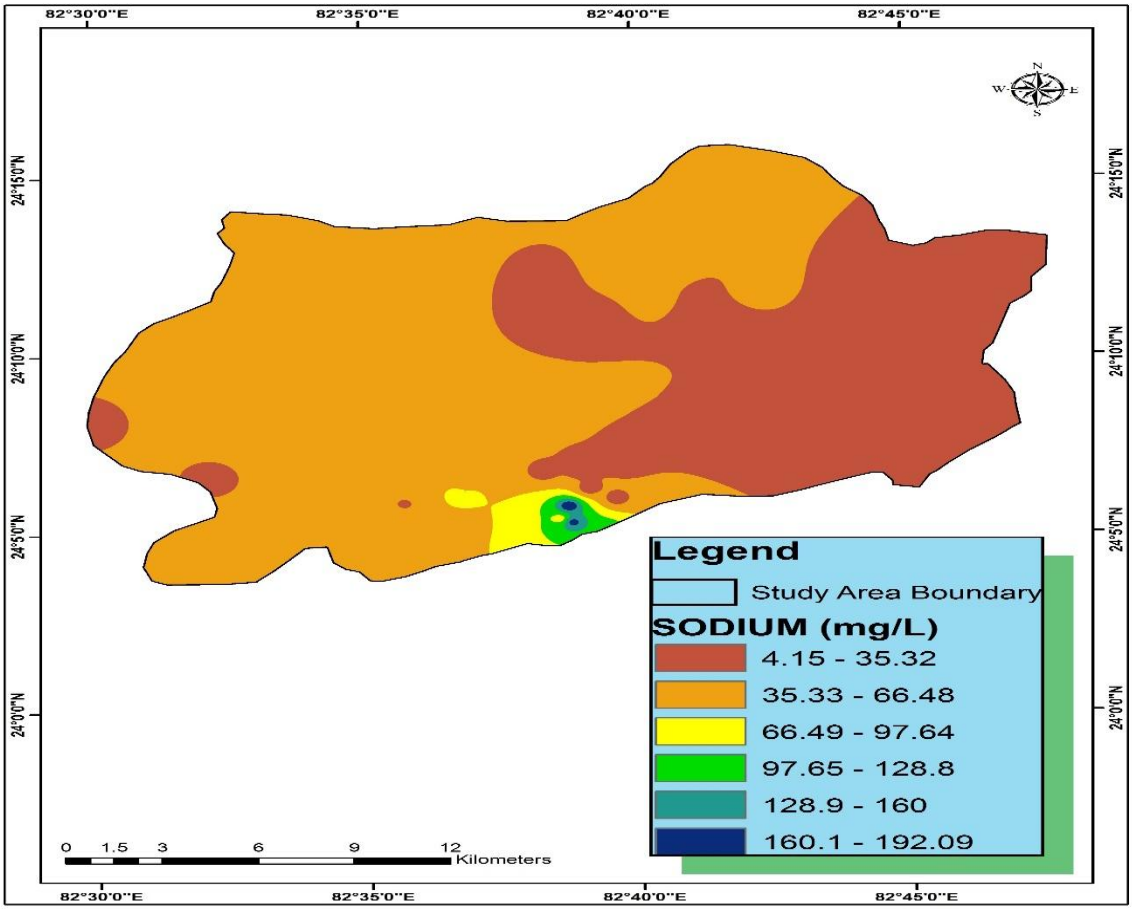

Figure 5.26 Spatial distribution of Sodium in the study area

5.4.1.11 Potassium (K^+)

The potassium concentration in groundwater mostly increases by the weathering of potash silicate minerals, the application of potash fertilizers and the usage of surface water for irrigation (Jain et al. 2010).The potassium concentration varies between 00.26 to 20.75 mg/l with an average of 1.01 mg/l in the study region. The maximum concentrations of potassium was found in the groundwater samples (GW-8,9,15,16,18 and 25) and exceeded the allowable limit (>15 mg/l) recommended by WHO (2011).The spatial distribution of potassium concentration in the groundwater of the study area is shown in Figure 5.27.

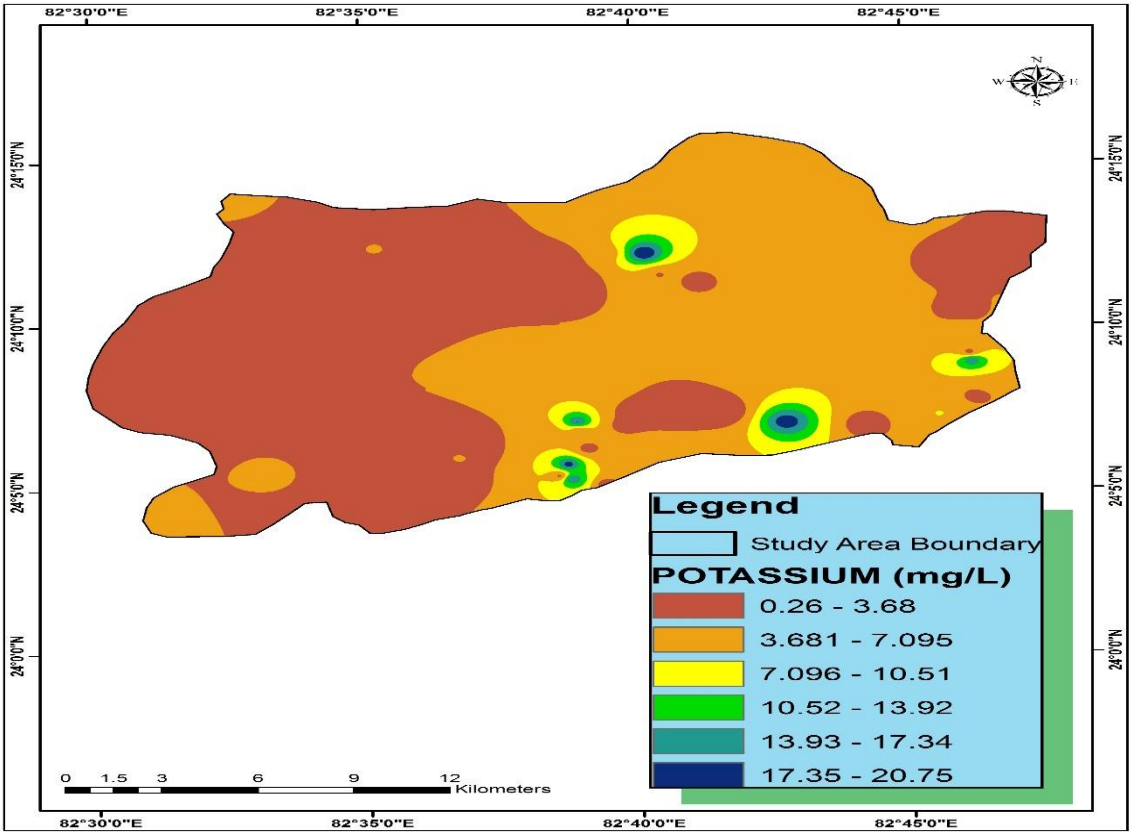

Figure 5.27 Spatial distribution of Potassium in the study area

5.4.1.12 Total Hardness (TH)

The hardness of water refers to soap neutralizing the power of water. Hardness refers to reaction with soap and scale formation. It increases the boiling point of water and does not have any adverse effect on the health of humans. The principal natural sources of hardness in water are dissolved polyvalent metallic ions from sedimentary rocks, seepage, and runoff from soils. Calcium and magnesium, the two principal ions, are present in many sedimentary rocks, the most common being limestone and chalk (WHO 2011). Total hardness (TH) ranges from 16.30 to 540.28 mg/l of the study area and mean 199.69 mg/l. Among the 46 groundwater samples, sample no-44 shows concentration value exceeds the limit (>500 meq/l) recommended by WHO (2011).

5.4.1.13 Iron (Fe)

Iron is the second most abundant metal in the earth's crust, of which it accounts for about 5%Elemental Fe is rarely found in nature, as the Fe ions Fe^{+2} and Fe^{+3} readily combine with oxygen- and sulphur-containing compounds to form oxides, hydroxides, carbonates, and sulphides. It is most commonly found in nature in the form of its oxides (Elinder, 1986; Knepper, 1981).Mines can produce a variety of Fe pollution problems in groundwater (Barnes and Clarke, 1964; Emrich and Merritt, 1969; Mink, 1972). The yellowish colour of water generally indicated the presence of iron in the water samples. The groundwater was yellowish or slightly yellowish in the central region (GW-3, 4) of the study area. The iron concentration varies between 0.71 and 1.48 mg/l with an average of 1.01 mg/l. The spatial distribution of Iron concentration in the groundwater of the study area is shown in Fig. 5.28.

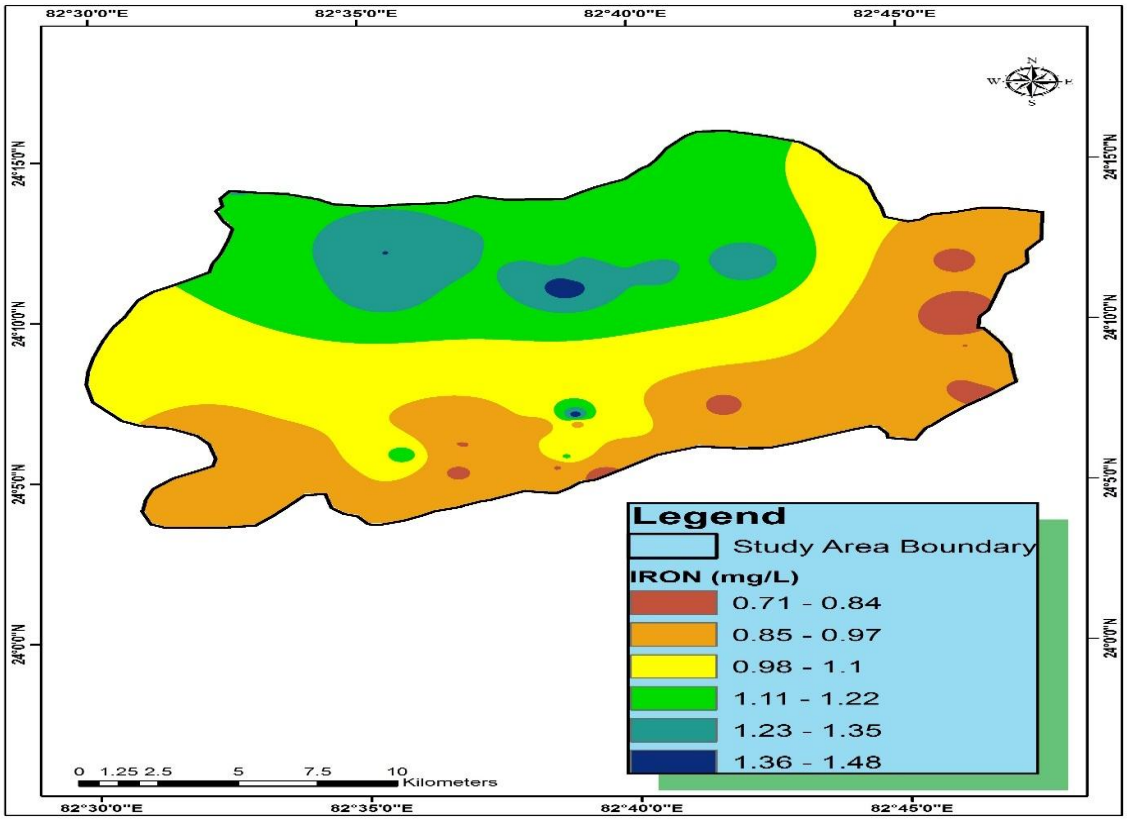

Figure 5.28 Spatial distribution of Iron in the study area

5.4.1.14 Copper (Cu)

Copper and Zn are also two main hazardous substances listed by ATSDR (2011). High concentrations of Copper (Cu) are toxic to the ecosystem and human health although they are essential microelements for plants and human bodies (Michaud et al. 2008; Wu et al. 2011). Continuous intake of high levels of Cu and Zn over an extended period can cause anemia, damage of the pancreas, liver, and kidney, and a decrease in the levels of high-density lipoprotein cholesterol (ATSDR 2004, 2005). Heavy metals originate from two primary sources: natural sources and anthropogenic activities (such as agriculture, industrialization and mining). The concentrations of copper (Cu) were observed in groundwater samples ranges from 1.10 to 1.674 mg/l and the mean value is 1.30 mg/l. The spatial distribution of copper concentration in the groundwater of the study area is illustrated in Figure 5.29.

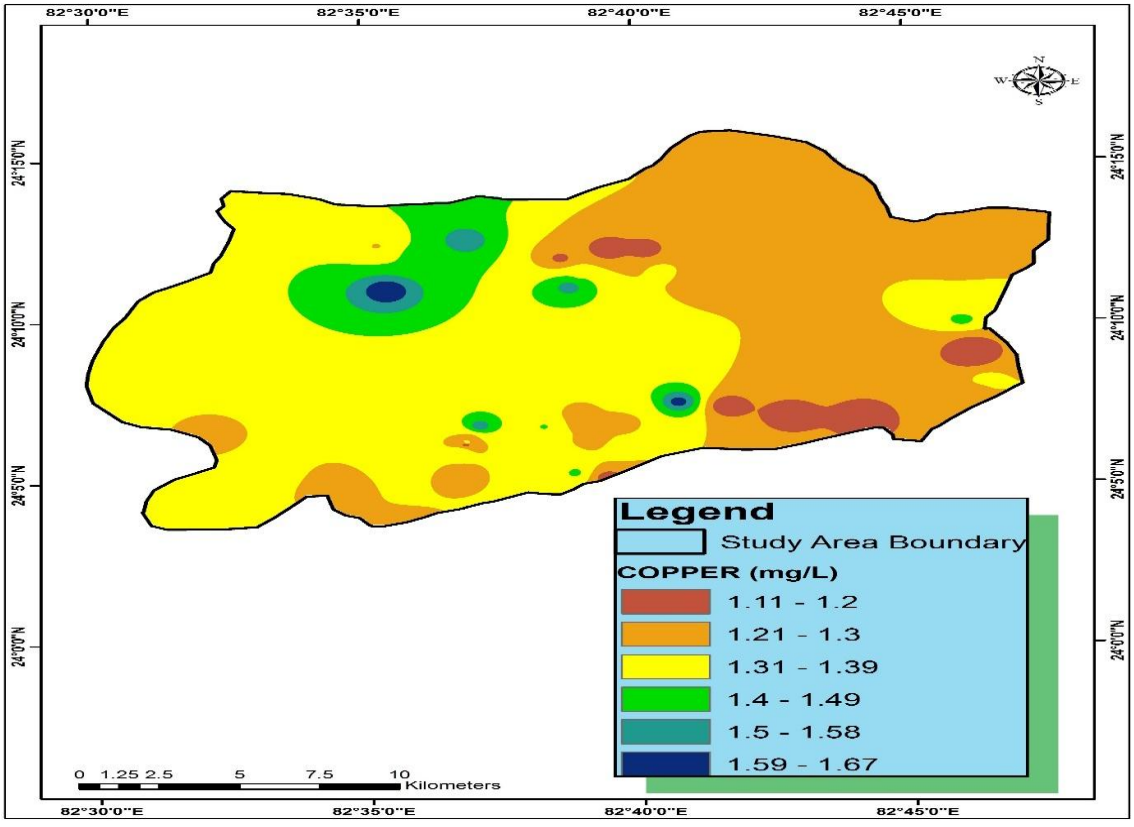

Figure 5.29 Spatial distribution of Copper in the study area

5.4.1.15 Lead (Pb)

Metal with high toxicity is lead that is carcinogenic to humans, causing serious chronic health disorders such as including headaches, blood pressure, abdominal pain, irritability, kidney and nerve damage, brain tumors, and cancer of the lungs (Keshav Krishna and Mohan 2016). Children and neonatal are very sensitive and more vulnerable to lead. Complicated health issues, such as dementia and behavioural disorders, may be caused as a result of exposure to excessive concentrations of lead. Anemia may be caused as a result of extended exposure to lead (Jarup 2003; Mortada et al. 2001; Steenland and Boffetta 2000).The lead concentration varies between 0.11 and 0.33 mg/l with an average of 0.159 mg/l. The spatial distribution of lead concentration in the groundwater of the study area is shown in Figure 5.30.

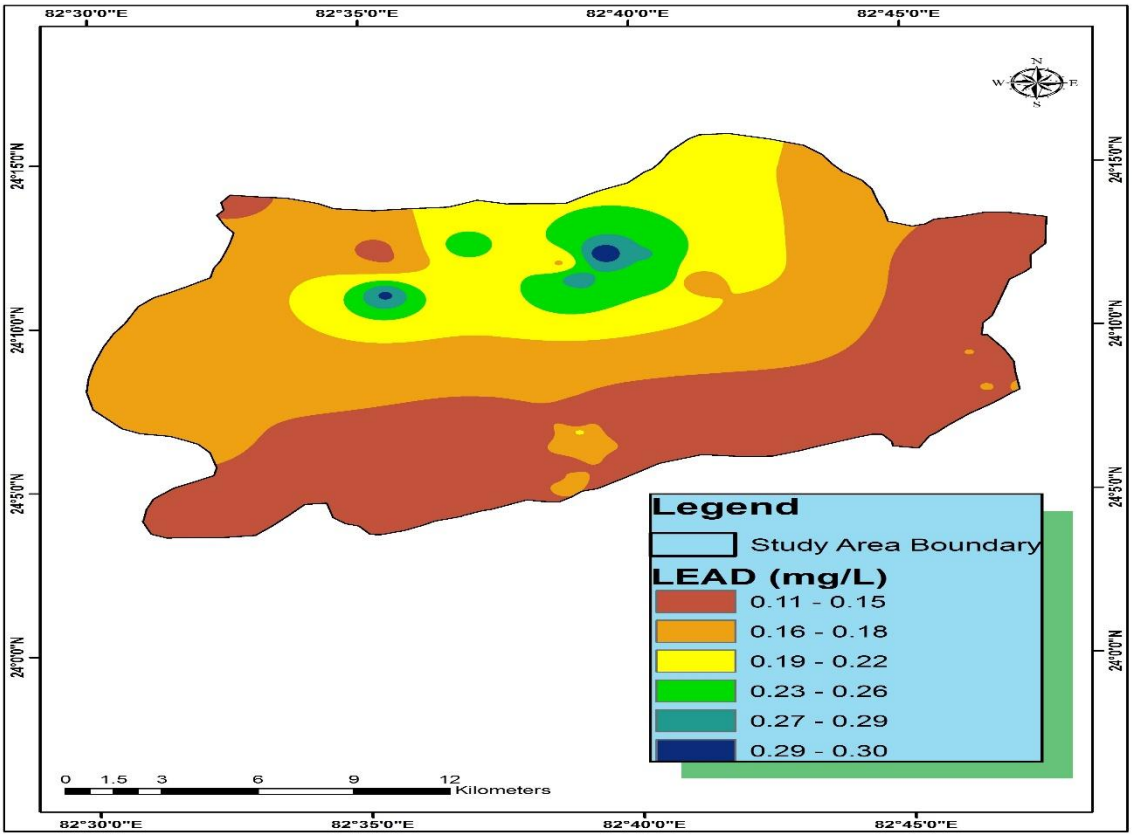

Figure 5.30 Spatial distribution of lead in the study area

5.4.1.16 Cadmium (Cd)

Cadmium is one of the most toxic and mobile elements in the environment (Alloway and Jackson 1991; Nies 1999, 2003). Anthropogenic Cadmium (Cd) sources include phosphate fertilizers, combustion emissions, sewage sludge, landfills, traffic, metal industry, mining, and environmental incidents (Merkel and Sperling 1998; Mirlean and Roisenberg 2006; Sprynskyy et al. 2011; Bigalke et al. 2017). Exposure to cadmium causes acute and chronic effects on living beings. These chronic issues include skeletal and kidney disorders. Experimental studies conducted on humans and animals show that cadmium may cause cancer in humans (Jarup et al. 2000; IARC1993; Nordberg et al. 2002). The concentrations of cadmium were observed in groundwater samples ranges from 0.012 to 0.198 mg/l and the mean value is 0.0849 mg/l. The maximum concentration is observed in the central portion of the study area. The spatial distribution of cadmium concentration in the groundwater of the study area is illustrated in Figure 5.31.

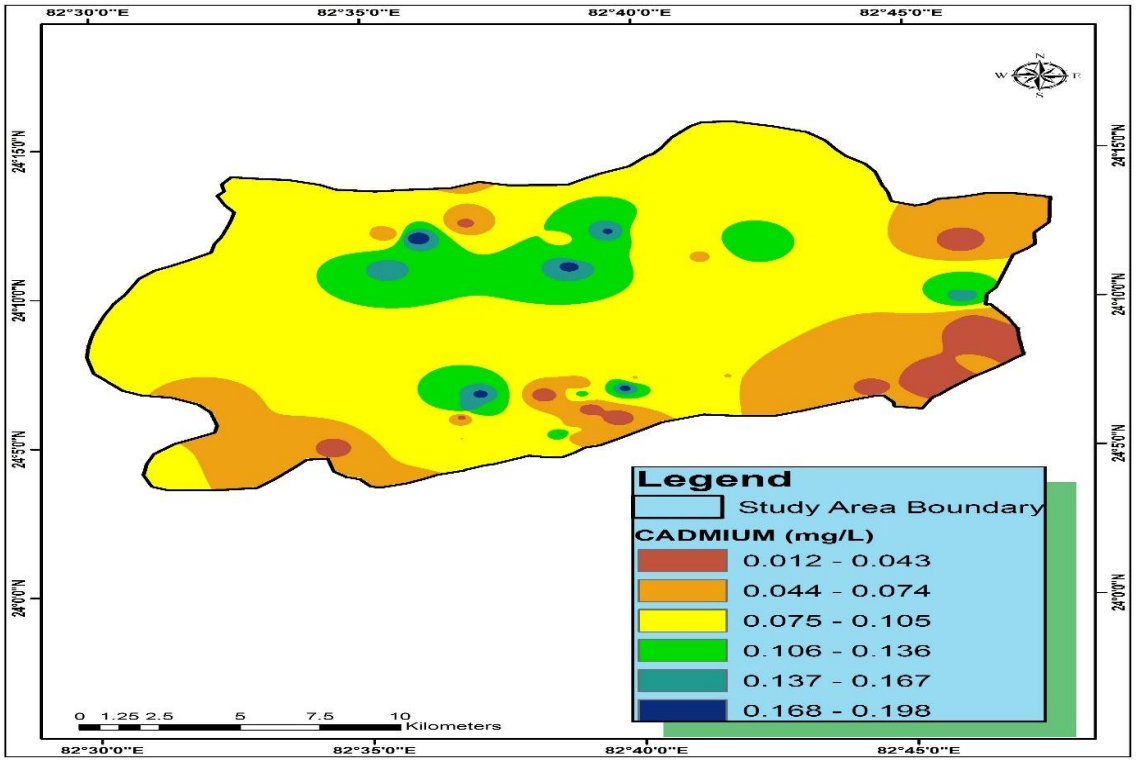

Figure 5.31 Spatial distribution of Cadmium in the study area

5.4.1.17 Chromium (Cr)

Chromium, which is included in the list of 126 priority pollutants of the United States Environmental Protection Agency (USEPA 2014), is the 21st most abundant element in the Earth's crust (Emsley 2001). Cr(VI) can also be directly released into the environment via several anthropogenic activities, such as coal combustion and the uncontrolled disposal of produced fly ash (Jacobs and Testa, 2004), as well as paint production, mining activities and phosphate fertilizer production among others (Molina et al., 2009). The mobility of Cr (VI) in groundwater is significantly higher than that of Cr (III), due to its higher solubility and lower adsorption capacity onto aquifer materials (Calder, 1988). Chromium concentrations in the study area have been found to range from 0.001 to 0.061 mg/l and the mean value is 0.0108 mg/l. The spatial distribution of chromium concentration in the groundwater of the study area is illustrated in Figure 5.32.

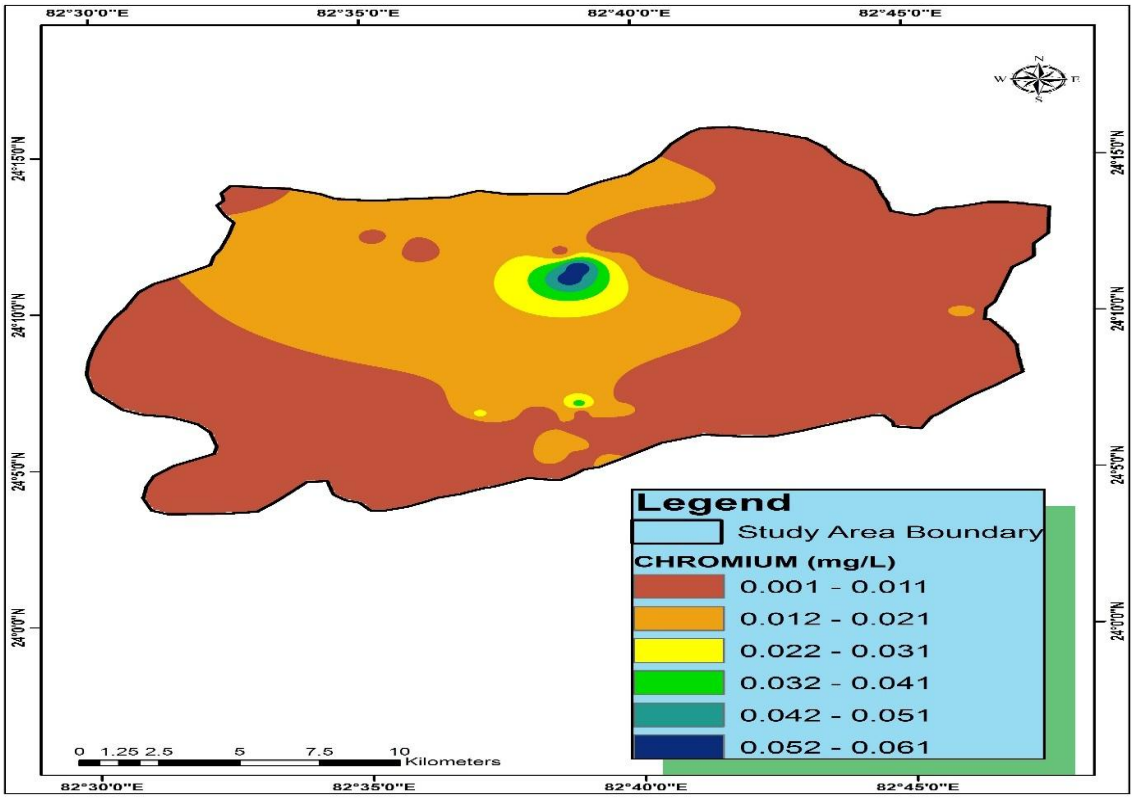

Figure 5.32 Spatial distribution of Chromium in the study area

5.4.1.18 Nickel (Ni)

Nickel present in the groundwater is particularly naturally released from rock and soil, which can be harmful to humans (Lehr J et al., 2006). Nickel concentrations in groundwater are influenced by soil type, pH level and sampling depth (WHO 2005). Excess concentrations have been reported where drinking water is contaminated with nickel waste discharge from chemical, industrial or mining plants (NHMRC 2004). The adverse health effects of nickel for humans depend upon the route of administration, water solubility (absorption) of nickel compounds, dose, body weight, sensitivity and duration of exposure (WHO 2005, Andersen KE et al. 1987; Grimsrud TK et al. 2005; Nielsen GD et al . 1999). The concentrations of nickel were observed in groundwater samples ranges from 0.092 to 0.294 mg/l and the mean value is 0.182 mg/l. The spatial distribution of nickel concentration in the groundwater of the study area is illustrated in Fig.5.33.

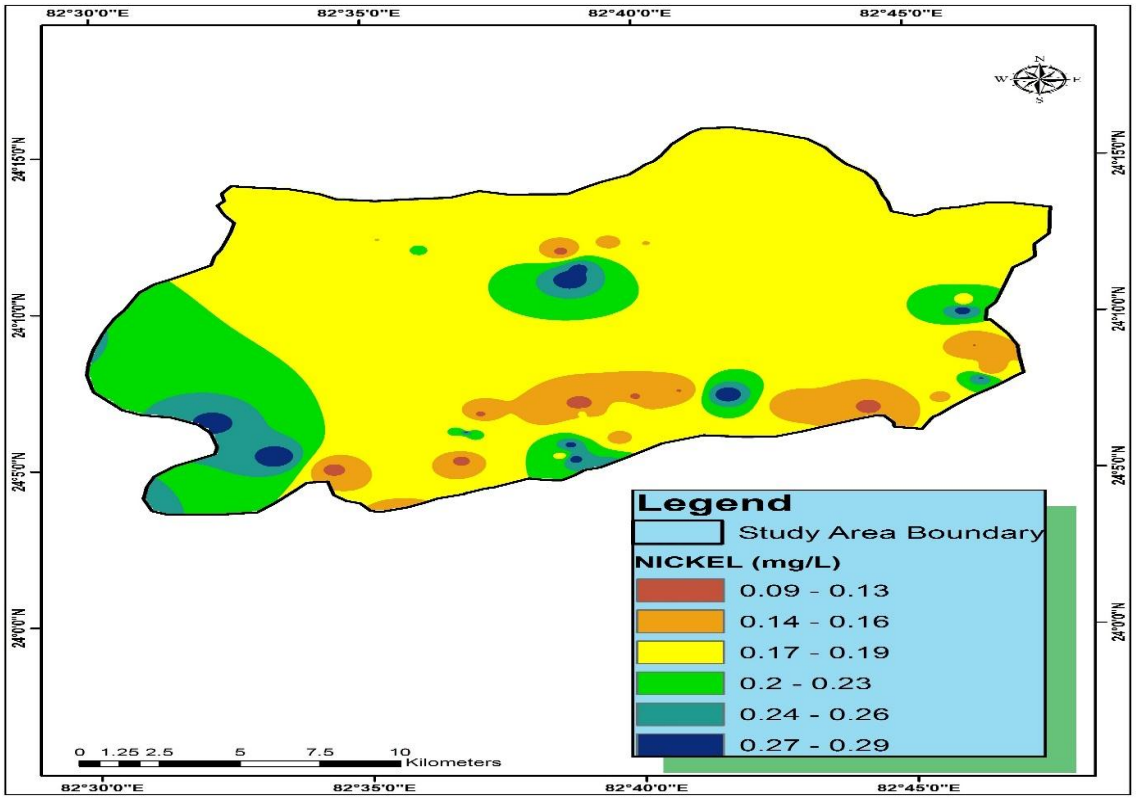

Figure 5.33 Spatial distribution of Nickel in the study area

5.4.1.19 Zinc (Zn)

Zinc occurs in small amounts in almost all igneous rocks (WHO 2003). Zinc is the main hazardous substances listed by ATSDR (2011). High concentrations of Zn are toxic to the ecosystem and human health although they are essential microelements for plants and human bodies (Michaud et al. 2008; Wu et al. 2011). Continuous intake of high levels of Zn over an extended period can cause anemia, damage of the pancreas, liver, and kidney, and decrease in the levels of high-density lipoprotein cholesterol (ATSDR 2004, 2005). Zinc concentrations in the study area have been found to range from 1.397 to 5.318 mg/l and the mean value is 3.204 mg/l. The maximum concentrations of zinc was found in the 06 groundwater samples (GW-3, 10,11,15,30 and 42) and exceeded the allowable limit (>5 mg/l) recommended by WHO (2011).The spatial distribution of zinc concentration in the groundwater of the study area is illustrated in Figure 5.34.

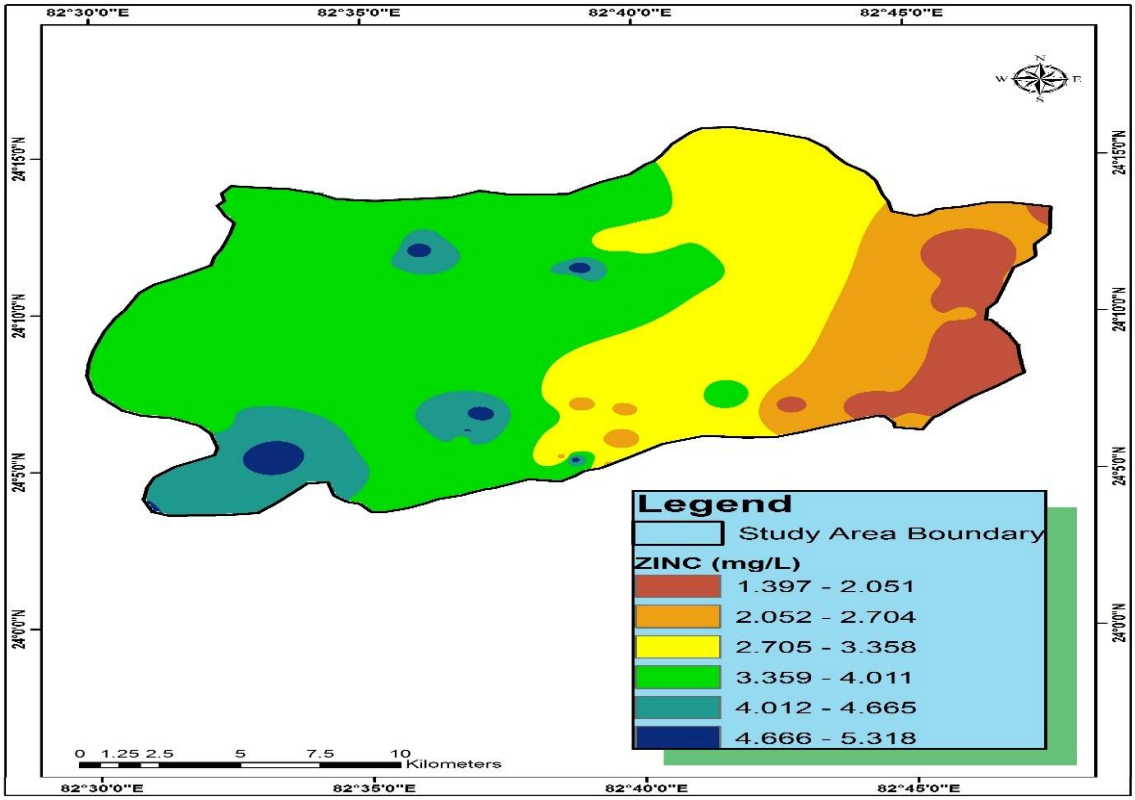

Figure 5.34 Spatial distribution of Zinc in the study area

5.4.2 Major Ion Chemistry

5.4.2.1 Anion Chemistry

The anion chemistry of the analyzed water samples of the study region shows Bicarbonate was generally dominant and representing on average 43% of the total anions. Chloride is the second dominant anion, representing an average of 28% of the total anions. Sulphate was less dominant ions and contributing 22% of the total anions respectively. Nitrate is the least dominant anion of the total anions. The order of mean abundance of major anions is $HCO_3^- > Cl^- > SO_4^{2-} > NO_3^-$. Percentage contributions and Box-plot diagram of individual anions in groundwater have shown in Fig. 5.35 and Fig. 5.36.

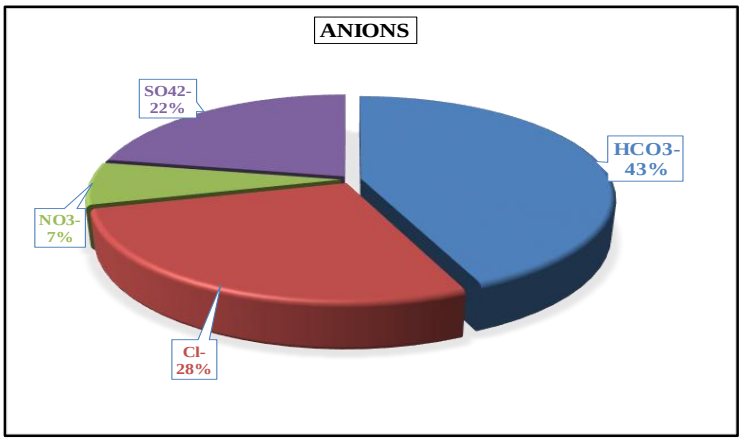

Figure 5.35 Percentage contributions of major anions

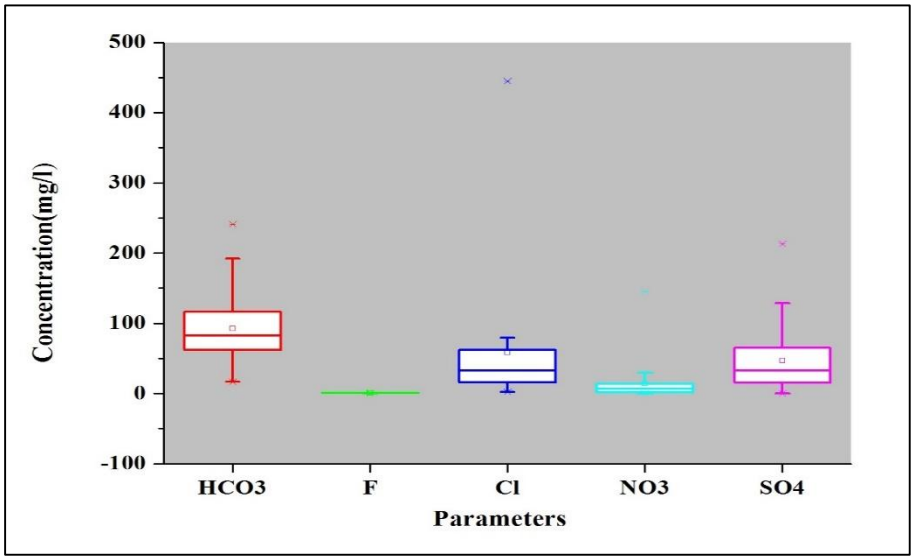

Figure 5.36 Box-whisker plot of major anions

5.4.2.2 Cation Chemistry

For the cations, Calcium was a dominant ion among all the cations and representing on average 40% of the total cations. Sodium is the second dominant cations, representing an average of 38% of the total cations. Magnesium was less dominant ions and contributing 18% of the total cations. The Potassium was the least dominant cations, representing 4% of the total cations. The order of mean abundance of major cations is $Ca^{2+} > Na^{+} > Mg^{2+} > K^{+}$. The Potassium values are generally low as compared with Ca^{2+}, $Na^{+,}$ and Mg^{2+} in the aquifer system. Percentage contributions and Box-plot diagram of individual cations in groundwater have shown in Fig. 5.37 and Fig. 5.38.

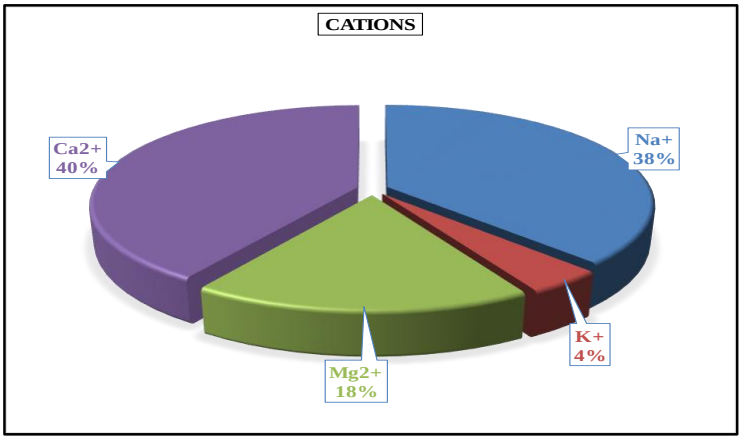

Figure 5.37 Percentage contributions of major cations

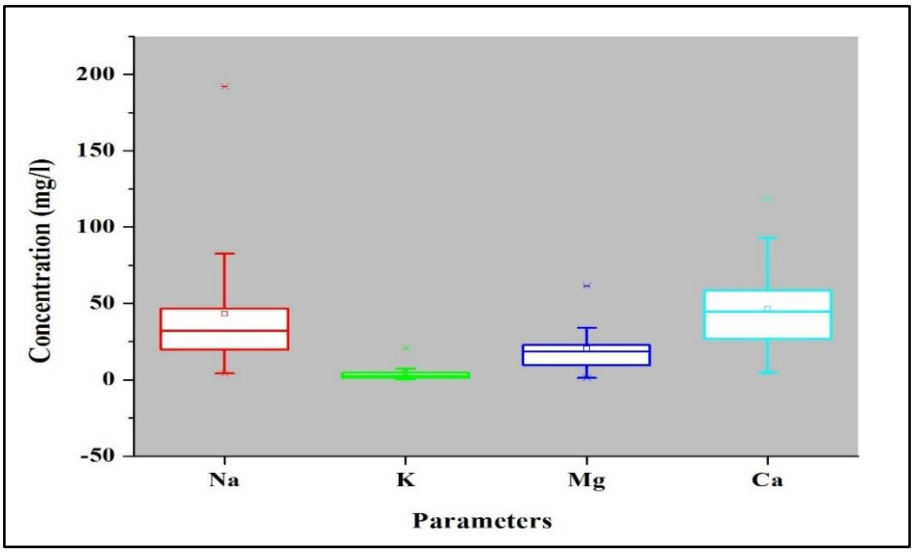

Figure 5.38 Box-whisker plot of major cations

5.4.3 Correlation Analysis

A correlation coefficient is a measure of the extent to which the measured variables (x and y) "vary together". The correlation coefficient is scaled so that its value is independent of the units in which the two measured variables (x and y) are expressed. The value of any correlation coefficient is between −1.0 and +1.0 (Ramadan, 2003; Elbeih and El-Zeiny 2018). The correlation analysis tool, embedded in the Microsoft Excel Data analysis pack, was used to test each pair of measurement variables to determine: whether the two measurement values tend to move together (positive correlation), whether small values of one variable tend to be related with large values of the other (negative correlation), or whether values of both variables tend to be unrelated (correlation near to zero). In other words, when the coefficient of correlation is near to zero, this indicates that the independent variable x is of help in reducing the uncertainty in predicting y.

The correlation coefficients (r) among the 20 groundwater quality parameters of the study area have been calculated and the numerical values are tabulated as shown in Table 5.6. Out of 210 correlation coefficients, 76 negatives, and 134 positive correlation coefficients. The high positive correlation coefficients is observed between TDS and EC (r =0.999), SO_4^{2-} and EC (r=0.872), SO_4^{2-} and TDS (r=0.871), SO_4^{2-} and Cl^-(r=0.817), TH and Ca^{+2} (r=0.807), Cl^- and TDS (r=0.774), Cl^- and EC (r=0.774),TH and Mg^{+2} (r=0.748),Ca^{2+} and EC (r=0.702), Ca^{2+} and TDS (r=0.699), Ca^{2+} and SO_4^{2-}(r=0684). The high Negative correlation coefficients is observed between K^+ and F^-(r=-0.316), Fe^{2+} and pH (r=0.311).

Table 5.6 Correlation coefficient matrix of water quality parameters

	pH	EC	TDS	F	Cl	NO_3	SO_4	HCO_3	Na	K	Mg	Ca	Fe	Cu	Pb	Cd	Cr	Ni	Zn	TH
pH	1																			
EC	-0.082	1																		
TDS	-0.077	0.999	1																	
F	0.378	-0.084	-0.082	1																
Cl	-0.217	0.774	0.774	-0.118	1															
NO_3	-0.200	0.534	0.535	-0.095	0.635	1														
SO_4	-0.258	0.872	0.871	-0.079	0.817	0.732	1													
HCO_3	-0.025	0.678	0.684	-0.071	0.468	0.516	0.543	1												
Na	0.076	0.635	0.635	-0.085	0.443	0.243	0.533	0.177	1											
K	-0.105	-0.080	-0.082	-0.316	-0.122	-0.212	-0.125	-0.222	0.328	1										
Mg	0.066	0.321	0.317	0.029	0.196	0.297	0.235	0.297	0.228	-0.031	1									
Ca	0.103	0.702	0.699	0.237	0.654	0.511	0.684	0.479	0.264	-0.291	0.212	1								
Fe	-0.311	-0.125	-0.132	-0.266	-0.077	-0.065	-0.099	-0.219	-0.114	0.075	-0.156	-0.213	1							
Cu	0.111	0.129	0.134	-0.002	-0.042	-0.069	0.033	0.089	0.035	-0.210	-0.246	0.014	0.304	1						
Pb	-0.206	-0.090	-0.093	-0.368	-0.012	0.035	0.026	-0.199	-0.014	-0.019	0.004	-0.223	0.605	0.237	1					
Cd	-0.041	0.040	0.045	-0.087	0.135	0.027	0.096	-0.031	0.010	-0.266	-0.025	0.142	0.258	0.329	0.314	1				
Cr	0.069	-0.166	-0.168	-0.169	-0.001	0.055	-0.118	-0.154	-0.081	0.006	-0.195	-0.126	0.511	0.380	0.337	0.283	1			
Ni	0.158	0.212	0.214	-0.108	0.153	0.260	0.254	0.099	0.395	-0.031	-0.023	0.056	-0.082	0.088	0.175	0.175	0.248	1		
Zn	-0.007	0.217	0.210	-0.016	0.101	0.137	0.283	-0.090	0.255	-0.181	-0.044	0.258	0.322	0.456	0.276	0.360	0.195	0.171	1	
TH	0.110	0.670	0.666	0.179	0.562	0.527	0.606	0.505	0.317	-0.216	0.748	0.807	-0.239	-0.139	-0.149	0.081	-0.204	0.024	0.149	1

5.4.4 CCME Water Quality Index of Groundwater

The Canadian Council of Ministers of the Environment Water Quality Index (CCMEWQI) is a useful and efficient method for assessing the quality of water (Lumb et al. 2006; Magesh and Chandrasekhar 2011). Based on the CCME WQI the water quality is ranked in the following five categories.

Table 5.7 Classification of CCME WQI range and category of water

CCME WQI Value	Rating	Remarks
95-100	Excellent	Water quality is protected with a virtual absence of threat or impairment; conditions very close to natural or pristine levels
80-94	Good	Water quality is protected with only a minor degree of threat or impairment; conditions rarely depart from natural or desirable levels.
65-79	Fair	Water quality is usually protected but occasionally threatened or impaired; conditions sometimes depart from natural or desirable levels.
45-64	Marginal	Water quality is frequently threatened or impaired; conditions often depart from natural or desirable levels.
0-44	Poor	Water quality is almost always threatened or impaired; conditions usually depart from natural or desirable levels.

CCME Water Quality Index provides information on a rating scale from zero to hundred. Zero (0) value signifies very poor water quality, whereas values close to 100 signifies excellent water quality. An index can be used to reflect the overall and ongoing condition of the water. Spatial variation and Bar chart of CCME WQI of study area is shown in Fig.5.40 and Fig.5.39. CCME WQI and details of sampling location along with the status of groundwater quality is presented in Table 5.8.

The lower value of CCME WQI was found due to the higher concentration values of major ions and heavy metals in the groundwater which directly influences the groundwater quality**.** The value of calcium and magnesium were significantly interrelated and indicates that the hardness of the water in nature.

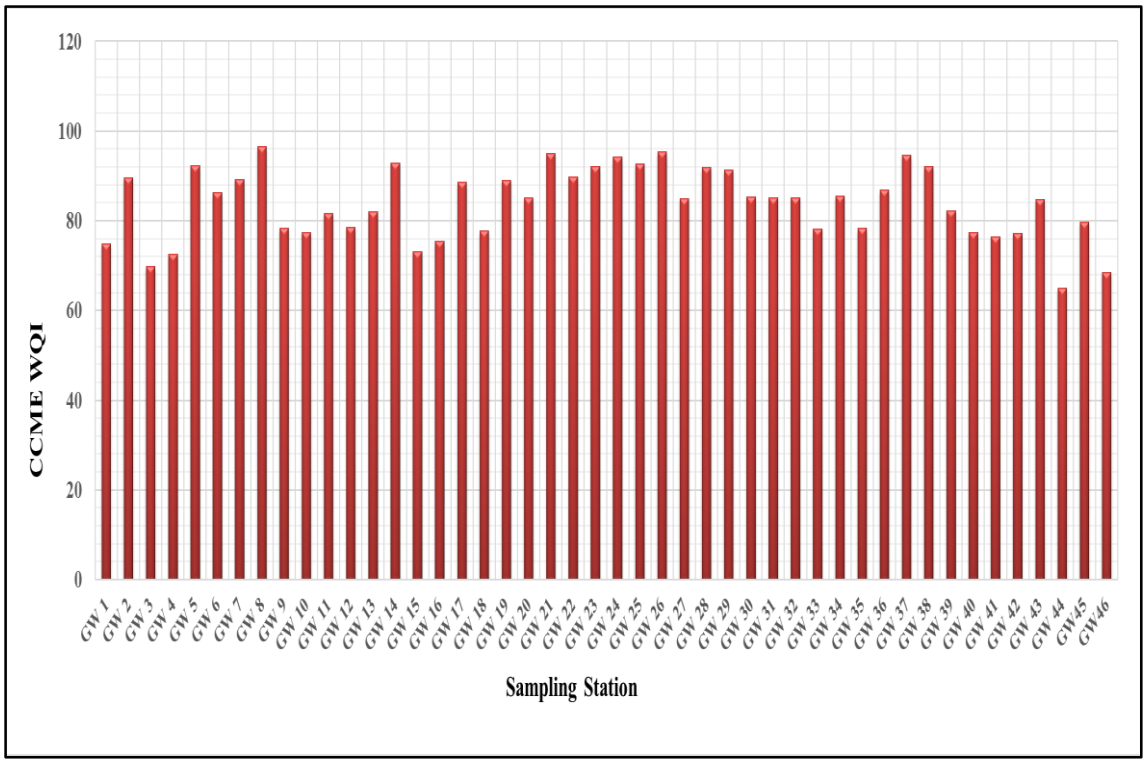

Figure 5.39 Graphical representation of water quality index

The CCME WQI of groundwater samples was found in the range of 64.90 to 96.52. Almost 56% of the total water samples were found in the range good category, 35% were found in fair category, 7 % were found in excellent category and 2 % were found in the marginal category, respectively. The CCME WQI categories (%) of groundwater samples as shown in Fig. 5.41.

Sample no. GW-8, GW-21, GW-26 were found in the excellent category. Sample no. GW-8 showed the highest CCME WQI values (96.52). While the sample no. GW-44 showed the lowest CCME WQI values (64.90). It can be seen that from CCME WQI spatial variation map, the central and few portions of the northern and southern regions of the study area indicated lower CCME WQI values. Whereas the eastern and western regions of the study area showed higher CCME WQI values. The spatial variation map

of CCME WQI showed that the major portion of the study area has CCME WQI greater than 80 and suitable for drinking purposes.

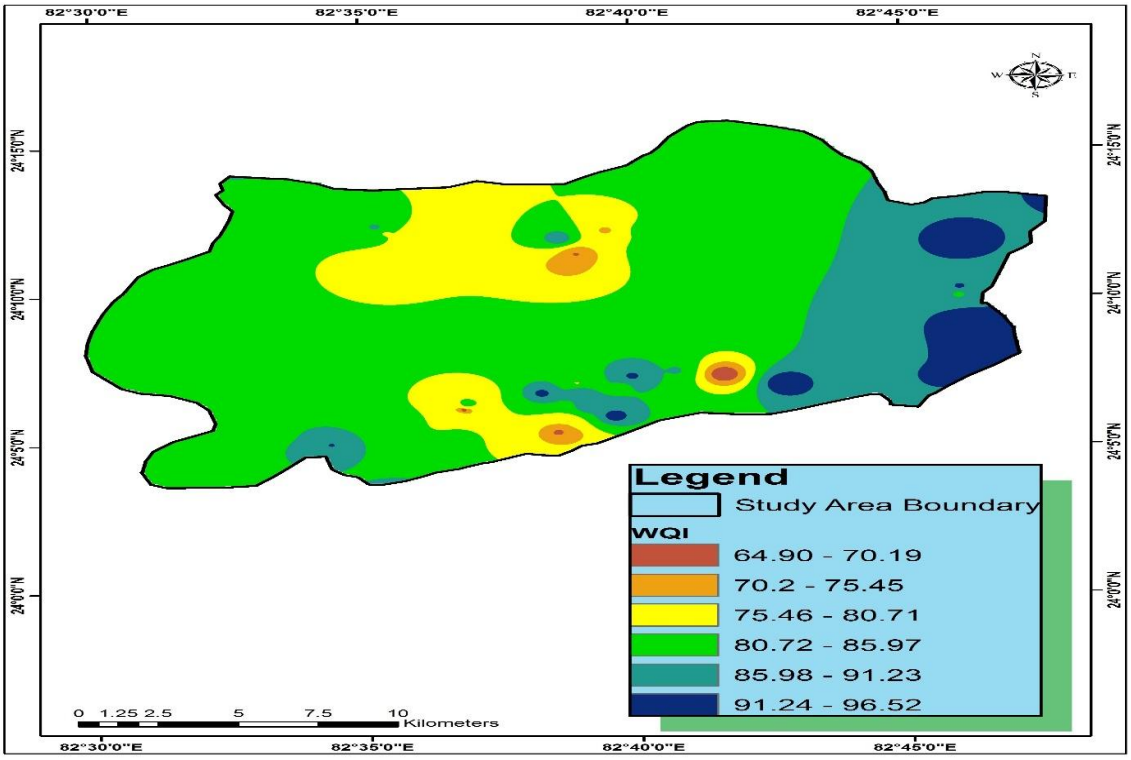

Figure 5.40 Spatial distribution of CCME WQI in the study area

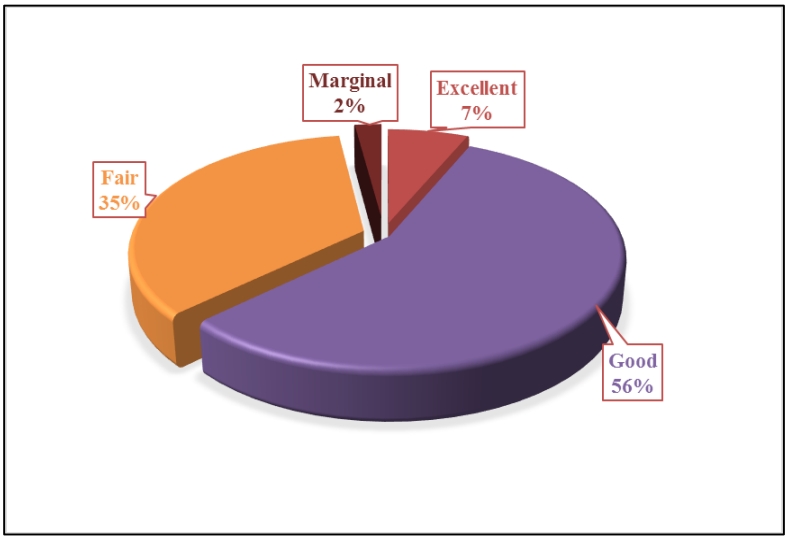

Figure 5.41 Pie chart representing CCME WQI categories

Table 5.8 CCME Water Quality Index for groundwater of study region

S.No.	Sample Code	Latitude	Longitude	CCME WQI	Description
1	GW 1	24º12'13"	82º39'30"	74.87	Fair
2	GW 2	24º11'57"	82º38'38"	89.67	Good
3	GW 3	24º11'25"	82º38'57"	69.79	Fair
4	GW 4	24º11'04"	82º38'47"	72.57	Fair
5	GW 5	24º07'18"	82º39'56"	92.34	Good
6	GW 6	24º07'29"	82º40'45"	86.28	Good
7	GW 7	24º07'21"	82º41'38"	89.25	Good
8	GW 8	24º07'02"	82º42'46"	96.52	Excellent
9	GW 9	24º07'04"	82º38'55"	78.35	Fair
10	GW 10	24º06'46"	82º37'05"	77.40	Fair
11	GW 11	24º06'16"	82º36'50"	81.69	Good
12	GW 12	24º06'00"	82º36'44"	78.58	Fair
13	GW 13	24º05'17"	82º36'43"	82.06	Good
14	GW 14	24º06'44"	82º38'16"	92.93	Good
15	GW 15	24º05'19"	82º38'48"	73.17	Fair
16	GW 16	24º05'46"	82º38'44"	75.38	Fair
17	GW 17	24º06'15"	82º39'06"	88.53	Good
18	GW 18	24º12'00"	82º40'12"	77.75	Fair
19	GW 19	24º06'47"	82º38'57"	89.07	Good
20	GW 20	24º06'57"	82º39'45"	85.08	Good
21	GW 21	24º07'02"	82º39'36"	95.03	Excellent
22	GW 22	24º06'56"	82º44'13"	89.70	Good
23	GW 23	24º07'15"	82º45'35"	92.03	Good
24	GW 24	24º08'03"	82º46'27"	94.14	Good
25	GW 25	24º08'52"	82º46'12"	92.61	Good
26	GW 26	24º09'08"	82º46'10"	95.37	Excellent
27	GW 27	24º10'0.8"	82º46'0.4"	85.02	Good
28	GW 28	24º10'15"	82º46'1.3"	91.85	Good
29	GW 29	24º05'01"	82º34'21"	91.33	Good
30	GW 30	24º05'26"	82º33'19"	85.24	Good
31	GW 31	24º06'31"	82º32'10"	85.11	Good
32	GW 32	24º11'32"	82º40'29"	85.22	Good
33	GW 33	24º11'46"	82º42'6.9"	78.17	Fair
34	GW 34	24º11'21"	82º41'10"	85.59	Good
35	GW 35	24º12'09"	82º35'26"	78.34	Fair
36	GW 36	24º12'21"	82º35'15"	86.78	Good
37	GW 37	24º11'48"	82º45'58"	94.63	Good
38	GW 38	24º07'49"	82º46'19"	92.15	Good
39	GW 39	24º05'51"	82º35'42"	82.32	Good
40	GW 40	24º12'30"	82º36'52"	77.34	Fair
41	GW 41	24º10'59"	82º35'25"	76.47	Fair
42	GW 42	24º12'02"	82º35'58"	77.22	Fair
43	GW 43	24º06'23"	82º36'53"	84.82	Good
44	GW 44	24º06'12"	82º36'49"	64.90	Marginal
45	GW45	24º05'02"	82º39'28"	79.71	Fair
46	GW46	24º05'25"	82º38'34"	68.52	Fair

5.4.5 Hierarchical Cluster Analysis (HCA)

Cluster analysis is an automatic technique that is used to classify individuals or objects into mutually exclusive groups (called clusters) based on similarities of measurements that have been collected on these objects. Hierarchical Cluster Analysis or dendrogram representation is used for grouping water samples by similar monitoring sites in their chemical composition. The multiple water quality parameters can be clustered based on their dependency (Routroy et al., 2013). The sampling locations can be clustered based on chemical similarity or WQI similarity in samples collected from various sites in the study area (Singh et al., 2005; Shreshtha and Kazama, 2006). Dendrograms are the pictorial representation techniques that classify data with high homogeneity within the cluster (group) and heterogeneity between the different clusters. The horizontal axis shows the dissimilarity or improper correlation in the group of data. The clusters linked at a height near to zero have a strong correlation or the variation of in the data is less than the other clusters at comparatively more height. As these diagrams help to link the properties or the set of properties of a particular entity, they are also referred to as Linkage Diagrams.

The results of Hierarchical Cluster Analysis are given as a dendrogram was presenting in Fig. 5.42. As seen from this figure, the sampling stations have mainly grouped into three Clusters: cluster I, II and III.

Cluster I consist of sampling location GW-9, GW-35, GW-12, GW-45, GW-11, GW-18, GW-13, GW-33, GW-39, GW-6, GW-36, GW-30, GW-32, GW-20, GW-31, GW-27, GW-43, GW-34, GW-4,GW-15,GW-1,GW-16,GW-10,GW-40,GW-42 and GW-41 shows similar values of water quality index.

Cluster II consist of GW-21,GW-16,GW-24,GW-37,GW-8,GW-2,GW-22,GW-7,GW-19,GW-17,GW-23,GW-38,GW-28,GW-5,GW-25,GW-14,GW-29 this group of samples have similar properties but different from the Cluster I group.

Cluster III consists of GW-3, GW-46, GW-44 which are differed from Cluster I and Cluster II. Thus the linkage diagram (or dendrogram) helps in associating areas with similar values of water quality index.

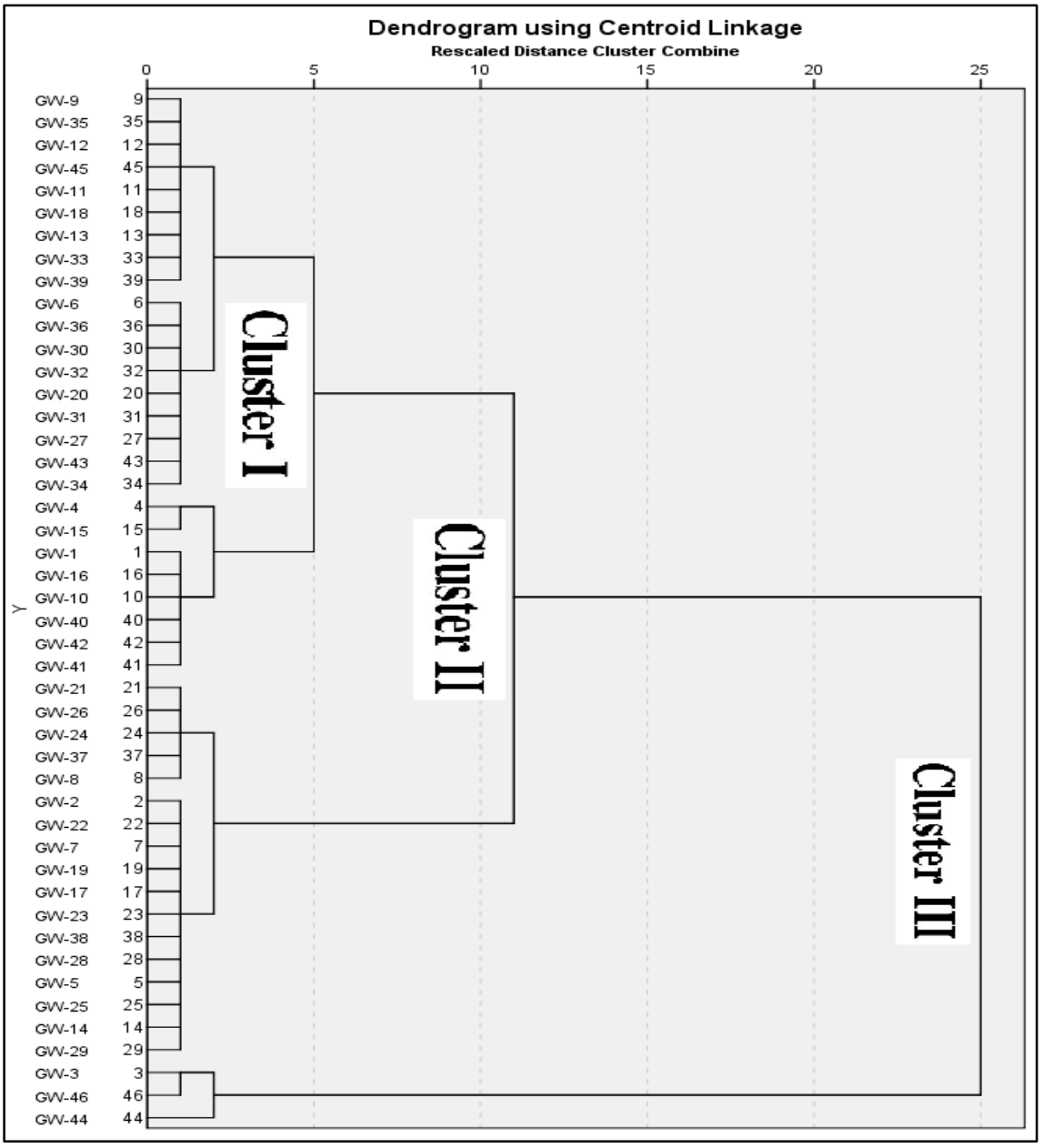

Figure 5.42 Dendrogram of the HCA based on WQI of the sampling stations

5.4.6 Geochemical classification and hydrogeochemical facies of the groundwater

5.4.6.1 Piper Trilinear Diagram

The Piper trilinear diagram (Piper, 1944) is a graphical presentation of the major ions to quickly determine the hydrochemical facies of groundwater in the study area. The diagram shows the similarities and differences among water samples as those with similar qualities will tend to fall in the same group (Todd 1980; Ramesh et al. 2014). The word "Hydrochemical facies" describes the occurrence of groundwater modes in an aquifer system differing in their chemical compositions and is primarily a function of geology, the kinetics of the solution and aquifer flow patterns (Todd 1980).

This diagram consists of three distinct fields including two triangular fields and a diamond-shaped field. The left triangle is represented by presence of cations such as Magnesium, Calcium, Sodium and Potassium whereas the right triangle consist of anions like Chloride, Bicarbonate, Carbonate and Sulphate. On both the triangles these ions are plotted in terms of percentage. However, the Diamond-shaped plot present in between the two triangles exhibits the convergence point of two triangles consisting of both cations and anions in form of a single point representing the composition of water in the study area.

The groundwater samples collected from the area under study show that nearly 11% of the samples fall under Magnesium type, approximately 17% were in Calcium type, 6% occurred in Sodium or Potassium type while the remaining 66% of the samples fall in No Dominant type in cation facies. Contrary to it, 9% of the samples appeared in Chloride type, approximately 41% into Bicarbonate type whereas the rest 50% of the samples fall under No Dominant type in anion facies. The diamond-shaped part of the plot reveals that nearly 48% of the ground water samples collected from the study area laid under Ca-Mg-

HCO_3 category indicating the percolation and dissolution of minerals such as Calcite and Dolomite which are predominant in the geology of the area of sample collection. However, approximately the same percentage of samples i.e. 46% of the samples fall under Ca-Mg-Cl-SO_4 group representing the presence of anthropogenic activities like continuation of mining activities and presence of thermal power plant in the study area. Apart from this, only 4% and 2% of the ground water samples collected from the study area appeared under NaCl-SO_4 and NaK-HCO_3 groups respectively showing the process of dissolution of minor minerals present in the area. Hence, the above explanation can be verified by Fig 5.43 and Fig 5.44 showing the Piper diagram for describing the hydro-geo-chemical facies variations and Modified Piper Plot of the Classification Scheme for hydro-geo-chemical facies variations respectively.

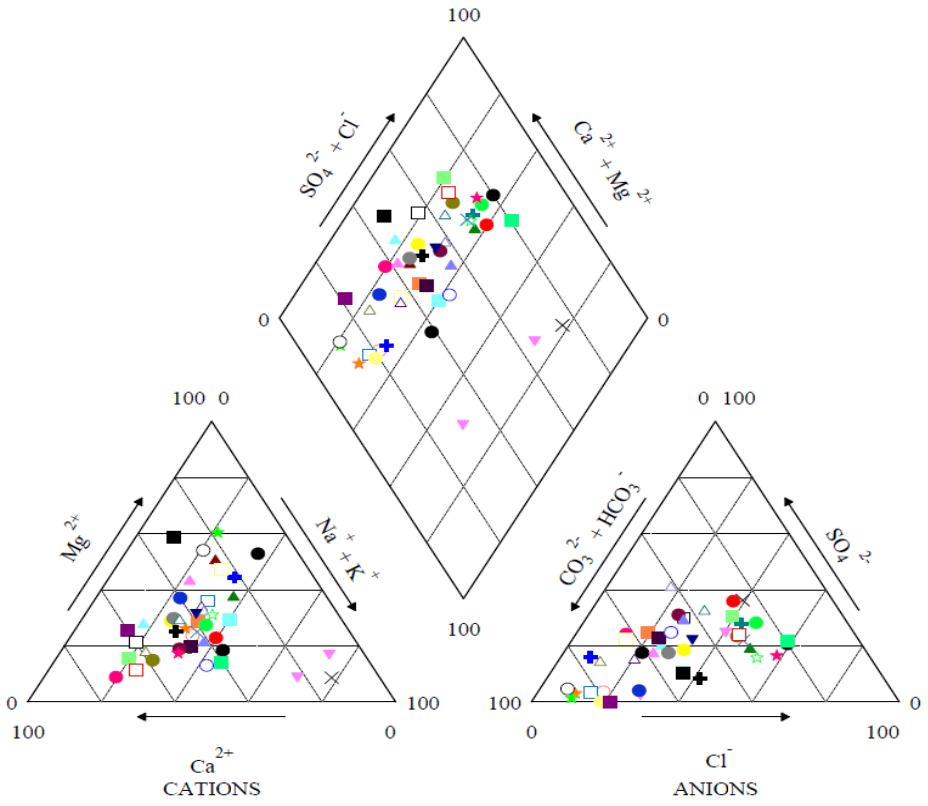

Figure 5.43 Piper diagram for describing the hydro-geo-chemical facies variations

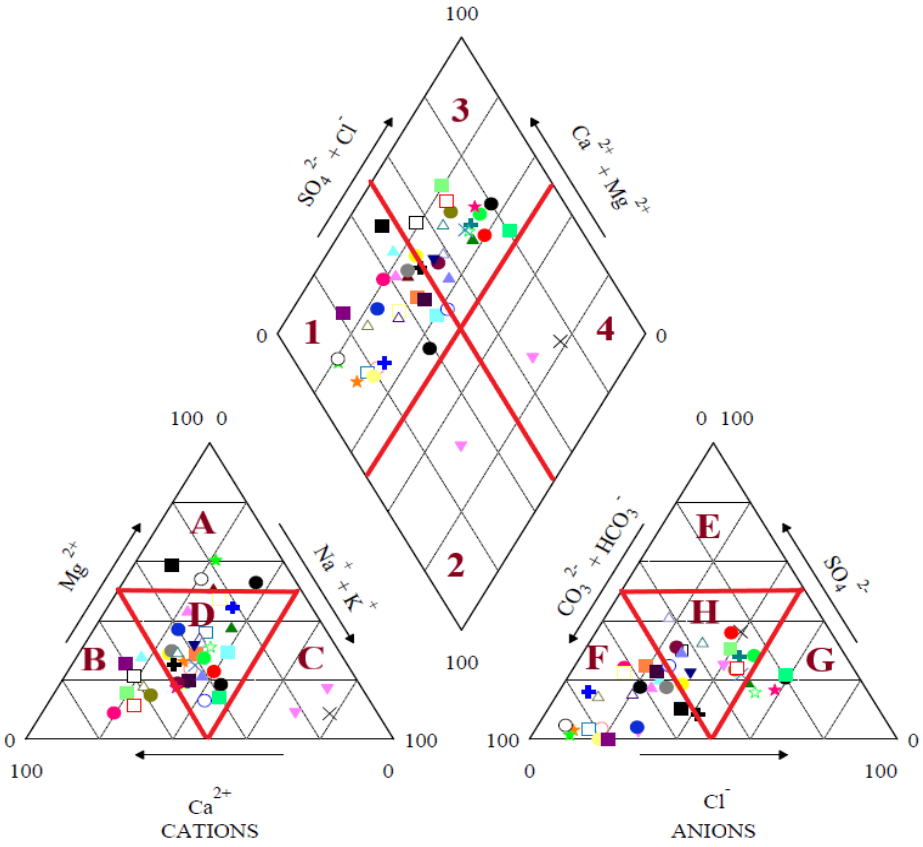

Figure 5.44 Modified Piper plot of the classification scheme for hydro-geo-chemical facies variations

The Legends used in Fig 5.44 has been listed below as follows:-

A - Magnesium type

B - Calcium type

C - Sodium or Potassium type

D - No dominant type

E - Sulphate type

F – Bicarbonate type

G - Chloride type

H - No dominant type

1 – $CaMg\text{-}HCO_3$

2 – $NaK\text{-}HCO_3$

3 – $Ca\text{-}Mg\text{-}Cl\text{-}SO_4$

4 – $NaCl\text{-}SO_4$

5.4.6.2 Gibb's Diagram

Gibbs diagram also used to analyze the effect of hydro-geochemical processes such as precipitation, rock-water interaction, and evaporation on groundwater geochemistry of the study area (Gibbs, 1970; Li et al., 2013). Gibb's diagram shows three different regions like precipitation dominance, evaporation dominance, and rock–water interaction dominance are shown in the Gibbs diagram (Gibbs, 1970). The rock–water interaction dominance field indicates the interaction between rock chemistry and the chemistry of the percolated waters under the subsurface. Gibb's diagram is explained on the basis of two ratios, one is for cation and another one is for anion, as a function of total dissolved solids (TDS).

$$\text{Gibbs ratio I (for cations)} = \frac{(Na^+ + K^+)}{(Na^+ + K^+ + Ca^{2+})} \quad (5.6)$$

$$\text{Gibbs ratio II (for anions)} = \frac{Cl^-}{(Cl^- + HCO_3^-)} \quad (5.7)$$

The Gibbs ratio of the groundwater samples is plotted against their respective TDS and calculated Gibbs equation values. Gibbs diagram (Fig. 5.45a, b) indicates that the majority of the water samples fall under the rock water dominance field and few samples are placed under the evaporation dominance zone. In the present study, the majority of the water samples fall in rock dominance for both ratios (cations & anions) which means that the quality of groundwater is being affected by the chemical weathering of rock minerals. The evaporation process is not only a common phenomenon in surface water but also in the groundwater system (Jankowski and Acworth 1997).

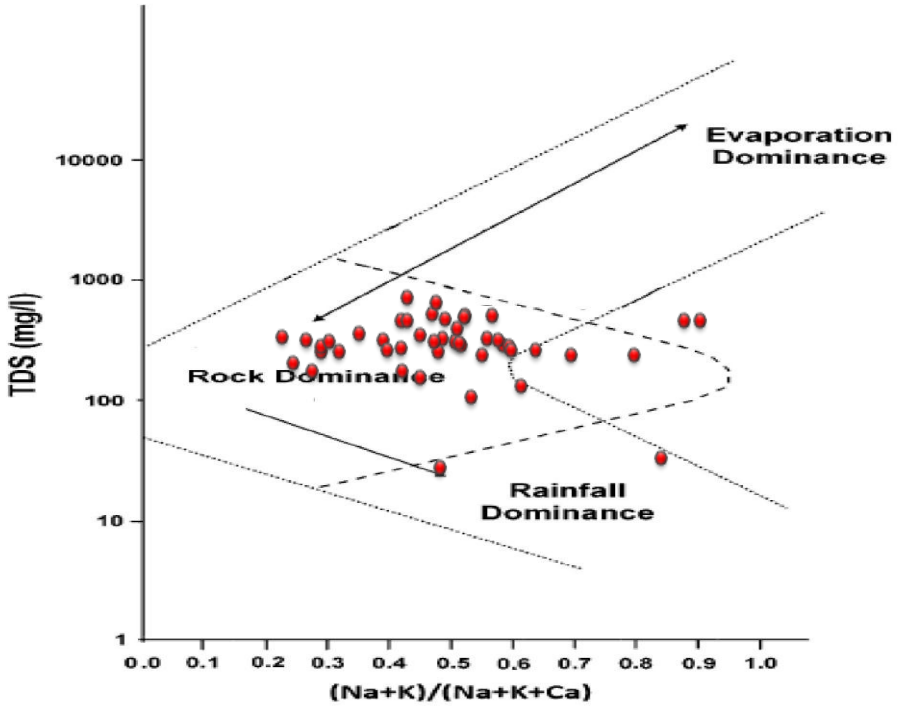

(a)

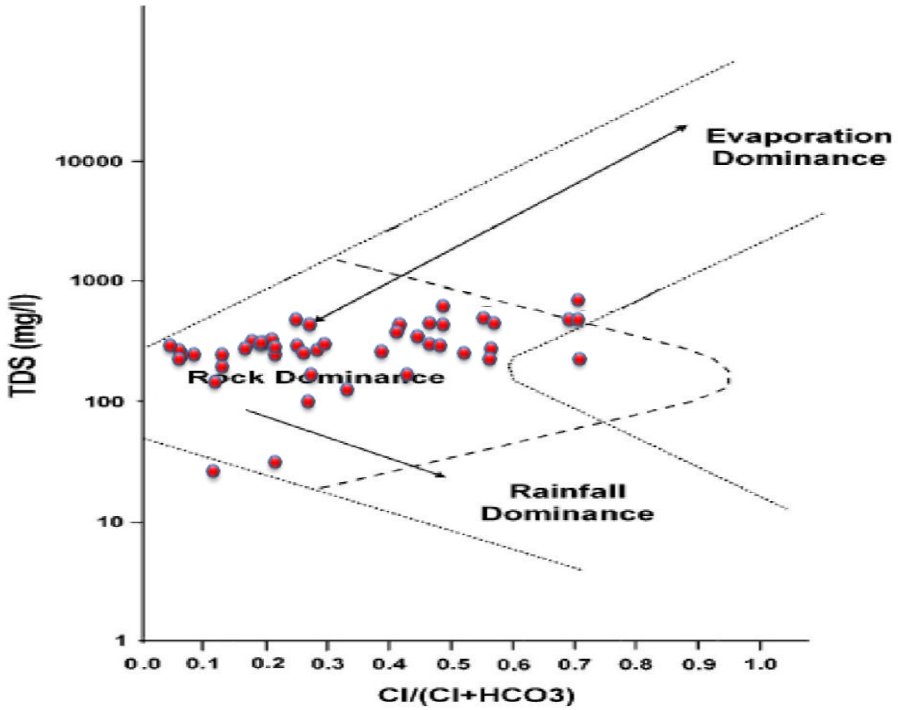

(b)

Figure 5.45 Gibbs Diagrams for groundwater samples (a) Gibbs ratio I (for cation), and (b) Gibbs ratio II (for anion)

5.4.7 Suitability of groundwater for irrigational purposes

The suitability of groundwater for irrigational applications depends on mineral constituents of water and its potential impacts on the soils and the plants (Todd and Mays, 2005). Excess amounts of salts in water could affect the structure and texture of the soil and result in changes in soil permeability and aeration, thereby impacting plant growth (Todd and Mays, 2005; Trivedy and Goel, 1984). It does not allow water to reach different parts of the plants, which in turn reduces agricultural productivity (Rao et al. 2013).

For long-term productivity, it is important to have knowledge of water quality used for irrigation to understand what management changes are essential (Jalali 2011; Srinivasamoorthy et al. 2014). The quality of irrigation water is decided by estimation of sodium adsorption ratio (SAR), percent sodium (%Na), Kelly's ratio and Magnesium Hazard.

5.4.7.1 Sodium Absorption Ratio (SAR)

The U.S. Salinity Laboratory (USSL) recommends using the Sodium Adsorption Ratio (SAR) to evaluate the alkalinity hazard or sodium hazard of water for irrigation (US Salinity Laboratory Staff, 1954). Sodium concentration is important in classifying the water for irrigation purposes because sodium concentration can reduce the soil permeability and soil structure (Todd 1980; Domenico and Schwartz 1990). The sodium hazard in the irrigation water is measured by the relative concentration of major cations, such as Na^+, Ca^{2+}, and Mg^{2+} (Khodapanah et al. 2009). SAR is calculated using the following equation (Hem 1985):

$$SAR = \frac{Na^+}{\sqrt{\frac{Ca^{2+} + Mg^{2+}}{2}}} \tag{5.8}$$

Where the concentration are reported in meq/L.The computed SAR values of the groundwater in the study area ranged from 0.40 and 7.20 meq/l with an average value of 1.36 meq/l. The combined effect of SAR and EC is shown in Fig 5.46. A classification of water for irrigation on the basis of SAR hazard is presented in Table 5.9. (Fipps, 2003). The SAR plot indicates that the water samples fall in the category C1-S1, C2-S1, C3-S1 and C3-S2. Majority of water samples fall under the C2-S1 (medium salinity and low alkali) and C3-S1 (higher salinity and low alkali) category, which can be used for irrigation purposes.

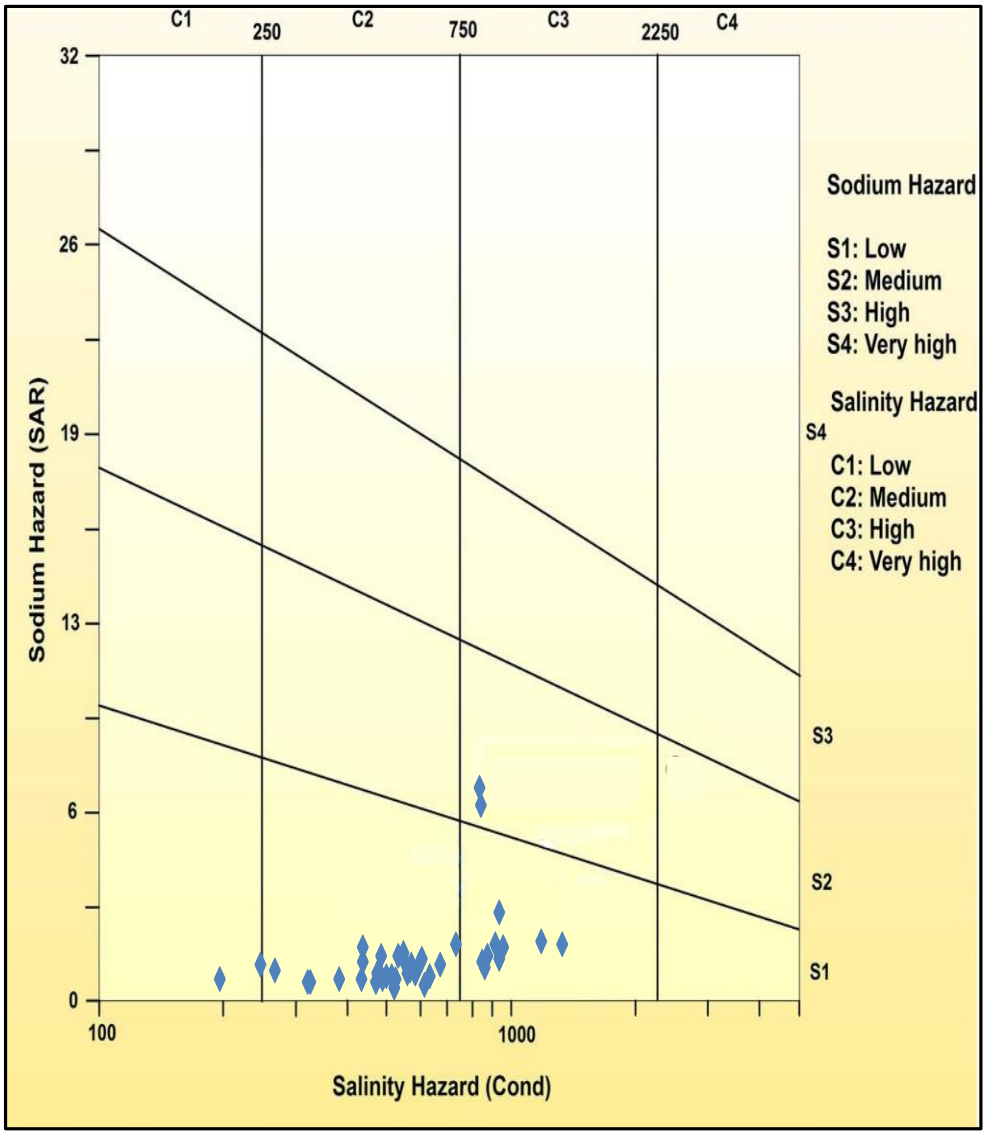

Figure 5.46 US Salinity diagram for the classification of irrigation water

The plot of data on the US Salinity diagram, in which the EC represents the salinity hazard and the SAR as alkalinity hazard. The measured value of EC is varied between 50 and 1331 μS/cm. Irrigation water was qualified by Richards (1954) into four categories on the basis of EC values. The zones (C1–C4) have the value of EC < 250 (low), 250–750 (medium), 750–2250 μS/cm (high) and more than 2250 μS/cm (Very high), respectively. As per Richards, it is observed that 67.39 % of the samples fall in moderately saline, 23.91% of the samples in the highly saline zone.

Table 5.9 Classification of water suitability for irrigation based on SAR

SAR	**Water class**	**Sample Code**	**Percentage**
0-10	low	GW-1,2,3,4,5,6,7,8,9,10,11,12,13,14,15,16,17, 18,19,20,21,22,23,24,25,26,27,28,29,30,31,32, 33,34,35,36,37,38,39, 40,41,42,43,44,45,46	100
10-18	Medium	Nil	0.00
18-26	high	Nil	0.00
>26	Very high	Nil	0.00

5.4.7.2 Sodium Percentage (%Na)

Sodium Percentage is also used to assess groundwater suitability for irrigation use (Purushothman et al., 2012). Excess amount of sodium content in water reduces soil permeability and limits air and water circulation, during winter. During the summer, it becomes hard and dry (Saleh et al., 1999). Sodium-saturated soils, by causing osmotic effects, may result in low agricultural yields (Raju, 2007). The percent sodium is calculated using the following equation:

$$\% \text{ Na} = \frac{(\text{Na}^+ + \text{K}^+)}{\text{Ca}^{2+} + \text{Mg}^{2+} + \text{Na}^+ + \text{K}^+} \times 100 \qquad (5.9)$$

Where the concentration are reported in meq/L.The soluble sodium percentage (%Na) of the analyzed groundwater samples of the study region varies from 10.31% to 78.24% with an average value of 32.27 %. A maximum Na% limit of 60% is recommended by BIS for irrigation water. Irrigation water quality based on sodium percentage is classified into five categories (Arumugam and Elangovan, 2009), are shown in Table 5.10.

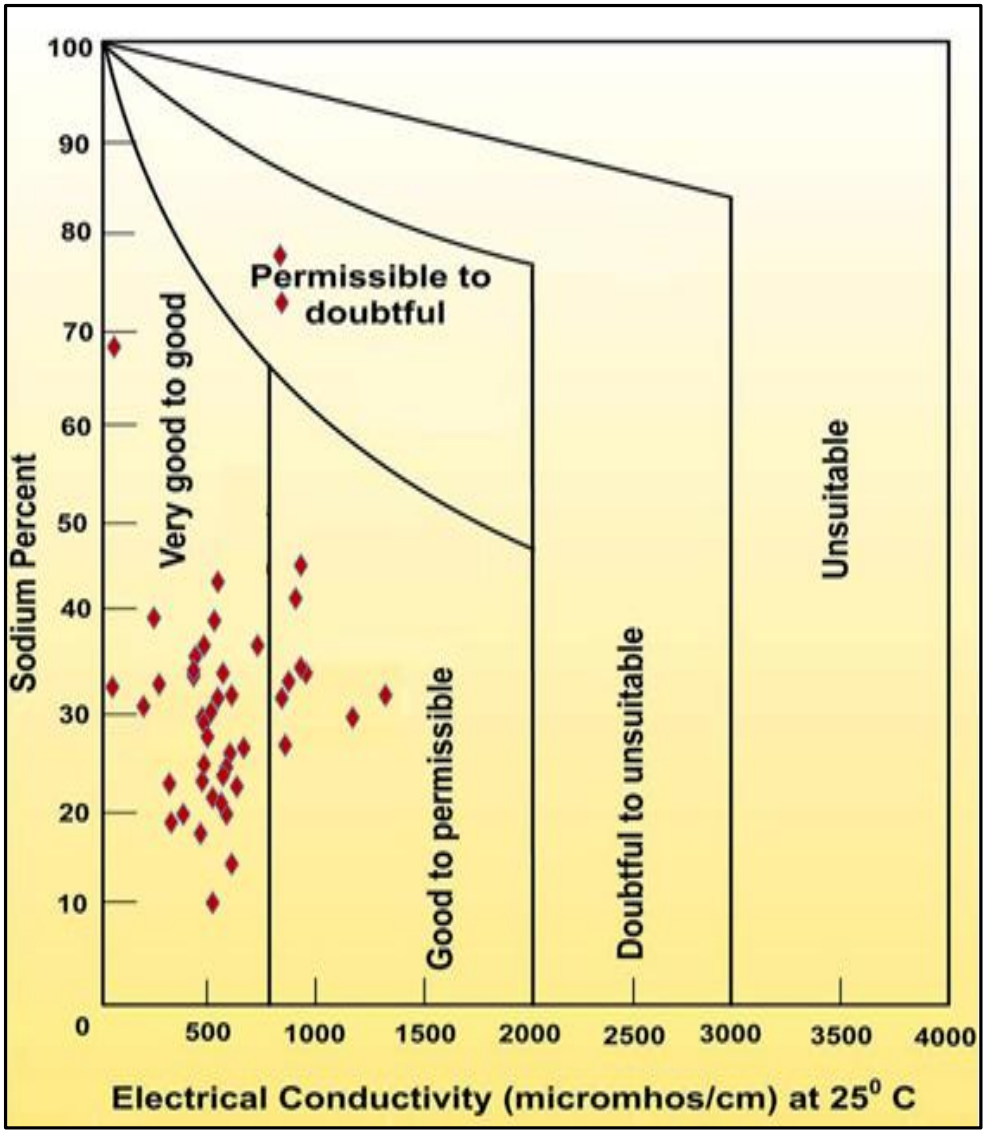

Figure 5.47 Classification of irrigation water based on the Wilcox plot

Wilcox (1948) suggested using the classification presented in Fig. 5.47. Based on this classification, about 76.08% of the water samples come under very good to good and

19.56 % of the samples come under good to permissible class, which may be used for irrigation purposes, whereas the rest of water samples (GW-15, 16) fall under the range of permissible to doubtful.

Table 5.10 Classification of water suitability for irrigation based on Na%.

% Na	Classification	Sample Code	Percentage
>20	Excellent	GW-7,11,17,19, 20 & 22	13.04
20-40	Good	GW-1,2,4,5,6,9,10,12,13,14,18,21,23, 24,25,26,27,29,30,31,32,33,34,35,36,37, 38,39,40,41, 43,44,46	71.73
40-60	Permissible	GW-3,28,42,45	8.69
60-80	Doubtful	GW-8,15,16	6.52
>80	Unsuitable	Nil	0.00

5.4.7.3 Kelly Ratio (KR)

Kelly's Ratio (KR) is used for the classification of water for agricultural uses. Sodium measured against calcium and magnesium is considered for calculating this parameter (Kelly 1940). The groundwater having Kelly's ratio > 1 is not suitable for irrigation and groundwater with low KR (<1) are suitable for irrigation (Sundaray et al. 2009; Srinivasamoorthy et al. 2014; Patel et al. 2016). The Kelly Ratio was calculated using the following formula (Kelly 1963).

$$\text{Kelly Ratio (KR)} = \frac{Na^{+}}{Ca^{2+} + Mg^{2+}} \quad (5.10)$$

Where the concentration are reported in meq/L.

Kelly's ratio is calculated for our study area which ranges from 0.11 to 3.40. Based on KR classification, about 95.65% of water samples are suitable and 4.35% of water samples are unsuitable for irrigation purposes. The classification of the quality of irrigation water based on KR is given in Table 5.11.

Table 5.11 Classification of irrigation water based on Kelly's ratio

KR	**Water Quality**	**Sample Code**	**Percentage**
< 1	Suitable	GW-1,2,3,4,5,6,7,8,9,10,11,12,13,14,17,18,19,20, 21,22,23 24,25,26,27,28,29,30,31,32,33,34,35, 36,37,38,39,40,41,42,43,44,45,46	95.65
> 1	Unsuitable	GW-15,16	4.35

5.4.7.4 Magnesium Hazard (MH)

The magnesium hazard are also used to classify water for irrigation uses. The Magnesium Hazard was determined using the following formula:

$$\text{Magnesium Hazard (MH)} = \frac{Mg^{2+}}{Ca^{2+} + Mg^{2+}} \times 100 \qquad (5.11)$$

Szabolcs and Darab (1964) proposed a MH value for irrigation water; above 50 meq/l magnesium ratio is recommended for unsafe and unsuitable for agricultural activity. From the analytical data, the MH values ranged from 10.97 to 82.84 meq/l with the mean value of 41.33 meq/l (Table 5.12). Among the 46 groundwater samples, 11 water samples (GW-1, 4, 13, 16, 20, 21,23,24,25,26 & 32) show MH value exceed the limit (>50 meq/l). Based on the above criteria, approx. 23.91% of the groundwater samples are not appropriate for irrigation purposes.

Table 5.12 Computed values of SAR, Na%, KR and MH in the study area

Sample Code	SAR	Na%	KR	MH
GW 1	1.73	36.24	0.54	82.84
GW 2	0.40	33.00	0.45	35.38
GW 3	1.14	40.27	0.65	49.30
GW 4	0.71	30.96	0.42	52.13
GW 5	0.74	23.23	0.29	22.95
GW 6	1.01	33.33	0.49	28.25
GW 7	0.63	19.65	0.24	10.97
GW 8	0.54	68.69	0.67	29.50
GW 9	0.90	29.79	0.31	37.34
GW 10	1.16	26.56	0.35	20.28
GW 11	0.82	19.73	0.24	19.40
GW 12	1.77	34.31	0.50	29.69
GW 13	1.29	25.91	0.35	67.85
GW 14	0.62	22.96	0.26	48.08
GW 15	7.20	78.24	3.40	39.85
GW 16	6.57	73.22	2.58	65.07
GW 17	0.50	14.37	0.16	29.96
GW 18	1.46	39.80	0.52	37.98
GW 19	0.57	17.72	0.19	33.48
GW 20	0.42	10.31	0.11	65.52
GW 21	0.67	21.47	0.25	76.89
GW 22	0.54	18.77	0.22	26.25
GW 23	0.84	20.74	0.23	68.16
GW 24	0.80	22.56	0.26	55.47
GW 25	0.69	34.05	0.33	67.22
GW 26	0.91	29.14	0.39	66.53
GW 27	0.80	30.38	0.38	48.49
GW 28	1.52	43.87	0.77	32.81
GW 29	1.35	32.03	0.47	41.91
GW 30	1.33	31.74	0.44	47.16
GW 31	0.88	24.60	0.30	38.26
GW 32	1.46	37.32	0.57	59.44
GW 33	1.29	34.66	0.50	47.55
GW 34	0.75	27.70	0.35	34.72
GW 35	1.48	33.54	0.49	37.59
GW 36	1.41	34.86	0.51	42.03
GW 37	1.14	34.40	0.50	30.11
GW 38	0.69	24.81	0.31	39.65
GW 39	0.93	23.76	0.30	15.04
GW 40	1.06	26.78	0.35	39.58
GW 41	1.30	31.78	0.46	27.76
GW 42	1.83	42.17	0.73	22.54
GW 43	1.85	37.37	0.59	33.56
GW 44	1.96	29.82	0.42	45.49
GW45	2.90	45.66	0.83	25.49
GW46	1.83	32.20	0.47	25.64

5.5 Analysis of land use / land cover (LULC) changes from 1990 to 2019

Six major land use land cover categories – built-up area, mining area, forest/hilly area, crop land, water body and fallow land were recorded in the study area. The land use/land cover maps of the study area for four different time periods (1990, 2000, 2009 and 2019) are presented in Fig. 5.48.

5.5.1 Areal statistics of LULC

Area statistics of six land use/land cover categories and percentages of the area covered by each land use land cover category are also shown in Table 5.13. The overall results of the LULC classification showed that the fallow land, cropland, and forest/hilly area was the most dominant. The built-up area shows increasing trend from 1990 to 2019 covering an area of 3.20 km^2 (0.71%) in the year 1990, 5.33 km^2 (1.19%) in the year 2000, 7.19 km^2 (1.61%) in the year 2009 and 9.24 km^2 (2.07%) in the year 2019.

The coal mining area that had spread over 19.56 km^2 in 1990 (4.39%), 32.27 km^2 (7.24%) in the year 2000, increased to 49.31 km^2 in 2009 (11.07%) and again it increased to 88.53 km^2 in the year 2019 (19.88%). The net increase of mining area is approx. 353% from the year 1990 to 2019. The mining area comprises the opencast coal mines and overburden dumps. As a consequence, the area of mining and overburden dumps showed a continuous increase in their aerial extents during the study period.

The forest/hilly area covered approximately 16.13% (2019) of the study area and forms a vital land cover class. It is observed that the forest/hilly area had decreased from 114.65 km^2 (25.75%) in the year 1990 to 101.76 km^2 (22.85%) in the year 2000, and further decreased to 71.82 km^2 (16.13%) by the year 2019. The decrease of forest cover may be due to establishment of thermal power plant and opening of new mine blocks as most of the coal mines are located in dense forest/hilly area.

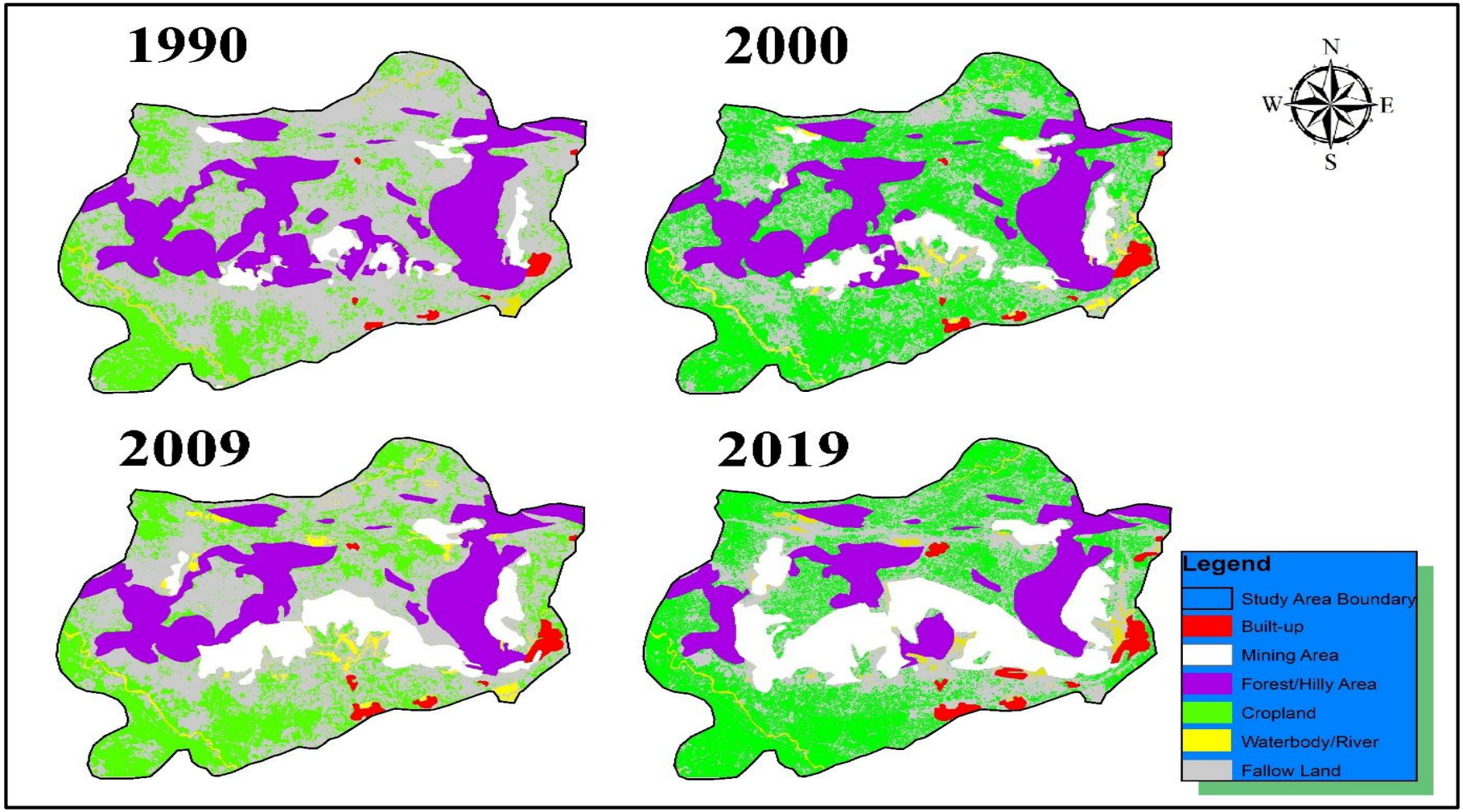

Figure 5.48 Classify land use / land cover (LULC) maps of the study area

Table 5.13 Areal classification of LULC classes in the study area

LULC Classes	1990		2000		2009		2019	
	Area (km^2)	Area (%)	Area (km^2)	Area (%)	Area (km^2)	Area (%)	Area (km^2)	Area (%)
Built-up Area	3.20	0.71	5.33	1.19	7.19	1.61	9.24	2.07
Mining Area	19.56	4.39	32.27	7.24	49.31	11.07	88.53	19.88
Forest/Hilly Area	114.65	25.75	101.76	22.85	89.54	20.11	71.82	16.13
Crop land	135.12	30.34	141.79	31.84	147.92	33.22	149.88	33.66
Water bodies/River	4.10	0.92	8.46	1.90	10.71	2.40	8.01	1.79
Fallow land	168.56	37.86	155.56	34.94	140.52	31.56	117.70	26.43
Total Area (km^2)	445.21		445.21		445.21		445.21	

The crop land covers approximately 34% of the study area. The crop land shows an increasing trend from 1990 to 2019 covering an area of 135.12 km^2 (30.34%) in the year 1990, 141.79 km^2 (31.84%) in the year 2000, 147.92 km^2 (33.22%) in the year 2009 and 149.88 km^2 (33.66%) in the year 2019.

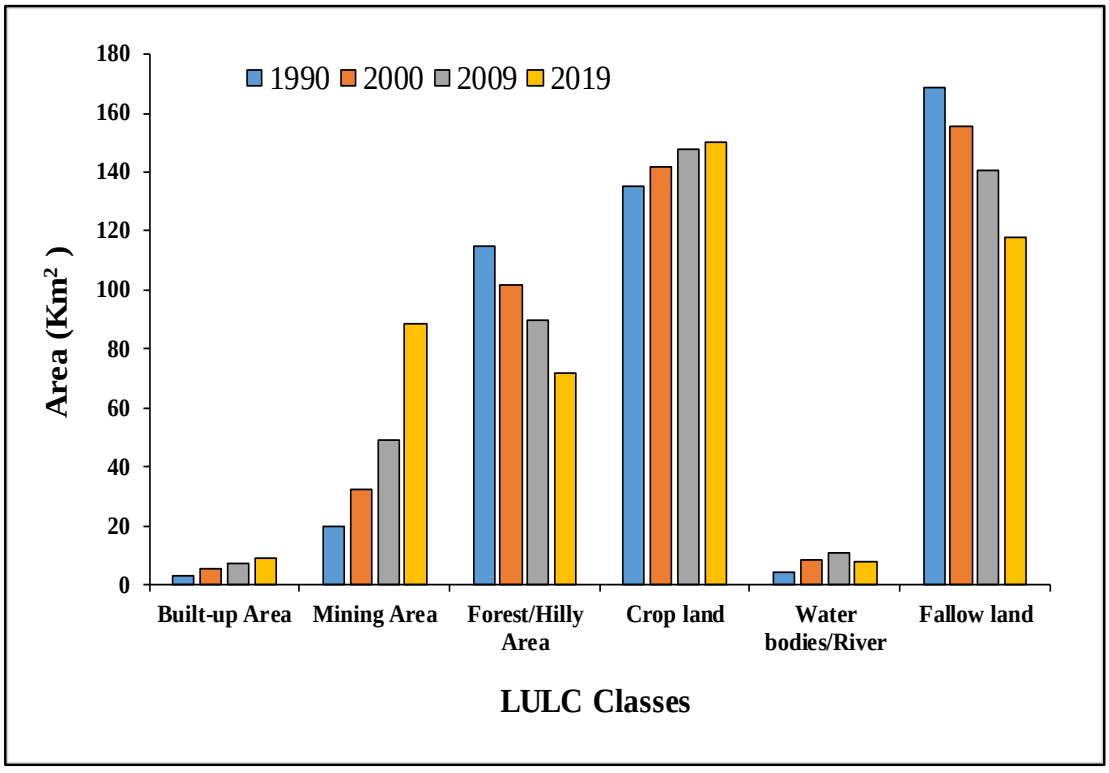

Figure 5.49 Bar showing LULC area distribution of the study area (1990–2019)

The water bodies/river of the study region shows increasing trend from 1990 to 2019 covering an area of 4.10 km^2 (0.92%) in the year 1990, 8.46 km^2 (1.90%) in the year 2000 and 10.71 km^2 (2.40%) in the year 2009.However, the total area of water body has decreased to 8.01 km^2 (1.79%) in the year 2019.

The fallow land covered the major part of the study area and which gradually decreased from 1990 to 2019. It is found that the Fallow land area had decreased from 168.56 km^2 (37.86%) in the year 1990 to 155.56 Km^2 (34.94%) in the year 2000, and further decreased to 114.70 km^2 (26.43%) by the year 2019.

5.5.2 Percent change analysis of LULC

Table 5.14 shows the area and percentage of change in different land use land cover classes in four year time period from 1990 to 2019.

Table 5.14 Net change in areal extent of LULC classes

LULC Classes	1990-2000		2000-2009		2009-2019		1990-2019	
	Net change		Net change		Net change		Net change	
	Area	%	Area	%	Area	%	Area	%
Built-up Area	2.13	66.56	1.86	34.90	2.05	28.51	6.04	188.75
Mining Area	12.71	67.98	17.04	52.80	39.22	79.54	68.97	352.61
Forest/Hilly Area	-12.89	-11.24	-12.22	-12.01	-17.72	-19.59	-42.83	-37.36
Crop land	6.67	4.94	6.13	4.32	1.96	1.33	14.76	10.92
Water bodies/River	4.36	106.34	2.25	26.60	-2.7	-25.21	3.91	95.37
Fallow land	-13	-7.71	-15.04	-9.67	-22.82	-16.24	-50.86	-30.17

As seen from the data in Table 5.14, Maximum positive change (352.61%) is observed in the mining area, particularly during 2009–2019, whereas maximum negative change is recorded in the Forest/Hilly (-37.36%) and Fallow land (-30.17%) area in the same period. Maximum increase in the mining area and consequently the maximum decrease in forest

cover and fallow land area are observed during 1990–2019. This was due to the expansion in coal mining activities as well as increases in the built-up area of that area.

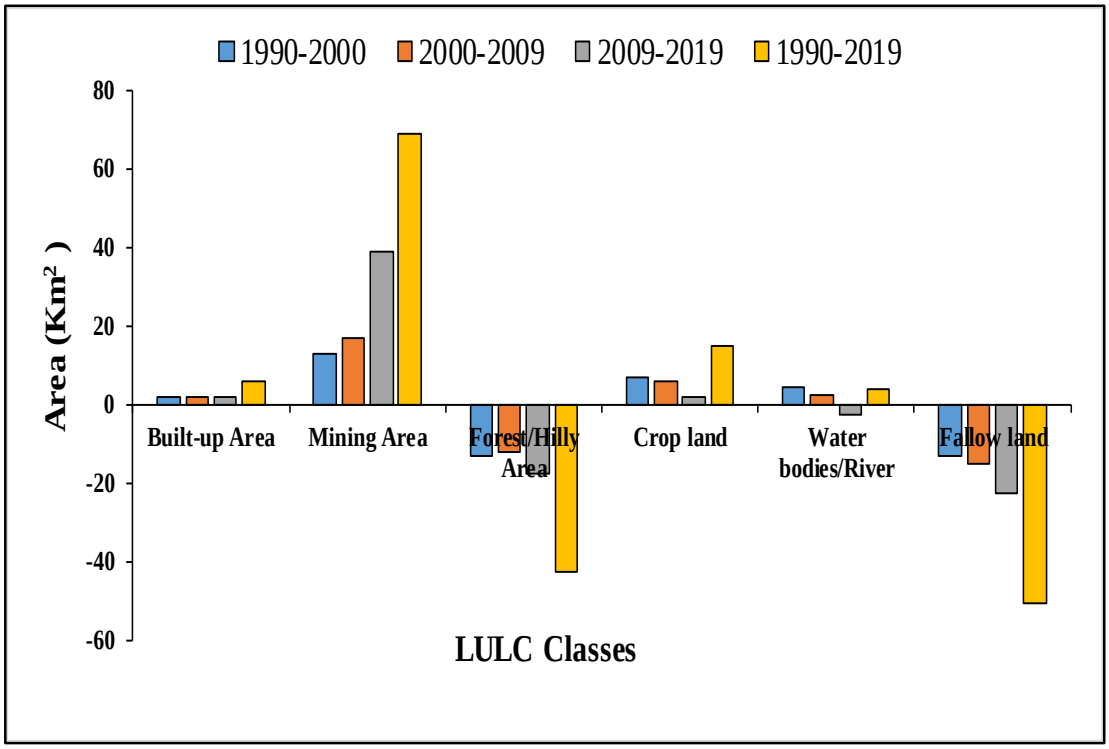

Figure 5.50 Bar showing change in LULC classes of the study area from 1990 to 2019

5.5.3 Rate of LULC changes

The rate of change of the land cover classes during the different time intervals (1990-2000, 2000-2009, 2009-2019 and 1990-2019) is shown in Table 5.15.It is observed that the built-up area shows an increase during the year 1990–2019. Which shows an increase in rate of change (0.21 km^2/year).Change rate of coal mining is observed increasing continuously during the study period with a net rate of change of 2.38 km^2/year. Coal mining areas observed maximum increment in change rate of 4.36 km^2/year during the period 2009-2019.The net positive rate of change of crop land is 0.51 km^2/year for the study period, while it is highest (0.68 km^2/year) during 2000–2009.The net rate of change of Forest/Hilly area is -1.48 km^2/year for the study period, while it is observed maximum decrease (-1.97 km^2/year) during 2009-2019.

The net rate of change of water bodies is 0.13 km^2/year for the study period, while recording maximum increase in change rate (0.44 km2/year) during the year 1990–2000, and maximum decrease in change rate (-0.30 km2/year) observed during the years 2009–2019.The Fallow land exhibits net negative rate of change of -1.75 km^2/year during the total study period (1990-2019).

Table 5.15 Rate of change in LULC classes of the study area

LULC Classes	**Rate of change (km^2/year)**			
	1990-2000	**2000-2009**	**2009-2019**	**1990-2019**
Built-up Area	0.21	0.21	0.23	0.21
Mining Area	1.27	1.89	4.36	2.38
Forest/Hilly Area	-1.29	-1.36	-1.97	-1.48
Crop land	0.67	0.68	0.22	0.51
Water bodies/River	0.44	0.25	-0.30	0.13
Fallow land	-1.30	-1.67	-2.54	-1.75

It is observed there is a direct impact of mining on forest/hilly area, fallow land and cropland due to the expansion of mining areas during the study period. The forest/hilly area, fallow land and cropland have played a significant role to improve the groundwater level. This study helps that in decision making for groundwater management in the Singrauli coalfield area of India.

The coalfield are the potential source of groundwater due to the occurrence of very soft friable sandstone (best aquifer) associated with coal. These aquifers are being damaged and disturb due to opencast coal mining. As a result of mining, the complete geology of the area are being disturbed and converted into mixed rocks unstable hillocks. Hence, the complete aquifer is destroyed. Generally, the life of the coal mine is 30 years or more. The discharge of groundwater continuously during the mining operation is extracting water from the nearby area and this discharged water is being collected in the sump of

coal mine. From the sump, through the pumping stations, the water is being continuously discharged into the nearby water bodies. Opencast mining is a process where all overlying rocks associated with coal and overburden are removed and disposed off somewhere else in the mining area. The leached water may infiltrate and contaminate groundwater as a result of development of joints, cracks, fractures developed due to blasting for breaking of rocks. Hence the groundwater quality has also degraded as a mining operation.